

EXPIRATION OF LIMITED EXCLUSIVE RIGHTS: The use, duplication and disclosure of this contractor report was formerly restricted under Limited Exclusive Rights. These Limited Exclusive Rights have expired and the contractor has been notified of the expiration. This report may be used, duplicated and disclosed, subject to NASA Langley Research Center's Scientific and Technical Information process and to any other restrictive notice(s).

1

Task 20

•

March 31, 1998

Prepared for

NASA LaRC Research Center
Hampton, Virginia 23665

[REDACTED]

[REDACTED]

[REDACTED]

[REDACTED] government contract No. NAS1-20220

WBS 2.1.7.2 Improved Aeroservoelastic Modeling

Relevant Milestones:

Incorporate Control Effects on Symmetric Flutter

PCD date: Dec 1997

Initial study of TCA with $\dot{\gamma}/V$ control law

Completed Dec 1997

Objective: Develop and/or improve methods for incorporation of the effects of control systems in the aeroelastic modeling, analysis, and structural sizing process. Apply these methods to the Technology Concept Airplane to assess the effects of defined control systems on the configuration aeroelastic behavior and resultant weight.

Accomplishments / Relation to Milestone

Flutter analysis that includes the effect of control systems has been developed and applied. Initial results for the TCA airplane, incorporating the longitudinal $\dot{\gamma}/V$ control law, show that the current control system has a significant detrimental effect on flutter mechanisms. Evaluations have been conducted at both the Seattle and Long Beach sites, using the ELFINI (Seattle) and NASTRAN (Long Beach) versions of the TCA finite element structural model. These analyses are described in two reports which are included in this deliverable. The two analyses confirm the basic finding of the control system effects on flutter. The Seattle analysis was performed at transonic ($M=0.95$) and supersonic ($M=2.60$) flight conditions. The effects of mean-axis sensors vs. "real" sensors at various locations, i.e. those including the effects of local structural motion were also examined. Comparisons were made between the traditional "p-k" flutter solution and stability analysis using root locus techniques based on the state-space representation of the model. The Long Beach analysis considered the effects of some possible modifications to the $\dot{\gamma}/V$ control law.

Task 20 - Technical Integration

Sub Task 7: Aeroservoelastic Design Studies

2.1.7.2 Evaluation of Aeroservoelastic Effects on Symmetric Flutter

(Level IV Milestone)

March 31, 1998

~~These data are subject to limited exclusive rights under Government Contract No. NAO1 20220. These data may be used, duplicated, and disclosed by or on behalf of the Government for Government purposes; used, duplicated, and disclosed by or on behalf of the Contractor for its purposes within the United States; and used and duplicated (but not further disclosed) by other recipients that have been designated or approved by NASA as participants in the program of which this contract is a part for their purposes within the United States, with the express limitation that any release or disclosure for any of the foregoing purposes are to be made subject to disclosure conditions that protect and preserve its limited exclusive rights. These limited exclusive rights shall be effective for 5 years from document release date. No other disclosure and use of these data is authorized without the written permission of The Boeing Company. This Notice shall be marked on any reproduction of these data, in whole or in part.~~

Task 20 - Technical Integration

Sub Task 7: Aeroservoelastic Design Studies

Evaluation of Aeroservoelastic Effects on Symmetric Flutter

March 31, 1998

Prepared by:

K. S. Nagaraja

K.S. Nagaraja

MS 67-MH 234-0158

Prepared by:

Larry R. Felt

Larry Felt

MS 67-MH 237-7478

Prepared by:

Raymond Kraft

Raymond Kraft

MS 6H-FA 965-2015

Approved by:

Kumar G. Bhatia

Kumar G. Bhatia

MS 67-HL 965-0899

Approved by:

Steve Precup

Steve Precup

MS 67-MH 234-3171

Approved by:

Ron Pera

For
Ron Pera

MS 6H-FJ 965-0159


BOEING®

Boeing Commercial Airplane Group
Technology and Product Development
P.O. Box 3707
Center
Seattle, Washington 98124-2207

Under Contract: NAS1-20220
Prepared for: National Aeronautics and Space
Administration, Langley Research
Hampton, Virginia 23665-5225

Foreword

This document is being submitted to satisfy the deliverable "Aeroservoelastic Design Studies" for WBS 2.1.7.2 under the High Speed Research II – Airframe Technologies Contract NAS1-20220. The document reports work being performed for aeroservoelasticity (2.1.7) tasks under the Technology Integration (2.1) effort. Boeing personnel performed the analysis work reported in this document.

Acknowledgments

The Aeroservoelasticity (ASE) Working Group at Boeing-Seattle coordinated the work reported in this document. The ASE Working Group members are:

William N Boyd
Kumar G Bhatia
Chris J Borland
Raymond H Kraft
Larry R Felt
K.S. Nagaraja
Steven R Precup
Steven C Stone
Payam Rowhani
Russ D Rausch
Skip Short
Eli Livine
Edward E Meyer

William N. Boyd and Steven C Stone provided the modified DITS dynamic models and the reference open-loop flutter solutions for validation purposes.

Table of Contents

Summary	1
Introduction	4
Approach	4
Aeroelastic Models	4
Control Laws	4
Results	5
Conclusions	9
Recommendations	9
Appendix A	64
Appendix B	75
Appendix C	85

List of Figures

Figure 1- Effect of Control system gain and phase on Symmetric Flutter Speed based on Ideal Sensors at IMU location, $M=0.95$, Mass Case M02.....	2
Figure 2- Effect of Control system gain and phase on Symmetric Flutter Speed based on Real Sensors at IMU location, $M=0.95$, Mass Case M02.	3
Figures 3-9 Flutter solutions based on Sensors at IMU location, $M=0.95$, Mass Case M02	9 to 15
Figures 10-13 Flutter solutions based on Sensors near C.G. location, $M=0.95$, Mass Case M02	16 to 19
Figures 14-18 Flutter solutions based on Sensors at IMU location, $M=2.60$, Mass Case M02	20 to 24
Figures 19-22 Flutter solutions based on Sensors near C.G. location, $M=2.60$, Mass Case M02	25 to 28

Figures 23-27 Flutter solutions based on Sensors at IMU location, $M=0.95$, Mass Case MT1	29 to 33
Figures 28 -32 Flutter solutions based on Sensors at IMU location, $M=2.60$, Mass Case MT1	34 to 38
Figures 33-37 Flutter solutions based on Sensors at IMU location, $M=0.95$, Mass Case MT4	39 to 43
Figures 38-42 Flutter solutions based on Sensors at IMU location, $M=2.60$, Mass Case MT4.....	44 to 48
Figures 43-52 Root Locus solutions based ^{on} MATLAB Analysis	49 to 58
Figures 53-57 Comparison between PK and State-Space Models	59 to 63

Summary

The HSCT Flight Controls Group is developing a longitudinal control law, known as $\Gamma \cdot V$, for the NASA HSR program. Currently, this control law is based on a quasi-steady aeroelastic (QSAE) model of the vehicle. This control law was implemented into the p-k flutter analysis process for closed loop aeroservoelastic analysis. The available flexible models, developed for the TCA aeroelastic analysis, were used to assess the effect of control laws on flutter at several different Mach numbers and mass conditions.

Significant structures and flight control system interaction was observed during the initial assessment. Figures 1 and 2 present a summary of the effect of total closed loop gain and phase on flutter mechanisms, based on ideal sensors and real sensors, for Mach 0.95 and mass M02 condition. Control laws based on ideal sensors gave rise to increased coupling between the rigid body short period mode and the first symmetric elastic mode. This reduced the stability margins for the first elastic mode and does not meet the required 6 dB gain margin requirement. The effect of "real" sensors significantly increased the structures and control system interactions. This caused the elastic modes to be highly unstable throughout most of the flight envelope.

State-space models were developed for several conditions and then MATLAB program was used for the aeroservoelastic stability analysis. These results provided an independent verification of the p-k flutter analysis findings. Good overall agreement was observed between the p-k flutter analysis and state-space model results for both damping and frequency comparisons. These results are also included in this document.

The following conclusions were made during this study:

- 1) The traditional QSAE control design strategies are not applicable; control laws need to be developed based on elastic models.
- 2) The location of sensors impacts various elastic modes differently.
- 3) A MIMO design strategy may be required. This would add complexity to the design architecture and raises the challenge for robust design.
- 4) The aeroservoelastic analysis using p-k and state-space formulations provided almost identical results.
- 5) The p-k based flutter analysis and state-space formulation analysis methods should be used concurrently for design and verification.

[B]: /acct/ksn8042/ASE/M95/M02/b595t5a6bgv2.esb
 [C]: /acct/ksn8042/ASE/M95/M02/b595t5a6bpv1.esb
 [D]: /acct/ksn8042/ASE/M95/M02/b595t5a6cpv6.esb
 [E]: /acct/ksn8042/ASE/PLOTS/GV/gvmach95.esb

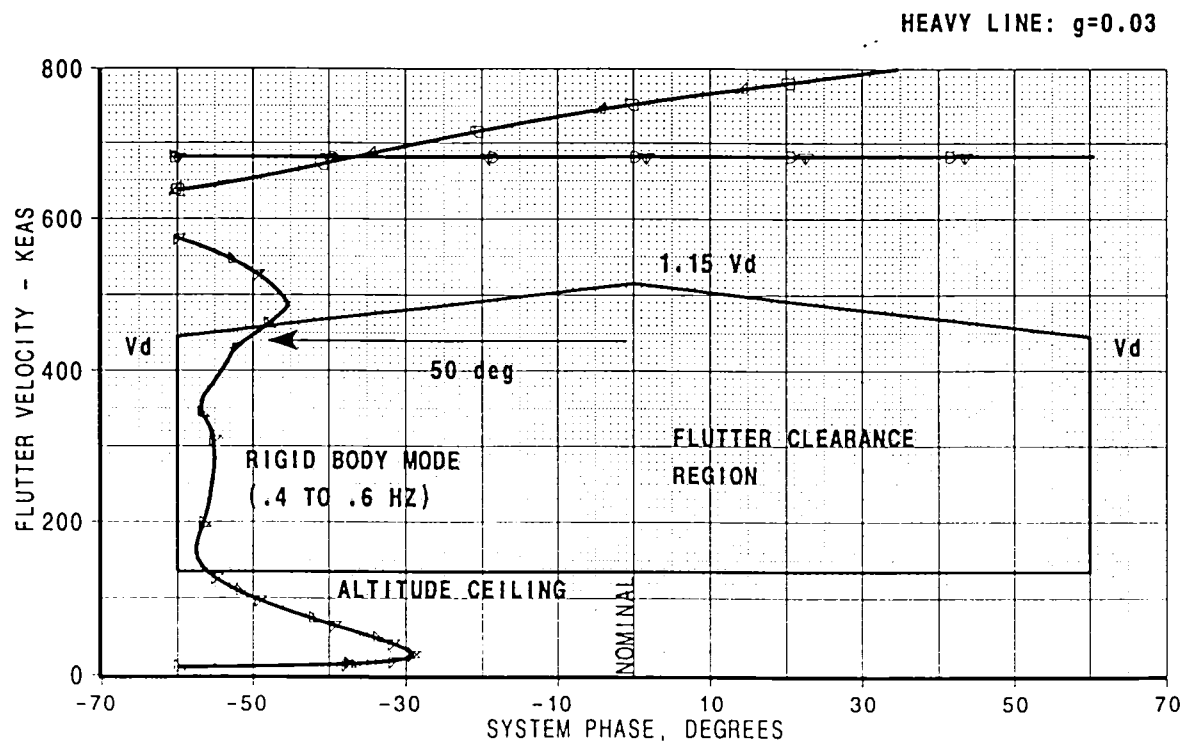
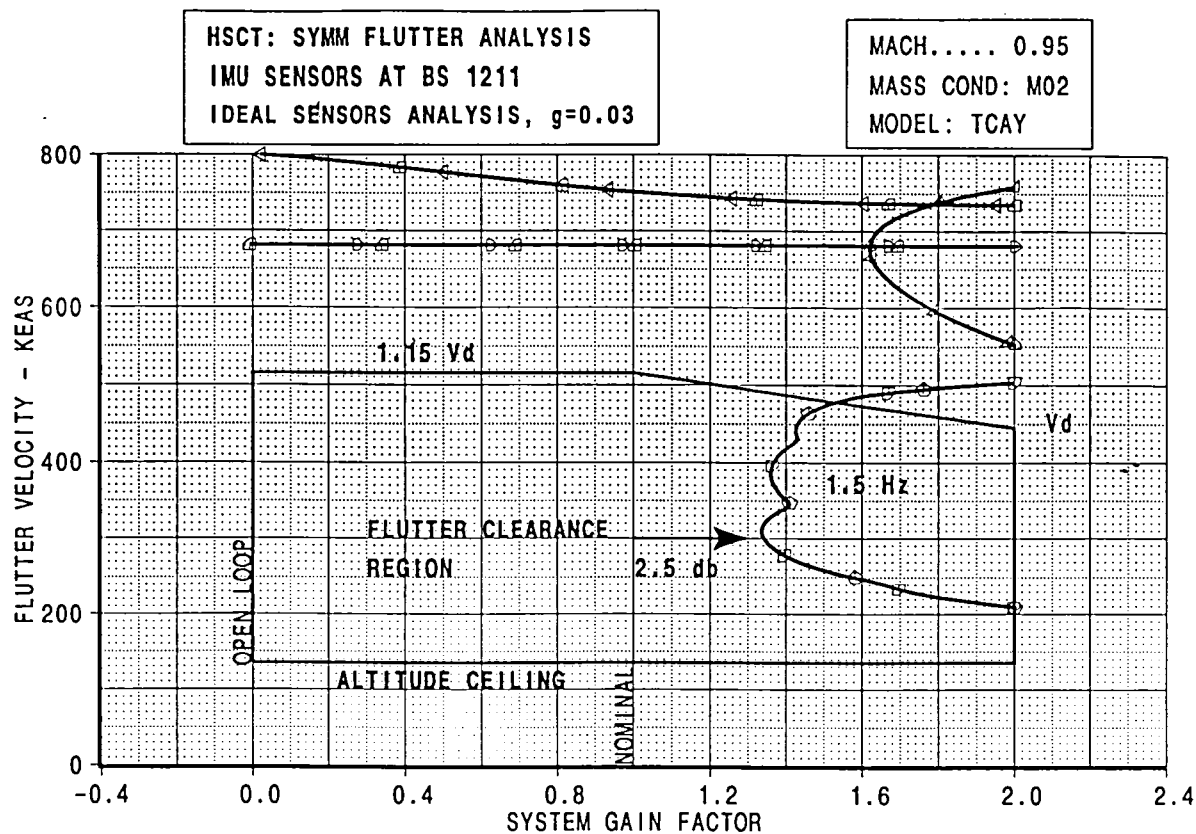
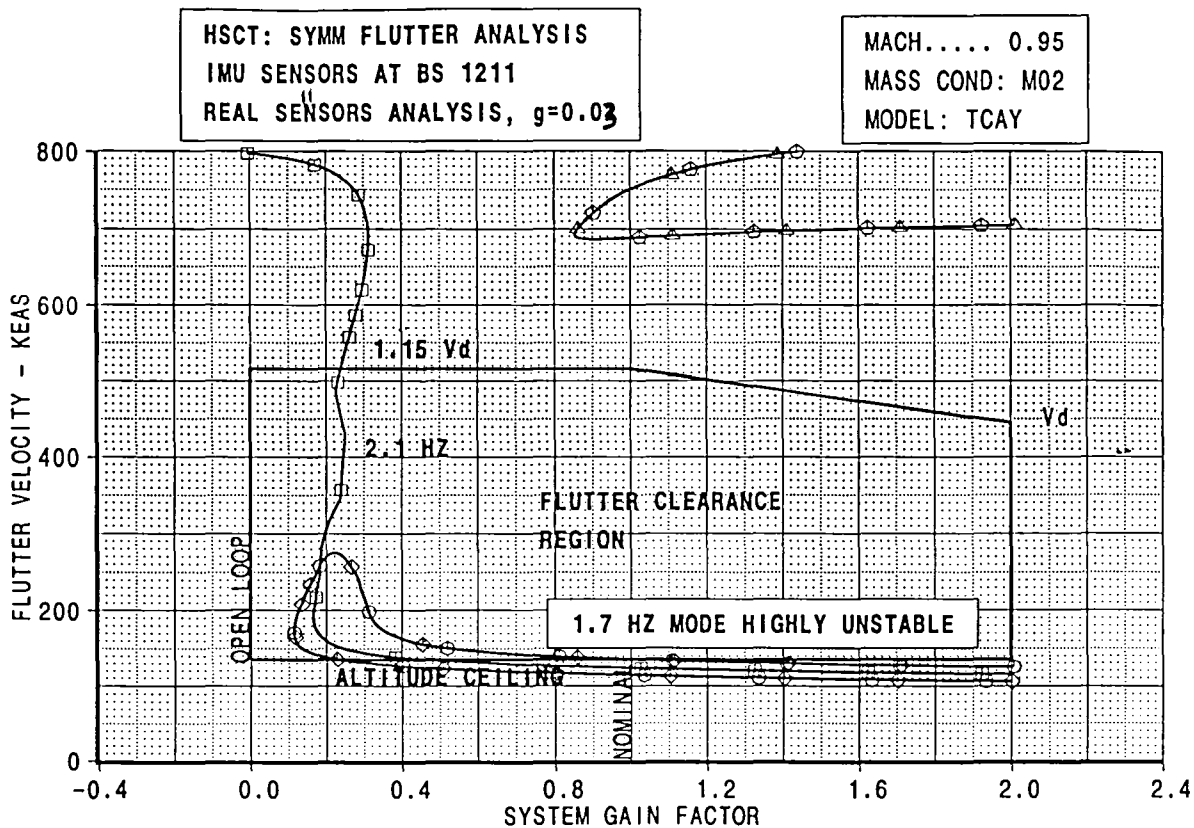


Figure 1 : Effect of Control system gain and phase on Symmetric Flutter speed based on Ideal sensors at IMU location, $M=0.95$, Mass Case M02

CALC	K.S.NAGARAJA	26Mar98	REVISED	DATE	CONTROL SYSTEM EFFECTS STRENGTH+FLUTTER SIZED AIRPLANE DITS MODEL TCAY BOEING	HSCT
CHECK						
APPD.						
APPD.						PAGE 2

1) : /acct/ksn8042/ASE/PLOTS/GV/gvmach95.esb
 [B] : /acct/ksn8042/ASE/M95/b595t5a2gv1.esb
 [C] : /acct/ksn8042/ASE/M95/b595t5a2pv1.esb



HEAVY LINE: g=0.03

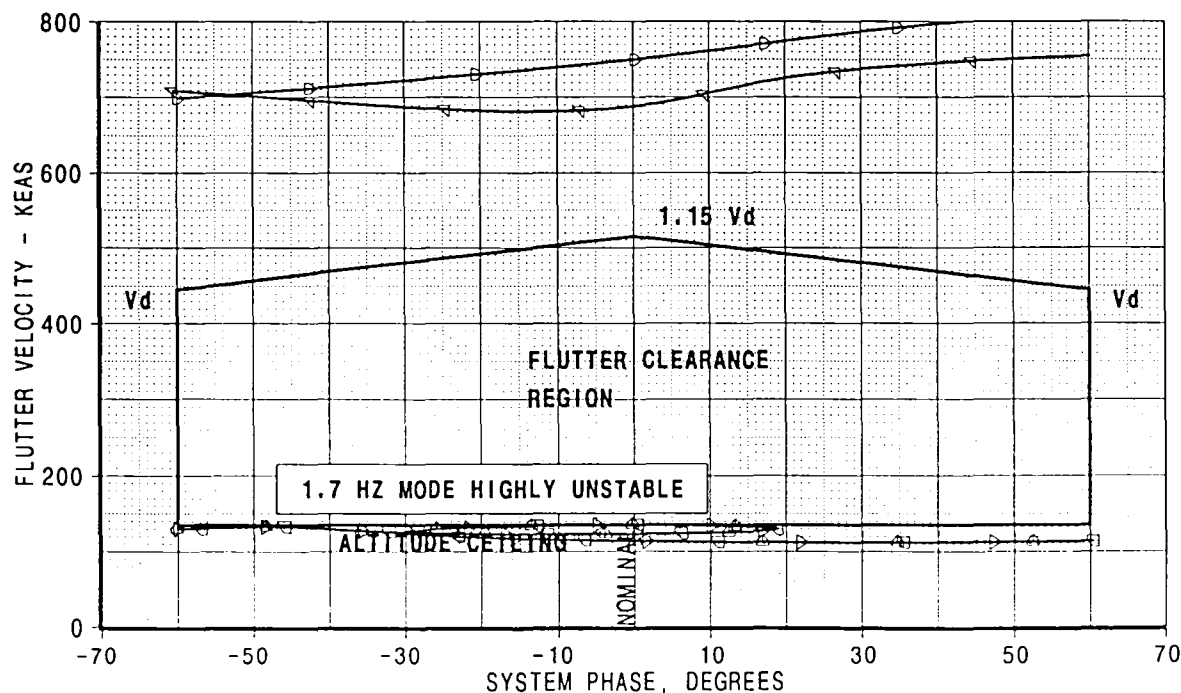


Figure 2: Effect of control system gain and phase on symmetric Flutter speed based on Real sensors at IMU Location, M=0.95, Mass Case M02

CALC	K.S.NAGARAJA	26Mar98	REVISED	DATE	CONTROL SYSTEM EFFECTS STRENGTH+FLUTTER SIZED AIRPLANE DITS MODEL TCAY BOEING	HSCT
CHECK						
APPD.						
APPD.						PAGE 3

Introduction

This report presents work performed by The Boeing Company to satisfy the deliverable "Evaluation of aeroservoelastic Effects on Symmetric Flutter" for Subtask 7 of Reference 1. The objective of this report is to incorporate the improved methods for studying the effects of a closed loop control system on the aeroservoelastic behavior of the airplane planned under NASA HSR technical Integration Task 20 work. Also, a preliminary evaluation of the existing pitch control laws on symmetric flutter of the TCA configuration was addressed. The goal is to develop an improved modeling methodology and perform design studies that account for the aero-structures-systems interaction effects.

Approach

Aeroelastic Models

Aeroelastic models developed for the TCA aeroelastic analysis, discussed in Reference 2, were considered for this study. Appendix A summarizes the analytical approach used for the control law assessment study. It presents the analysis process, Elfini FEM based dynamics models and aerodynamic mesh for the subsonic and supersonic linear aerodynamics. The dynamic math model utilized 60 flexible modes, 3 symmetric rigid body modes, and two assumed degrees of freedom for the stabilizer and elevator rotation modes required for control system closed loop representation. The mass cases considered for the study and the required flutter clearance speed envelope (V_d / M_d and $1.15 V_d / M_d$) are also provided in the Appendix A. The elastic models and the linear unsteady aerodynamic theories used for the aeroelastic analysis are discussed in Reference 2. The strength and flutter sized stiffness designed model (identified as TCAY) was used to assess the effect of control laws on flutter at several Mach numbers and mass conditions.

Control Laws

The HSCT Flight Controls Group is developing a longitudinal control law, known as $\Gamma\dot{V}$, for the NASA HSR program. Currently, this control law is based on a quasi-steady aeroelastic (QSAE) model of the vehicle. The Controller has an inner loop (SAS system), an outer loop (control path) and a feed forward direct control path. The command inputs to the stabilizer and elevator actuators are functions of flight path angle, angle of attack, pitch attitude, and pitch rate measured at the IMU location (BS1211). The various gains in the control law are schedule to be functions of dynamic pressure. The control law was transformed into inertial reference axis before implementation into the p-k flutter analysis. Also, the analysis utilized a simplified third order actuator model at the present time. The Apex based p-k flutter equations of

motion from Reference 3, simplified control law, sensor equations, and the actuator model used for the closed loop flutter analysis are summarized in Appendix A. The details of the longitudinal control law are presented in Appendix B.

Results

Flutter Analysis based on Apex p-k Solution Process:

Matched point flutter analyses were performed, for Mach numbers .95 and 2.6 and mass conditions M02, MT1, and MT4, to get a better assessment of the effect of longitudinal control law on flutter stability. Significant interaction between the structural modes and control system was observed in the low frequency range of up to 5 Hz. Initial assessment was focused on this frequency range and the results are summarized below.

Mach 0.95, Mass case M02:

Open loop analysis: Figure 3 shows that all the aeroelastic modes are stable in the speed range of interest.

Closed loop analysis based on ideal sensors (Mean axis feedback): This assumes that the sensors at the IMU location respond to rigid body motion of the airplane and do not respond to the elastic motion of the structure during the oscillations. Figure 4 shows the flutter solution that includes the effect of the control system for the nominal gain of the control law. The results show that there is increased coupling between the rigid body short period mode and the first elastic structural mode (1.45 Hz). This increased coupling contributed to the marginally unstable behavior of the first elastic mode. This does not meet the Vd flutter clearance requirement for zero structural damping. Figure 5 shows the flutter mode shape for this flutter mechanism. This exhibits significant elastic motion of the outboard nacelle and the wing combined with aft body vertical bending motion. Figure 6 shows the control system gain and phase variation effects on flutter speed, with a structural damping value of 0.03, and the gain and phase margins for the critical modes. These results show that the aeroservoelastic system does not meet the required 6 dB gain margin for the 1.45 Hz elastic flutter mode.

Closed loop analysis based on real sensors (Full structural feed back analysis): This analysis accounts for the real structural deformation feed back during the oscillations. Figure 7 shows the flutter solution for this situation and the control laws caused the 1.7 Hz flutter mode to become highly unstable in the speed range of interest. Figure 8 shows the flutter mode shape for this flutter mechanism and again exhibits significant elastic motion of the outboard nacelle and the wing combined with the whole body flexing of the airplane. Figure 9 shows the effect of system gain and phase variation effect on flutter speed. The

flutter mechanism is highly unstable and a significant level of gain attenuation is required to stabilize the flutter mode at this frequency either by reducing the system gain or by using a deep notch filter. This would result in a significant penalty on airplane performance. The IMU pitch rate feed back of the stability augmentation system was identified as the main cause for the increased structural / system interaction. An effort was made to study the effect of sensor location on the aeroservoelastic stability. Figures 10 - 13 show the effect on flutter speed based on sensors located near C.G. of the airplane. The results based on ideal sensors still exhibit low unstable damping for the 1.45 Hz mode. Also, the results based on real sensors (full structural feed back) show a different flutter mechanism (3.6 Hz) that is again highly unstable and does not meet 6 dB gain and 60 degree phase margin flutter requirements.

Mach 2.60, Mass case M02:

Open loop analysis: Figure 14 shows that all the aeroelastic modes are stable in the speed range of interest.

Closed loop analysis based on ideal sensors: Figure 15 shows a marginally unstable 1.6 Hz mode. This does not meet the Vd flutter clearance requirement for zero structural damping. However, Figure 16 show that the flutter mechanism exhibits adequate gain and phase margin with structural damping of 0.03.

Closed loop analysis based on real sensors: Figures 17 and 18 show flutter characteristics similar to Mach 0.95 solution discussed above and the results do not meet flutter clearance requirements. Again, the effect of sensor location (near C.G.) on flutter characteristics was examined and the results shown in Figures 19 through 22 demonstrate flutter characteristics very similar to the Mach 0.95 solution.

Mach 0.95,2.60 for Mass cases MT1 and MT4:

Figures 23 to 42 show the flutter analysis results for Mach numbers 0.95 and 2.60 and Mass cases MT1 and MT4. These results include the open loop solution, closed loop results including gain and phase variations based on mean axis analysis (ideal sensors), and full structural feed backs (real sensors). The results show the flutter characteristics to be very similar to the cases discussed above.

Stability Analysis based on State-Space Formulation Process:

The above aero-structures-systems interaction effects were independently validated by developing state-space models for several Mach / Mass conditions. The methodology used for this process is described in Appendix C. The analysis utilized 60 flexible modes, two rigid body modes, and two assumed stabilizer rotation and elevator rotation modes. Also, a sensitivity analysis, for number of

aerodynamic lag terms varying from 4 to 8, was performed. For comparison of results with p-k flutter analysis results it was decided to use 8 lag terms in the state-space formulation process. The stability analyses were performed for each of the models at various flight speed conditions using MATLAB program.

Figures 43 through 46 present the open loop root locus match point stability solution results for M02 and MT1 mass cases at Mach numbers 0.95 and 2.60. These results show that the aeroelastic modes are stable at all speeds considered in the 1.15 Vd envelop thereby validating the p-k open loop flutter solutions discussed earlier.

Figures 47 and 48 present the mean axis root locus match point stability solution results (ideal sensors) for M02 and MT1 mass cases at Mach numbers 0.95. The results show that the low frequency elastic mode is marginally unstable for nominal system gain predicting characteristics similar to the p-k flutter analysis results.

Figures 49 through 52 presents the root locus match point stability solution results based on full structural feed backs (real sensors) for the above mass case / Mach number combinations. The low frequency flutter mechanism exhibit high instability as predicted by the p-k flutter analysis process. In addition, there are additional high frequency mechanisms (8.0 to 9.5 Hz) that are highly unstable. Further work is needed to understand these high frequency flutter mechanisms.

Comparison of P-K Flutter and State-Space Model Analyses Results:

Mach 0.95 and 2.60 with mass case M02 conditions were considered for quantitative comparison of the stability analyses results of the two processes considered above. This was done by transforming the state-space model results into the frequency / damping format for comparison with p-k frequency / damping results. Figures 53 and 54 present the match point open loop comparison between the two sets for Mach numbers 0.95 and 2.60 respectively for M02 mass case. The results show good comparison of frequency between the two processes and acceptable level of damping comparison.

Figure 55 show similar results for the mean axis closed loop analysis for the mass / Mach combination case M02 / 0.95. Both the processes predicted similar level of low damping instability for the 1.45 Hz elastic mode. However, there is a significant difference in the short period mode frequency at higher speeds between the two methods. Further investigation would be done to understand this difference.

Figures 56 and 57 show results of comparison based on real sensors (full structural feed backs) analysis. The results show good comparison of frequencies between the two processes and acceptable level of comparison for

stable modal damping values. Also, the highly unstable damping value comparison between the two methods, for the low frequency mode 1.45 Hz, is considered to be good.

Conclusions

This aeroservoelastic investigation has demonstrated the following:

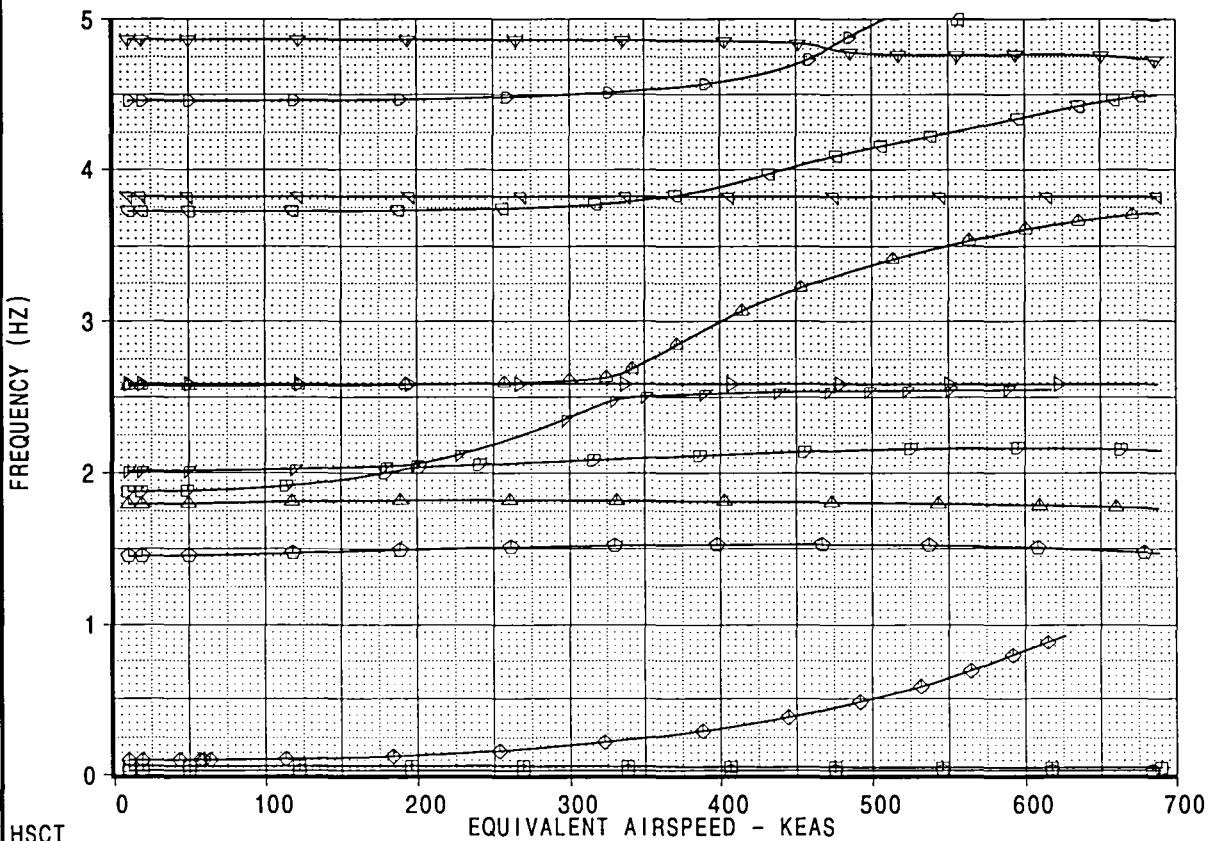
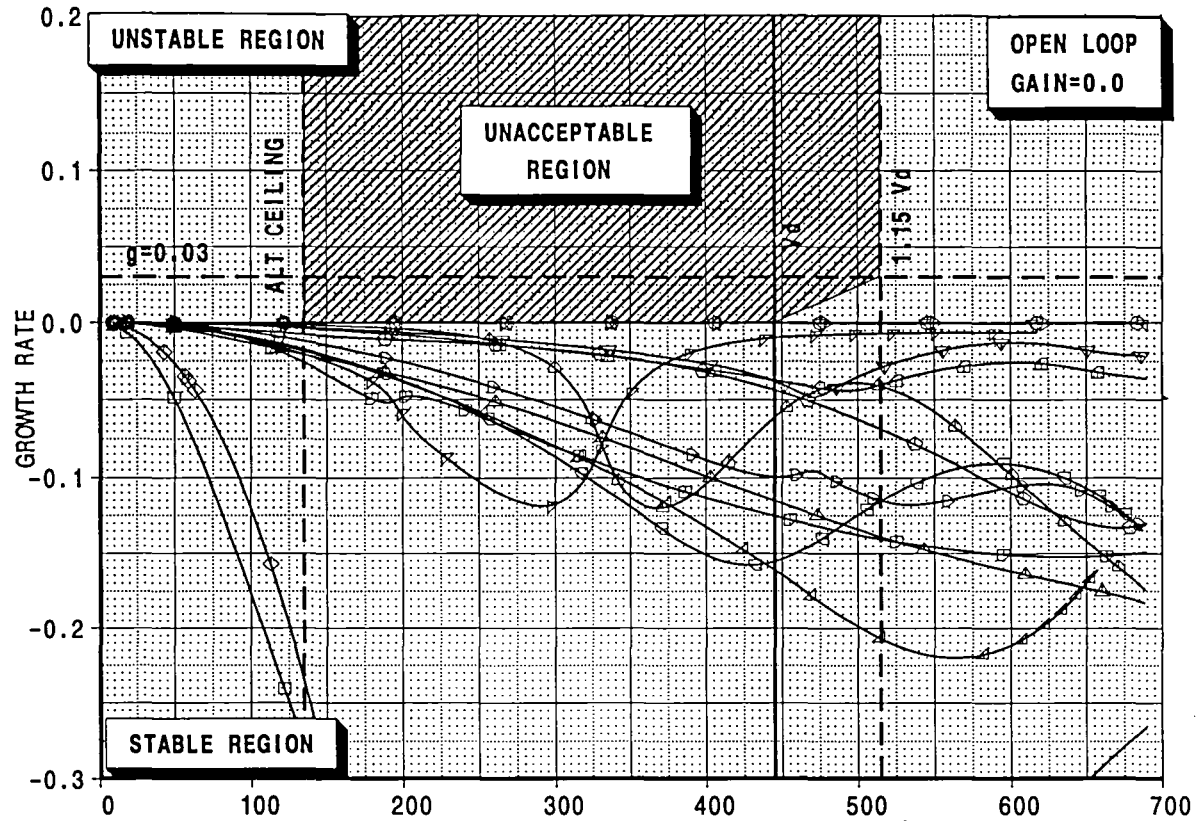
- 1) The QSAE based longitudinal $\gamma\dot{V}$ control law drastically violates the flutter stability requirements through most of the flight envelope.
- 2) Traditional QSAE control design strategies are not applicable.
- 3) Control laws need to be developed based on flexible dynamic models.
- 4) The location of sensors impact various elastic modes differently.
- 5) The aeroservoelastic analysis using p-k and state-space formulations provided almost identical results.
- 6) The p-k based flutter analysis method and state-space formulation analysis method should be used concurrently for design.
- 7) Early aeroservoelastic analysis for ASE wind tunnel model is required for defining control laws, and may impact wind tunnel model design.

Recommendations

- 1) Assess the effect of flexibility on other control laws such as flare, ride qualities and lateral/directional control.
- 2) Incorporate Long Beach P-transform state-space modeling approach into the Flight Controls / Structures tool suite.

HSCT MODEL TCAY, SYMMETRIC FLUTTER ANALYSIS, M=0.95
GAMMA-DOT V CONTROLLER, MASS:M02

- mode001
- mode002
- ◇ mode003
- △ mode004
- ▽ mode005
- ▽ mode006
- ▽ mode007
- △ mode008
- ▷ mode009
- ▽ mode010
- ▽ mode011
- ▷ mode012
- ▽ mode013
- △ mode014
- △ mode015



[A]: /acct/ksn8042/ASE/PLOTS/VGPLOTS/mach95.esb
[B]: /acct/ksn8042/ASE/M95/M02/DOC/b595t5a6b1C0.esb

HSCT

EQUIVALENT AIRSPEED - KEAS

CALC	K.S.NAGARAJA	26Mar98	REVISED	DATE
CHECK				
APPD.				
APPD.				
PLOT				

CONTROL SYSTEM EFFECTS
STRENGTH+FLUTTER SIZED AIRPLANE
DITS MODEL TCAY

BOEING

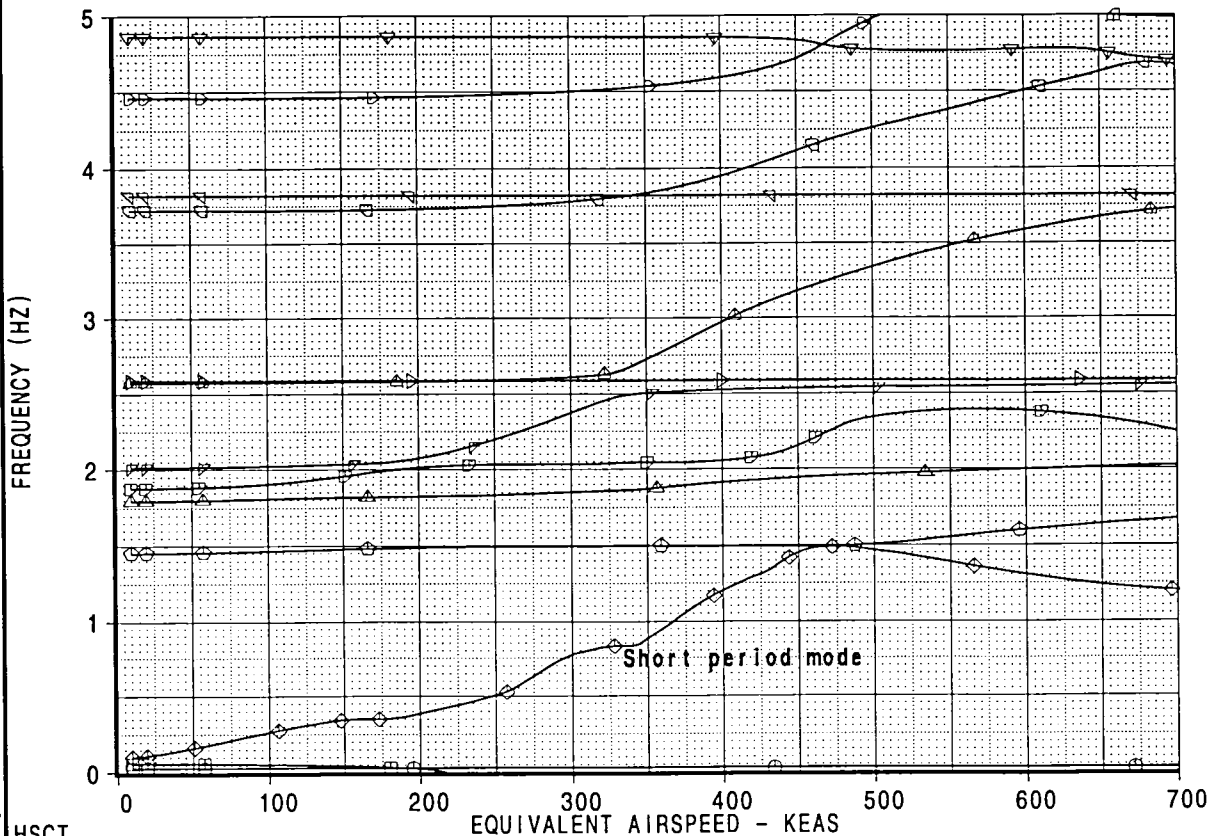
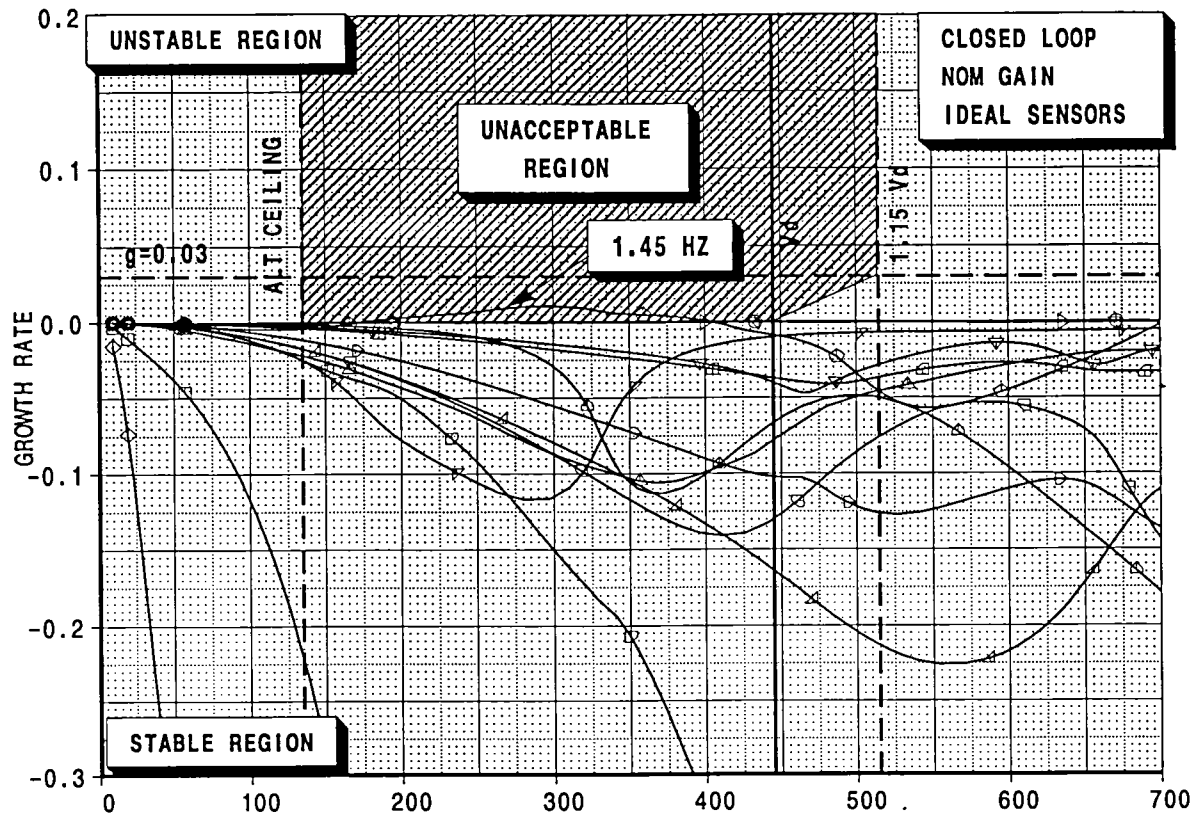
HSCT

FIGURE 3

PAGE

9

HSCT MODEL TCAY, SYMMETRIC FLUTTER ANALYSIS, M=0.95
GAMMA-DOT V CONTROLLER, MASS:M02



[A]: /acct/ksn8042/ASE/PLOTS/VGPLOTS/mach95.esb
[B]: /acct/ksn8042/ASE/M95/M02/DOC/b595t5a6aC1.esb

HSCT

CALC	K.S.NAGARAJA	26Mar98	REVISED	DATE
CHECK				
APPD.				
APPD.				
PLOT				

CONTROL SYSTEM EFFECTS
STRENGTH+FLUTTER SIZED AIRPLANE
DITS MODEL TCAY

BOEING

- mode001
- mode002
- ◇ mode003
- △ mode004
- ▽ mode005
- ◇ mode006
- ▽ mode007
- △ mode008
- ◇ mode009
- ▽ mode010
- ◇ mode011
- ▽ mode012
- △ mode013
- ◇ mode014
- ▽ mode015

HSCT

FIGURE 4

PAGE 10

Task 20 - Sub Task 7 - Aeroservoelastic Design Studies



Boeing, Seattle

High Speed Civil Transport

TCAV Closed Loop Symmetric Flutter Modeshape (Mean Axis Feedbacks)

1.45 Hz. - Mass MO2 - Mach 0.95

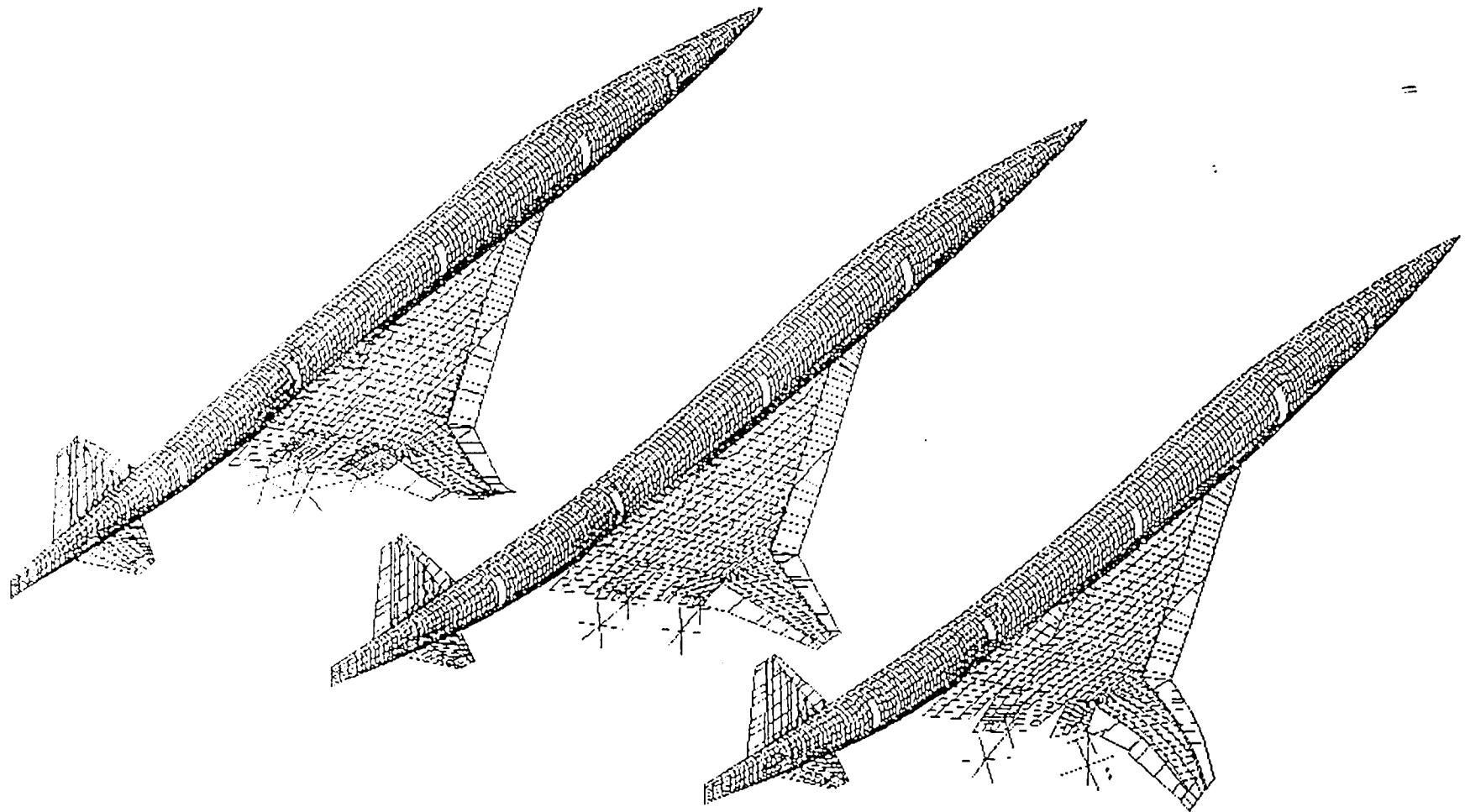
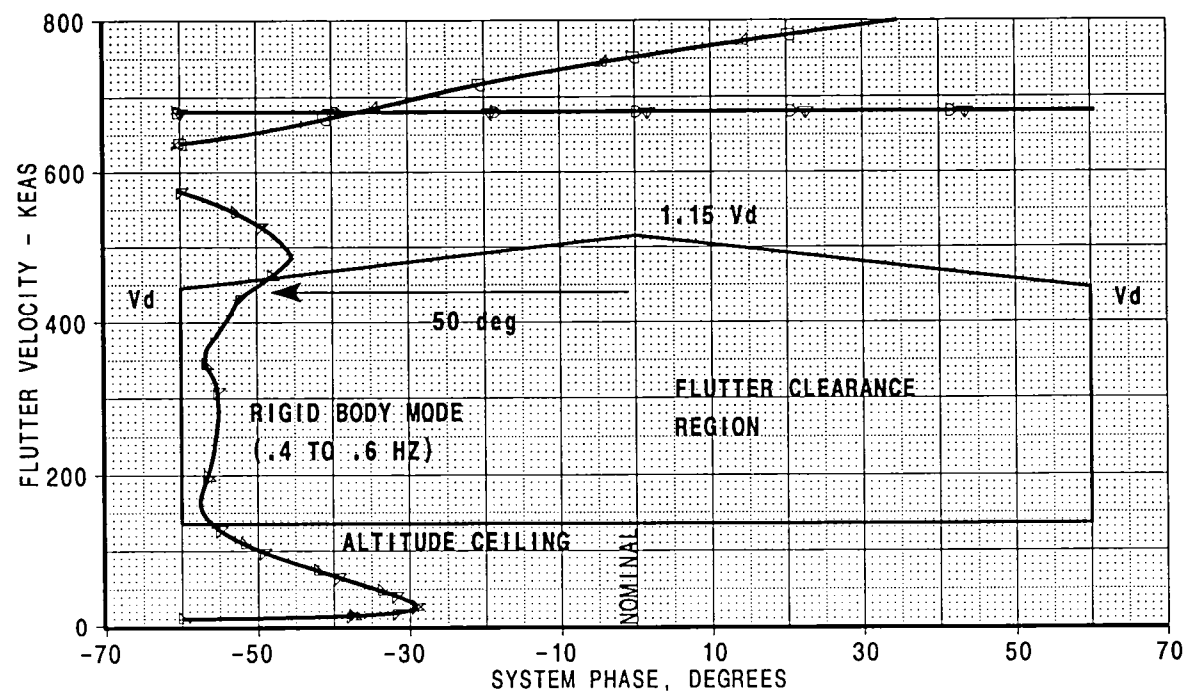
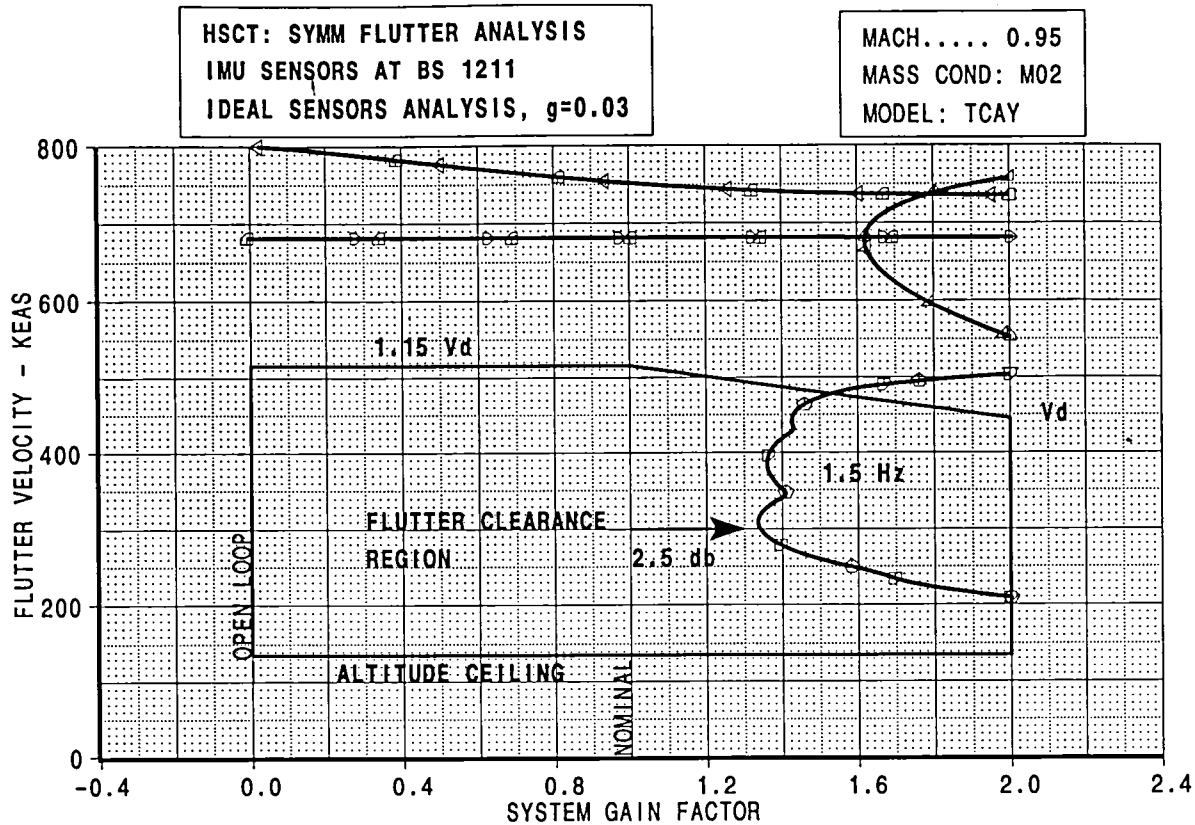


FIGURE 5

11

~~NOTICE - Limited Exclusive Right to Use~~

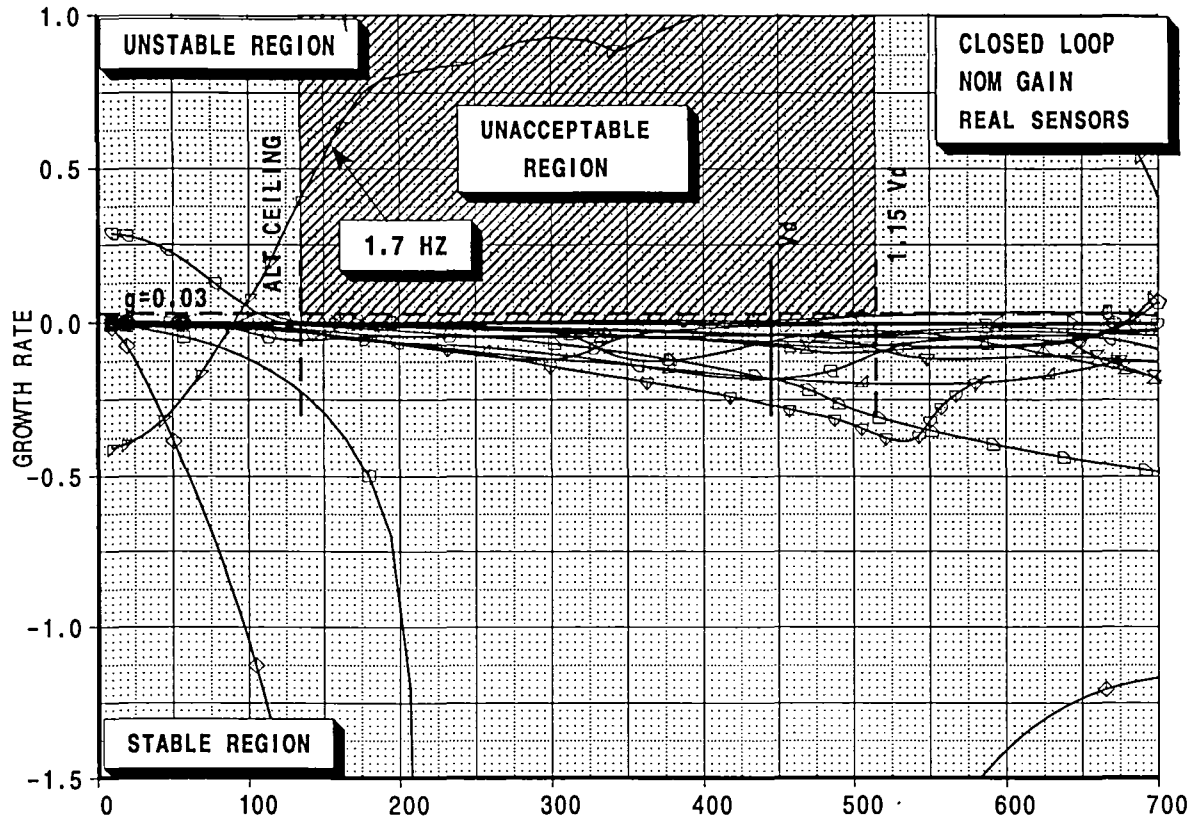
~~This information is sensitive. It is subject to export control restrictions. No export of this information is permitted without prior approval of the Department of Defense. No. NASC-20000~~



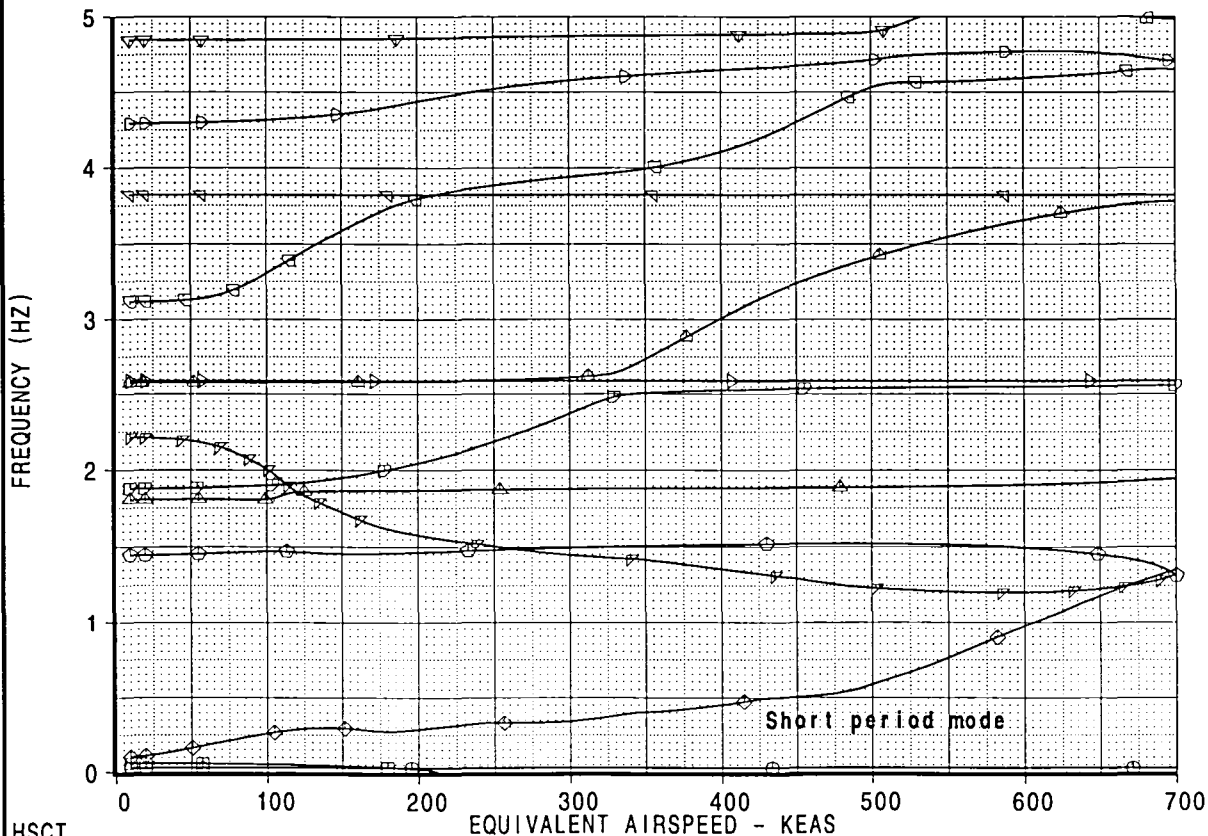
[B]: /acct/ksn8042/ASE/M95/M02/b595t5a6bgv2.esb
[C]: /acct/ksn8042/ASE/M95/M02/b595t5a6bpv1.esb
[D]: /acct/ksn8042/ASE/M95/M02/b595t5a6cpv6.esb
[E]: /acct/ksn8042/ASE/PLOTS/GV/gvmach95.esb

CALC	K.S.NAGARAJA	26Mar98	REVISED	DATE	CONTROL SYSTEM EFFECTS STRENGTH+FLUTTER SIZED AIRPLANE DITS MODEL TCAY BOEING	HSCT
CHECK						FIGURE 6
APPD.						PAGE
APPD.						12

HSCT MODEL TCAY, SYMMETRIC FLUTTER ANALYSIS, M=0.95
GAMMA-DOT V CONTROLLER, MASS:M02



- mode001
- mode002
- ◇ mode003
- ◇ mode004
- △ mode005
- ▽ mode006
- ▽ mode007
- △ mode008
- ▷ mode009
- ▽ mode010
- ▽ mode011
- ▷ mode012
- ▽ mode013
- △ mode014
- △ mode015
- ▽ mode016
- △ mode017
- ▷ mode018
- ▷ mode019
- ◇ mode020
- ◇ mode021
- + mode022
- × mode023
- mode024



[A]: /acct/ksn8042/ASE/PLOTS/VG/PLOTS/mach95.esb
[B]: /acct/ksn8042/ASE/M95/M02/DOC/b59515a6bC1.esb

HSCT	CALC	K.S.NAGARAJA	26Mar98	REVISED	DATE	CONTROL SYSTEM EFFECTS STRENGTH+FLUTTER SIZED AIRPLANE DITS MODEL TCAY BOEING	HSCT
	CHECK						FIGURE 7
	APPD.						PAGE
	APPD.						13
	PLOT						

Task 20 - Sub Task 7 - Aeroservoelastic Design Studies



Boeing, Seattle

High Speed Civil Transport

TCAV Closed Loop Symmetric Flutter Modeshape (Full Feedbacks)

1.70 Hz. - Mass MO2 - Mach 0.95

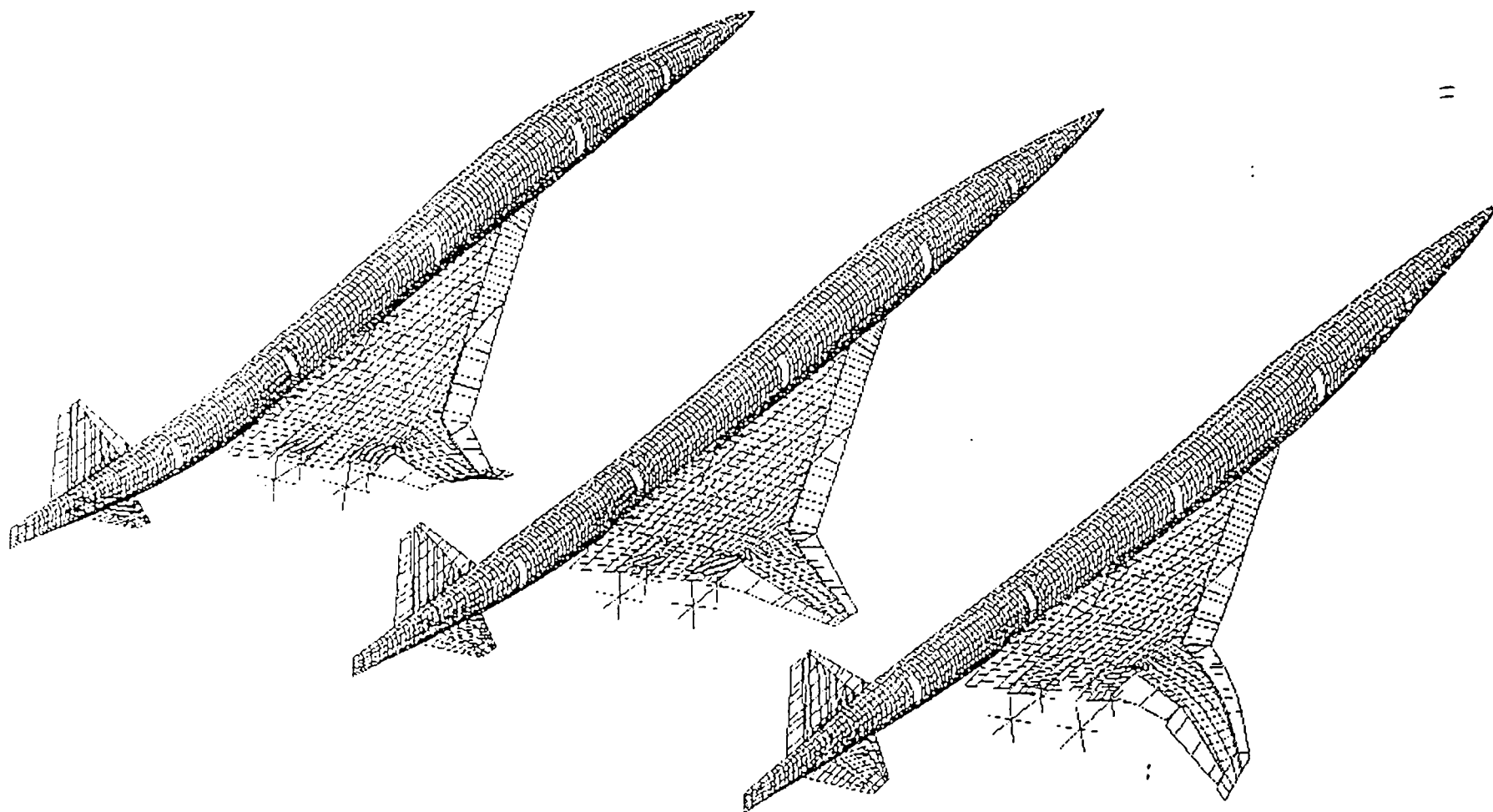
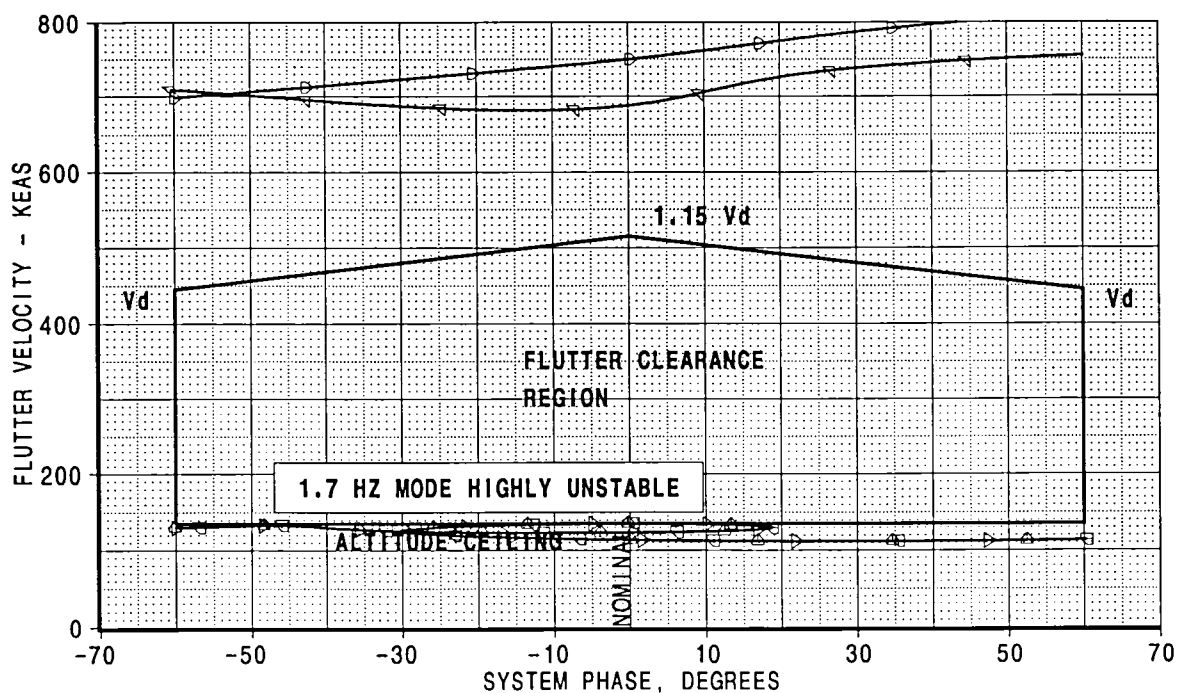
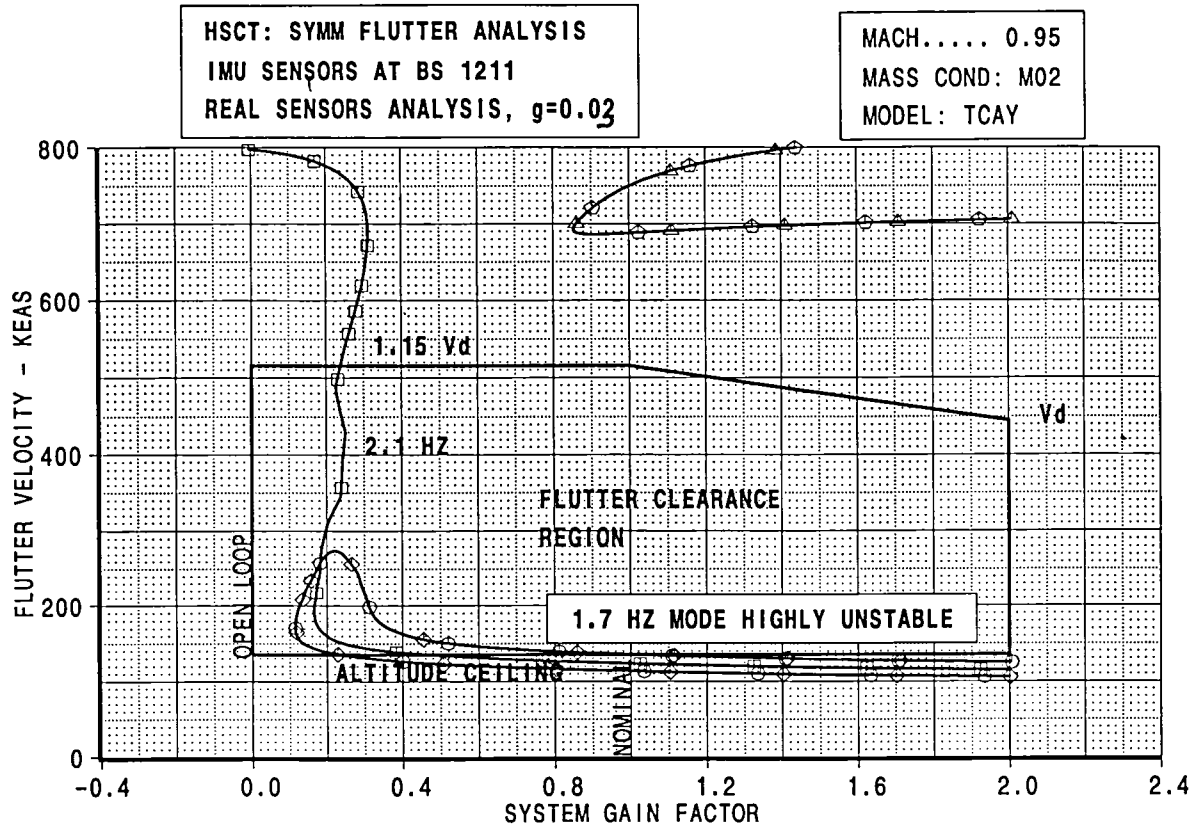


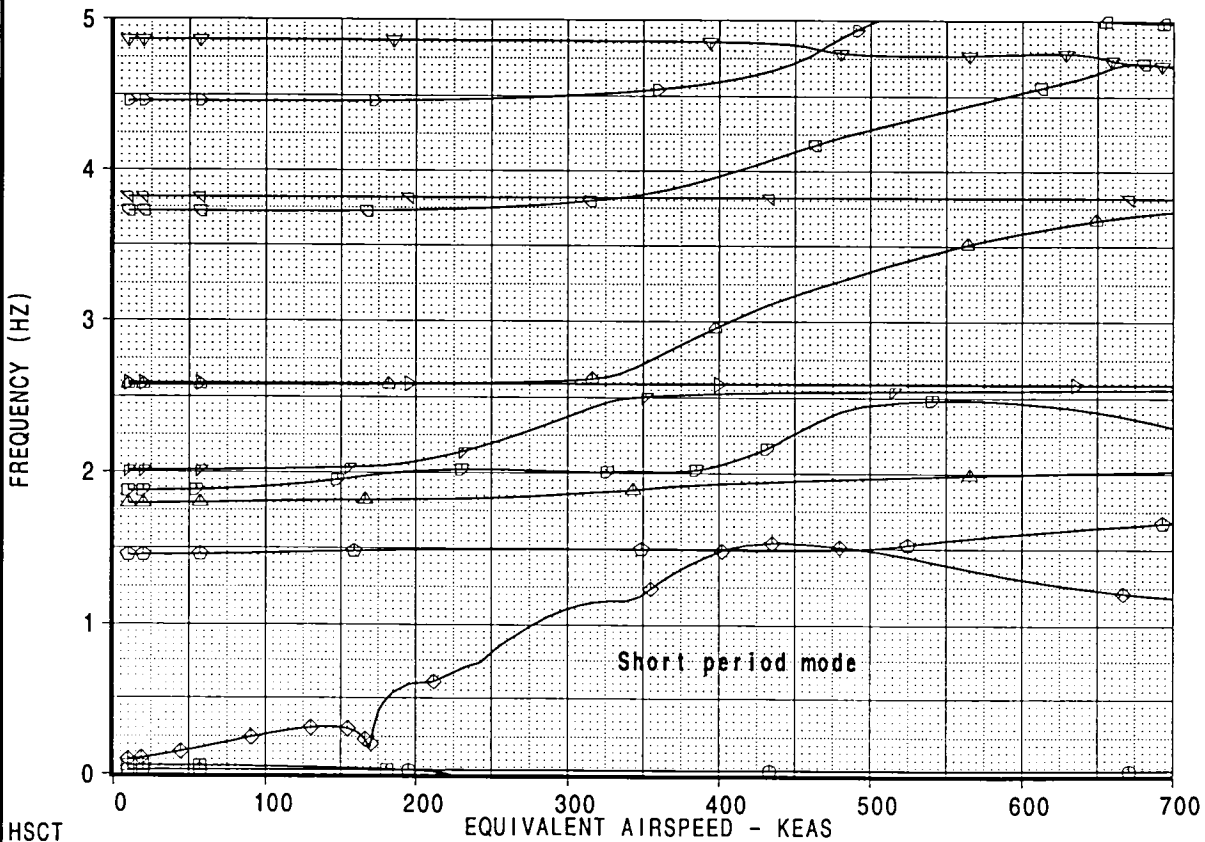
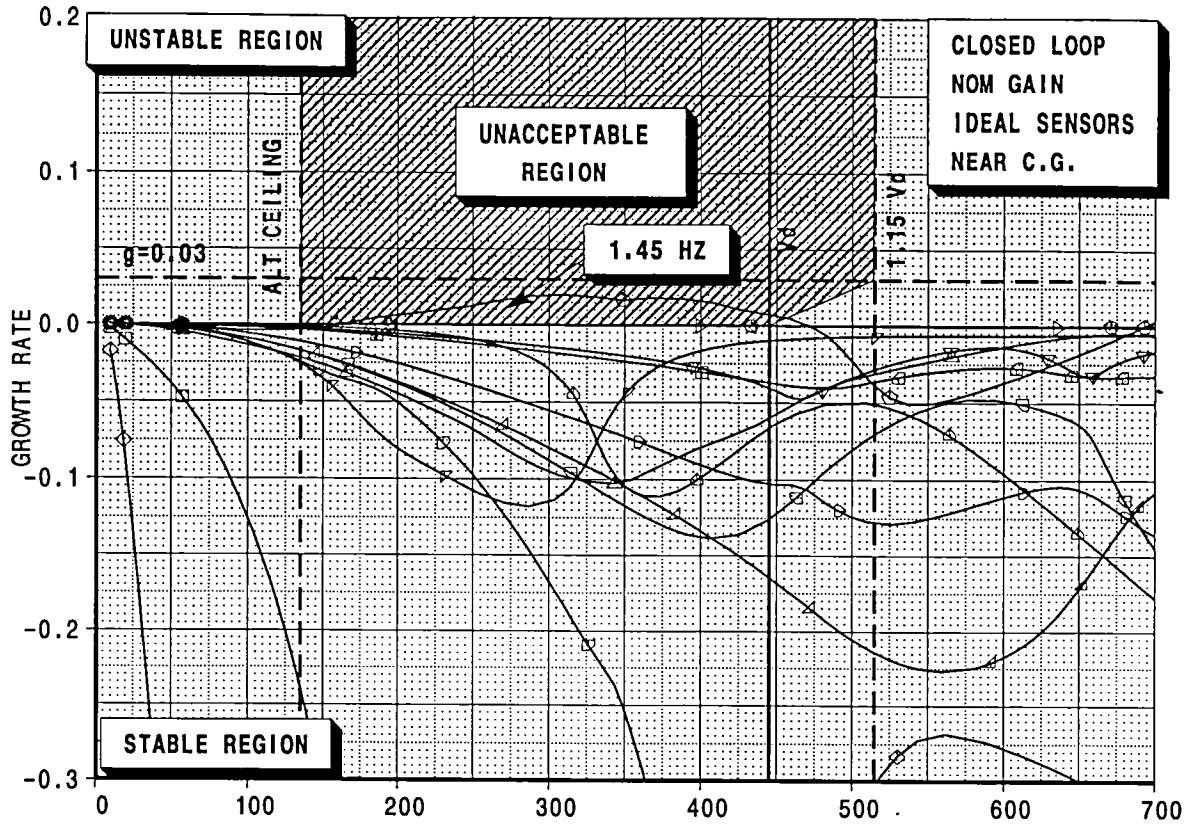
FIGURE 8

[A]: /acct/ksn8042/ASE/PLOTS/GV/gvmach95.esb
 [B]: /acct/ksn8042/ASE/M95/b595t5a2gv1.esb
 [C]: /acct/ksn8042/ASE/M95/b595t5a2pv1.esb



CALC	K.S.NAGARAJA	26Mar98	REVISED	DATE	CONTROL SYSTEM EFFECTS STRENGTH+FLUTTER SIZED AIRPLANE DITS MODEL TCAY BOEING	HSCT
CHECK						FIGURE 9
APPD.						PAGE 15
APPD.						

HSCT MODEL TCAY, SYMMETRIC FLUTTER ANALYSIS, M=0.95
GAMMA-DOT V CONTROLLER, MASS:M02



[A]: /acct/ksn8042/ASE/PLOTS/VGPLOTS/mach95.esb
[B]: /acct/ksn8042/ASE/M02/DOC/b59515a6d01.esb

HSCT

CALC	K.S.NAGARAJA	26Mar98	REVISED	DATE
CHECK				
APPD.				
APPD.				
PLOT				

CONTROL SYSTEM EFFECTS
STRENGTH+FLUTTER SIZED AIRPLANE
DITS MODEL TCAY

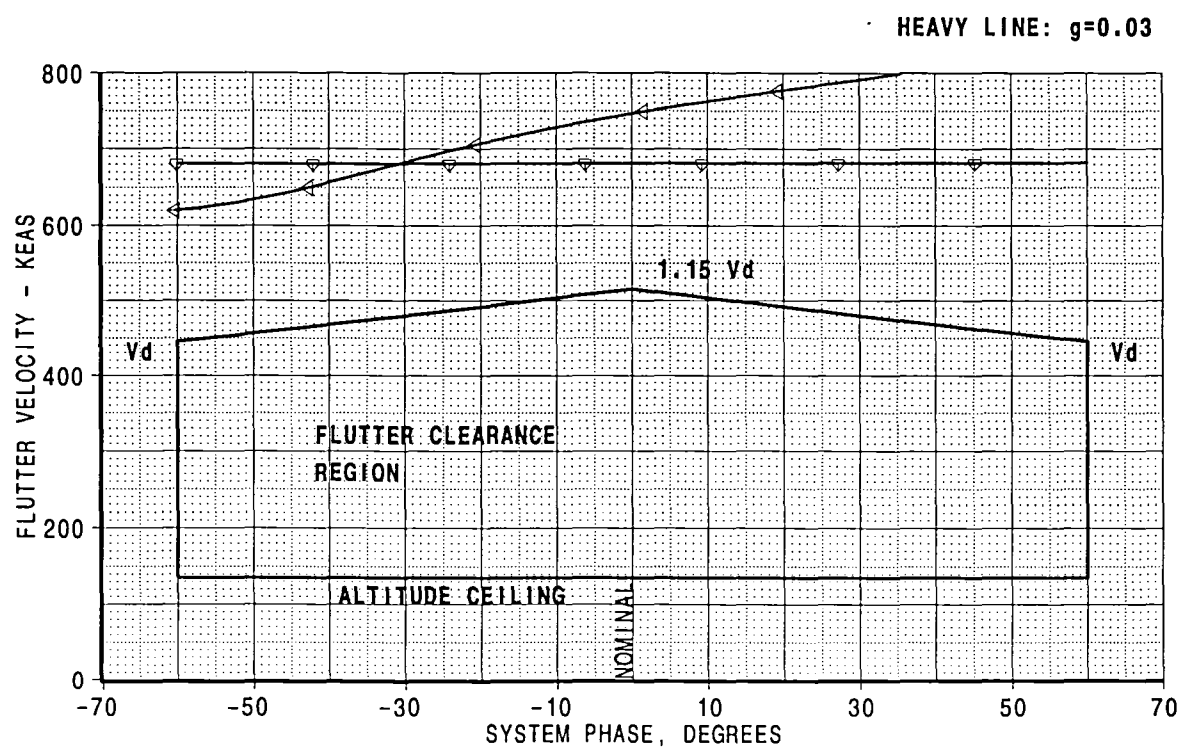
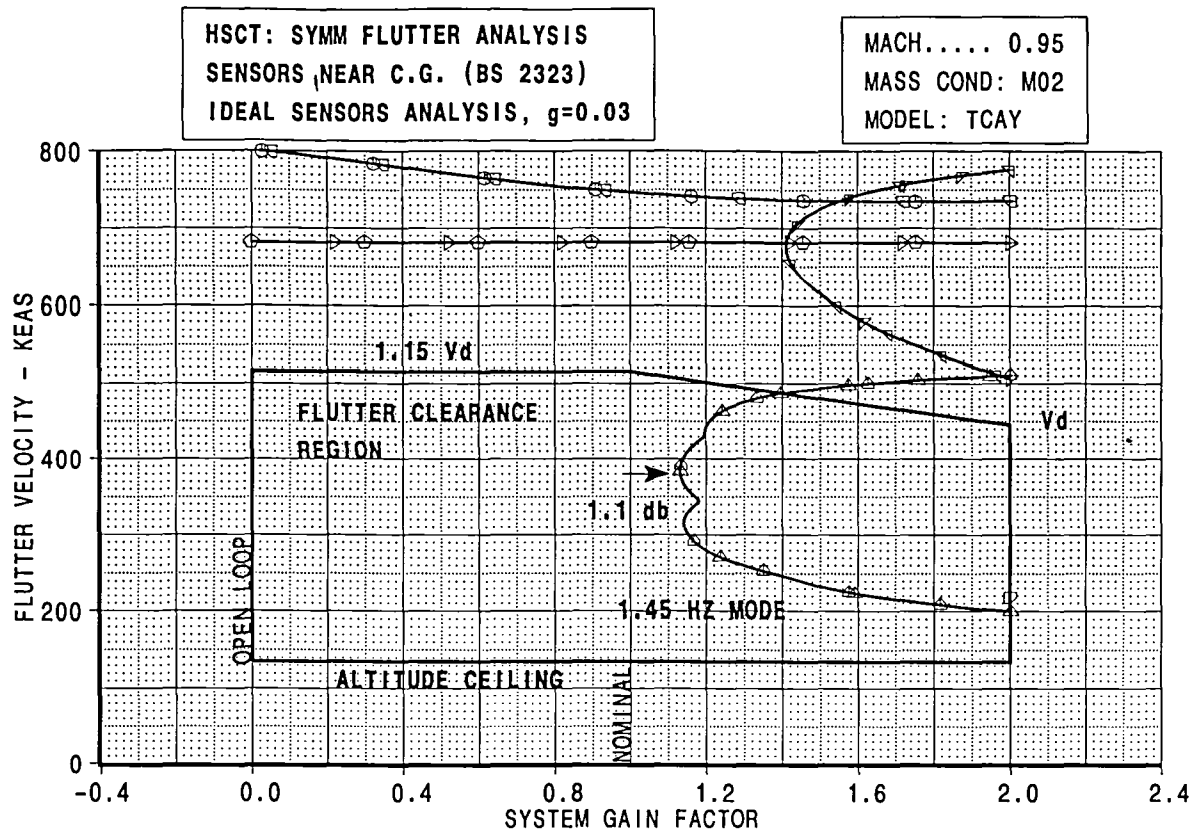
BOEING

HSCT

FIGURE 11

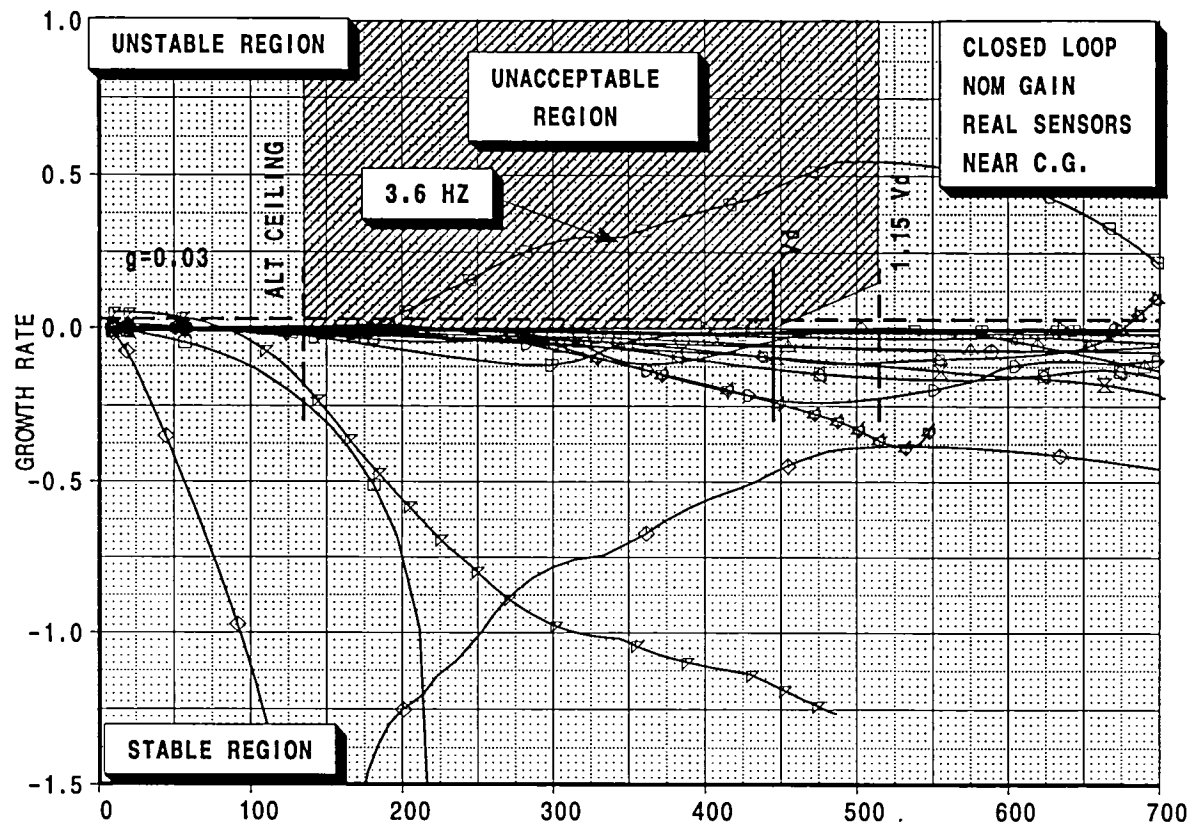
PAGE 16

[A]: /acct/ksn8042/ASE/PLOTS/GV/gvmach95.esb
 3]: /acct/ksn8042/ASE/M95/M02/DOC/b595t5a6dgv1.esb
 [C]: /acct/ksn8042/ASE/M95/M02/DOC/b595t5a6dgv2.esb
 [D]: /acct/ksn8042/ASE/M95/M02/DOC/b595t5a6dpv1.esb

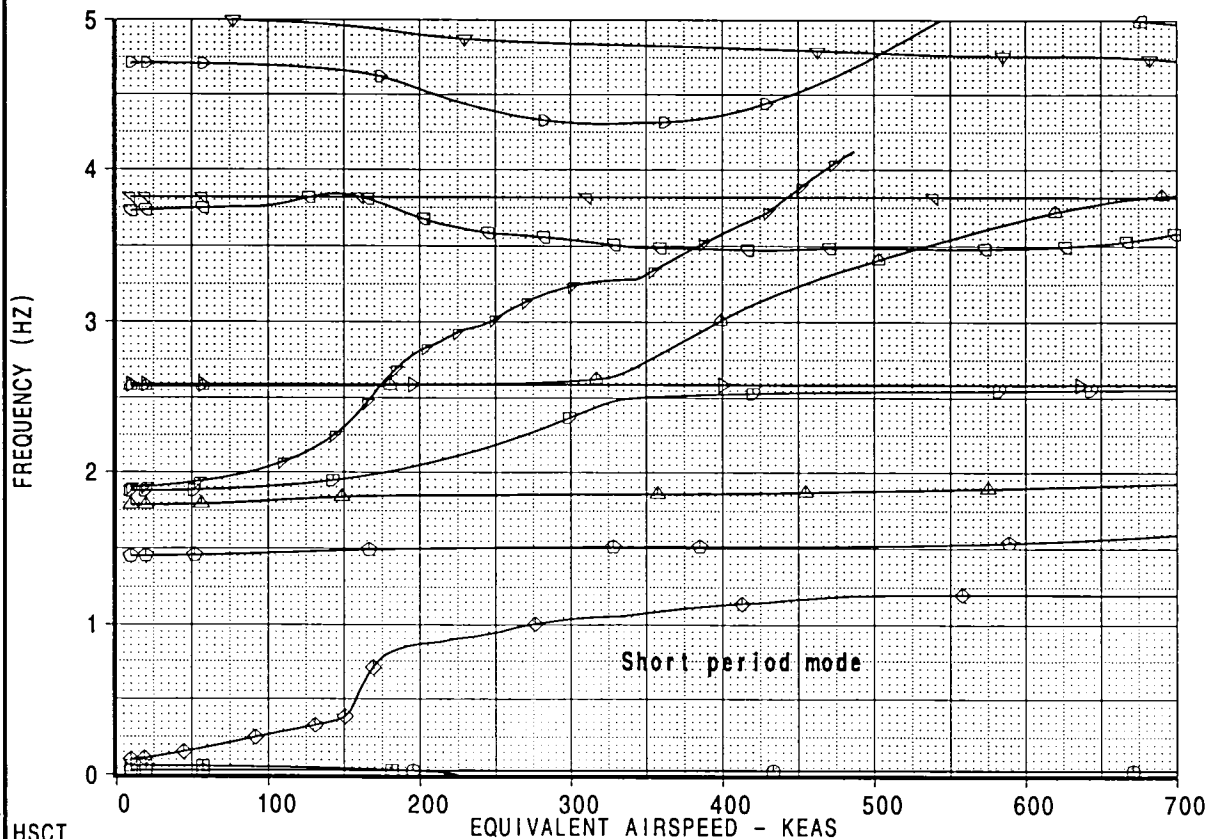


CALC	K.S.NAGARAJA	28Mar98	REVISED	DATE	CONTROL SYSTEM EFFECTS STRENGTH+FLUTTER SIZED AIRPLANE DITS MODEL TCAY BOEING	HSCT
CHECK						FIGURE 11
APPD.						PAGE
APPD.						17

HSCT MODEL TCAY, SYMMETRIC FLUTTER ANALYSIS, M=0.95
GAMMA-DOT V CONTROLLER, MASS:M02



- mode001
- mode002
- ◇ mode003
- ◇ mode004
- △ mode005
- ▽ mode006
- ▽ mode007
- △ mode008
- ▷ mode009
- ▽ mode011
- ▷ mode012
- ▽ mode013
- △ mode014
- △ mode015
- ▽ mode016
- ◇ mode017
- ▷ mode018
- ▷ mode019
- ◇ mode020
- mode021
- + mode022
- × mode023
- mode024
- ▷ mode009
- ▷ mode010

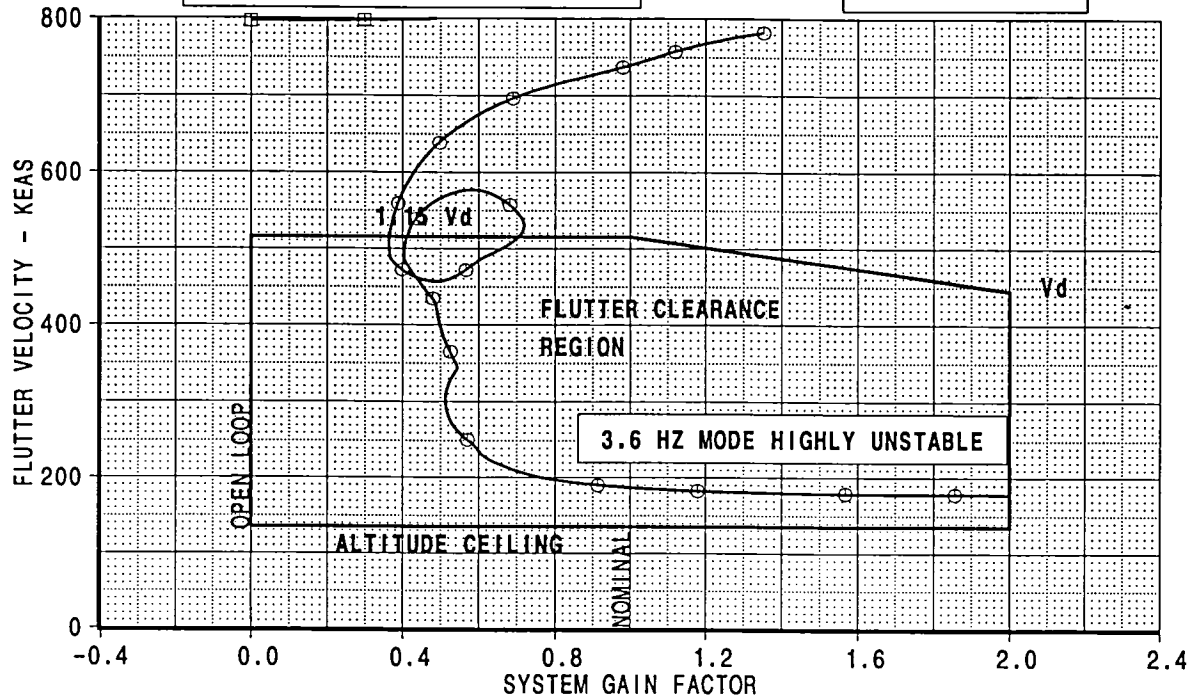


HSCT					EQUIVALENT AIRSPEED - KEAS		
CALC	K.S.NAGARAJA	26Mar98	REVISED	DATE	CONTROL SYSTEM EFFECTS STRENGTH+FLUTTER SIZED AIRPLANE DITS MODEL TCAY		
CHECK							
APPD.							
APPD.					BOEING		PAC
PLOT							

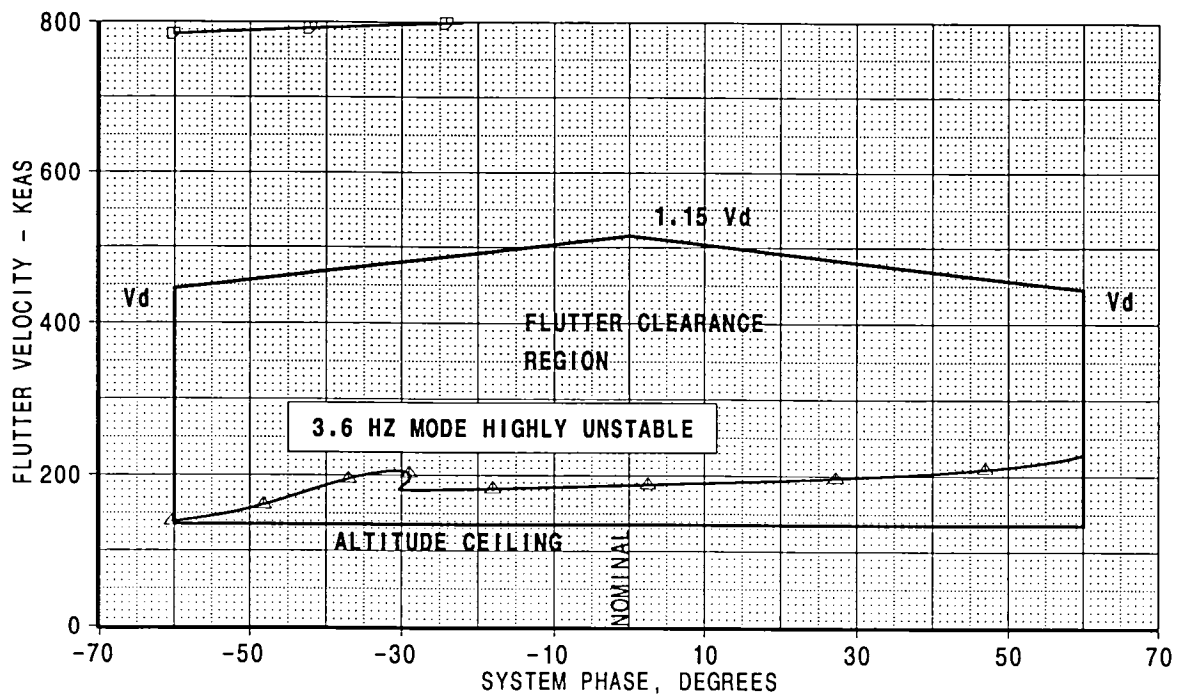
[] /acct/ksn8042/ASE/PLOTS/VGLOTS/mach95.esb
[B]: /acct/ksn8042/ASE/M95/M02/DOC/b595t5a6tC1.esb
[C]: /acct/ksn8042/ASE/M95/b595t5a4C1.esb

HSCT: SYMM FLUTTER ANALYSIS
SENSORS (NEAR C.G. (BS 2323)
REAL SENSORS ANALYSIS, $g=0.02$

MACH..... 0.95
MASS COND: M02
MODEL: TCAY



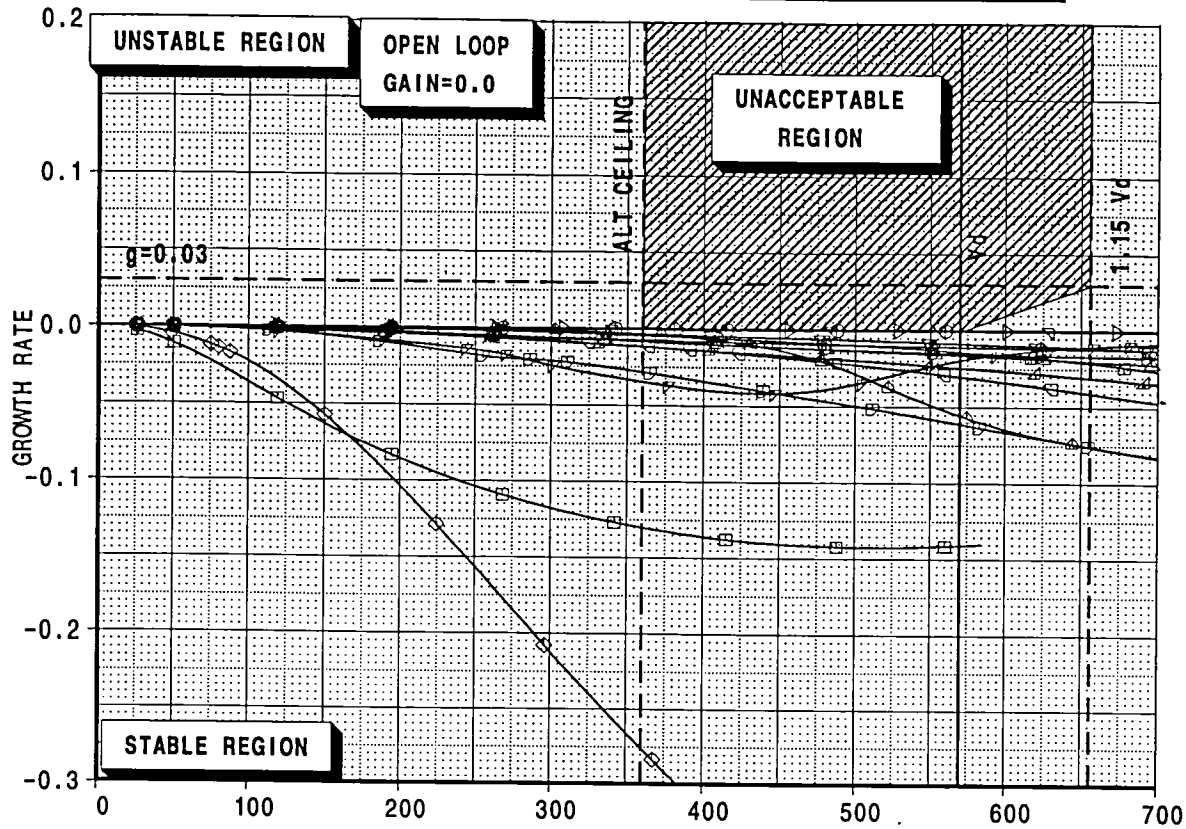
HEAVY LINE: $g=0.03$



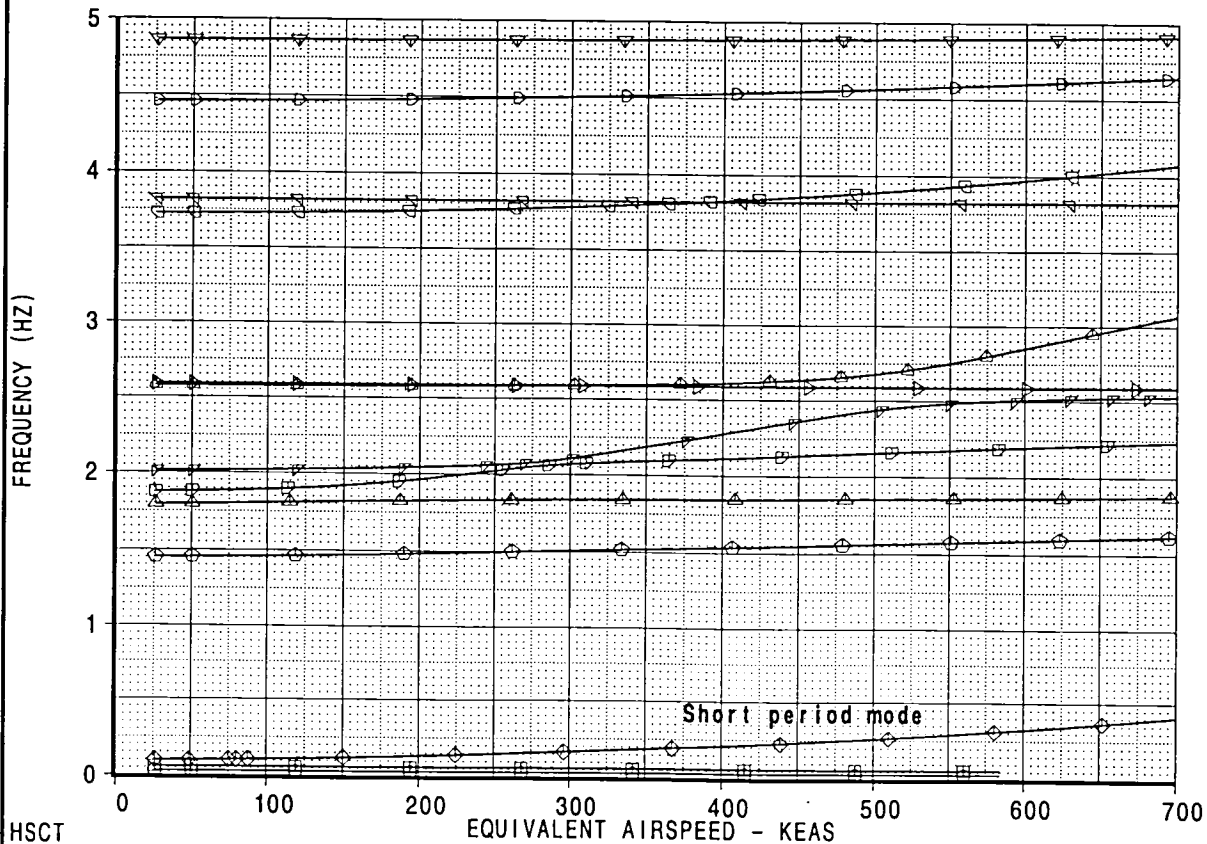
.J: /acct/ksn8042/ASE/PLOTS/GV/gvmach95.esb
[B]: /acct/ksn8042/ASE/M95/b59515a4gv1.esb
[C]: /acct/ksn8042/ASE/M95/b59515a4pv1.esb

CALC	K.S.NAGARAJA	26Mar98	REVISED	DATE	CONTROL SYSTEM EFFECTS STRENGTH+FLUTTER SIZED AIRPLANE DITS MODEL TCAY BOEING	HSCT
CHECK						FIGURE 13
APPD.						PAGE 19
APPD.						

HSCT MODEL TCAY, SYMMETRIC FLUTTER ANALYSIS, M=2.60
GAMMA-DOT V CONTROLLER, MASS:M02



- mode001
- mode002
- ◇ mode003
- ◇ mode004
- △ mode005
- ▽ mode006
- ▽ mode007
- △ mode008
- ▷ mode009
- ▽ mode010
- ▷ mode011
- ▷ mode012
- ▽ mode013
- mode014
- △ mode015

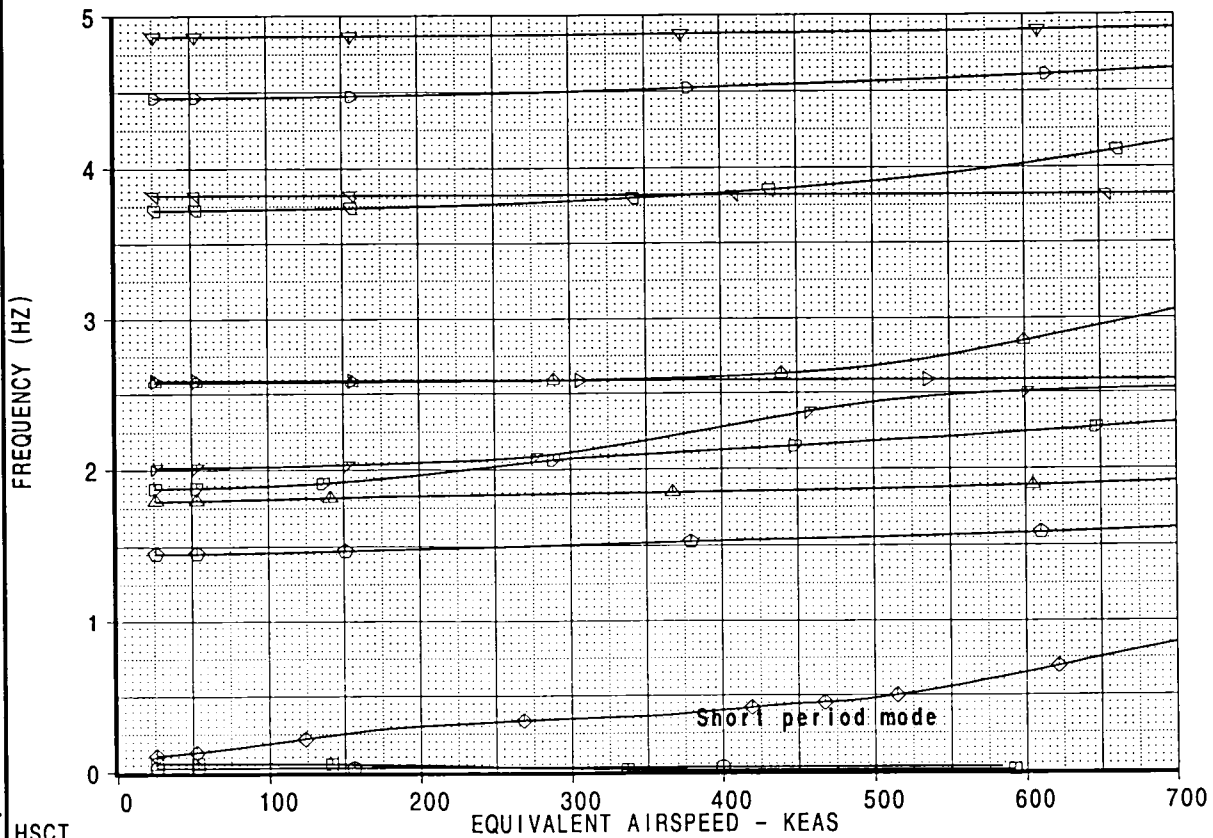
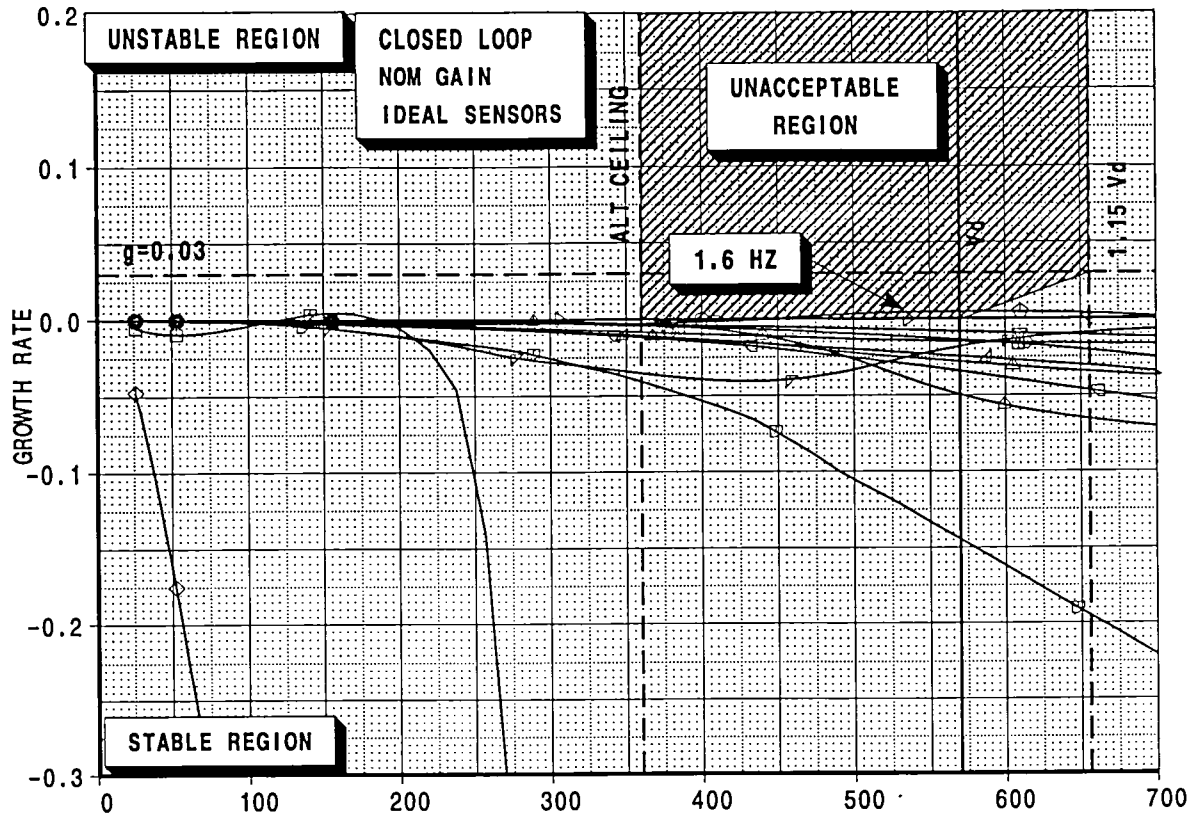


HSCT

CALC	K.S.NAGARAJA	26Mar98	REVISED	DATE	CONTROL SYSTEM EFFECTS STRENGTH+FLUTTER SIZED AIRPLANE DITS MODEL TCAY BOEING	HSCT
CHECK						FIGURE 14
APPD.						PAGE 20
APPD.						
PLOT						

[A]: /acct/ksn8042/ASE/PLOTS/VG/PLOTS/mach26.esb
[B]: /acct/ksn8042/ASE/M26/M02/DOC/b59515a6a1C0.esb

HSCT MODEL TCAY, SYMMETRIC FLUTTER ANALYSIS, M=2.60
GAMMA-DOT V CONTROLLER , MASS:M02

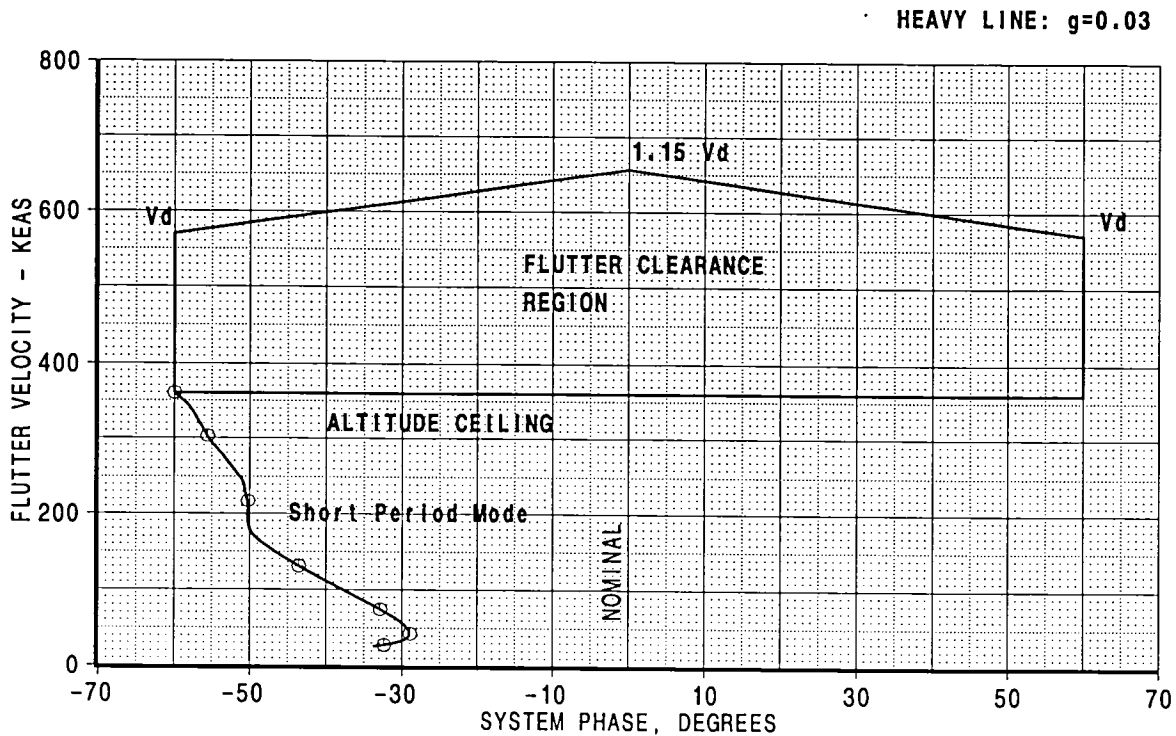
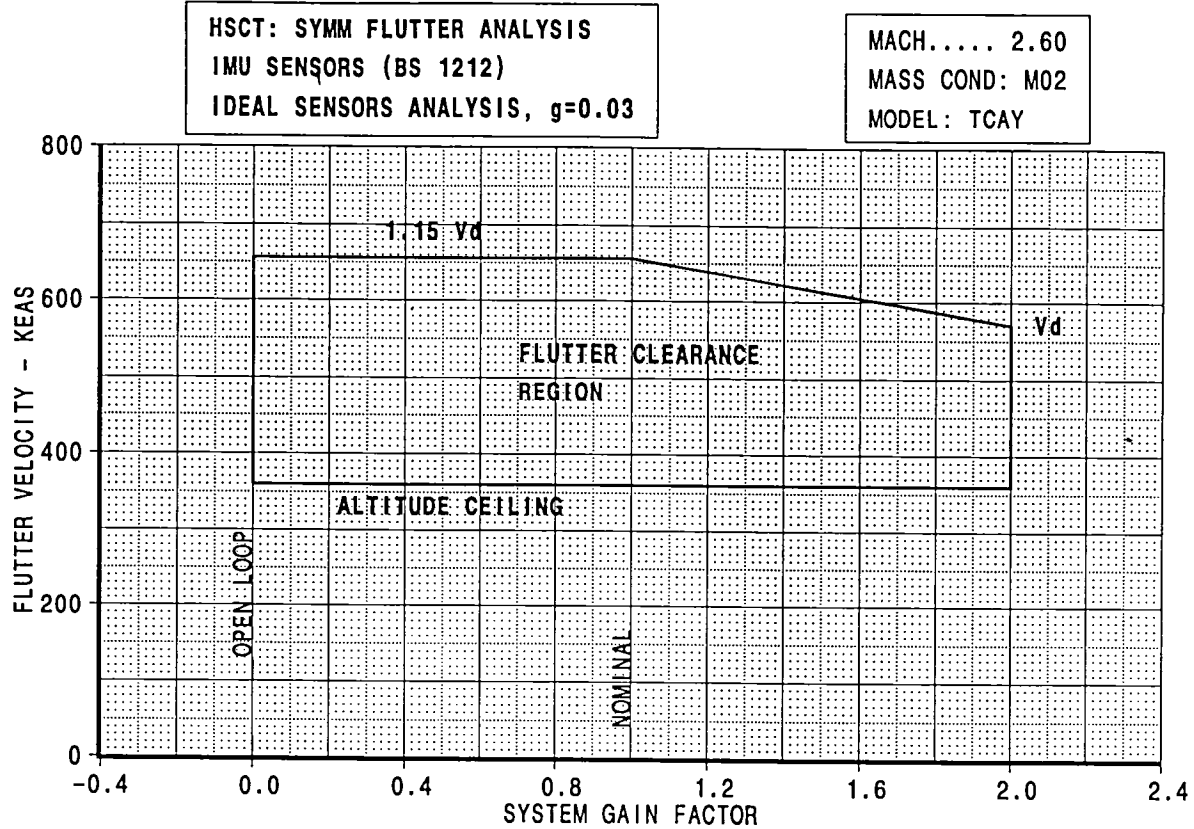


[A]: /acct/ksn8042/ASE/PLOTS/VGPLOTS/mach26.esb
 [B]: /acct/ksn8042/ASE/M02/DOC/b595t5a6aC1.esb

HSCT				CONTROL SYSTEM EFFECTS		HSCT
CALC	K.S.NAGARAJA	26Mar98	REVISED	DATE	STRENGTH+FLUTTER SIZED AIRPLANE	FIGURE 15
CHECK					DITS MODEL TCAY	
APPD.						PAGE 21
APPD.						
PLOT						

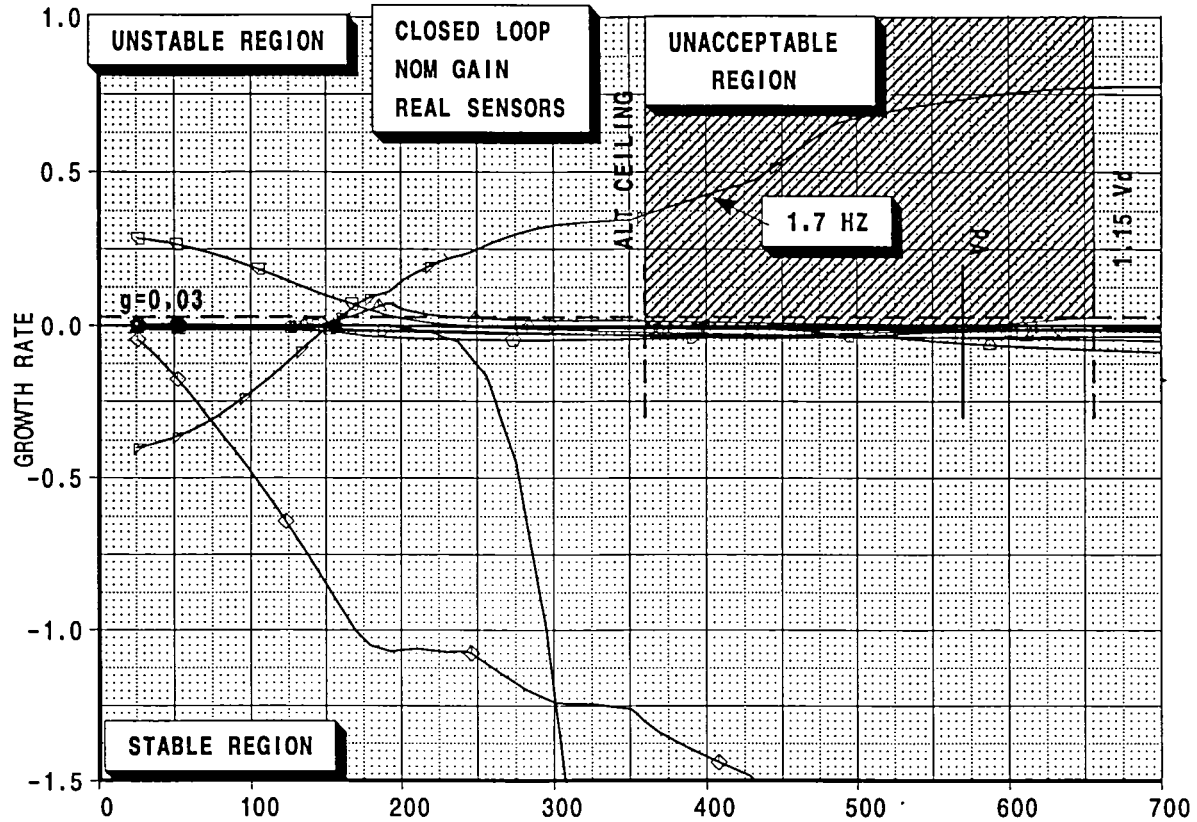
BOEING

[A]: /acct/ksn8042/ASE/PLOTS/GV/gvmach26.esb
 [B]: /acct/ksn8042/ASE/M26/M02/DOC/b59515a6a1pv1.esb
 [C]: /acct/ksn8042/ASE/M26/M02/DOC/b59515a6agv1.esb
 [D]: /acct/ksn8042/ASE/M26/M02/DOC/b59515a6agv2.esb

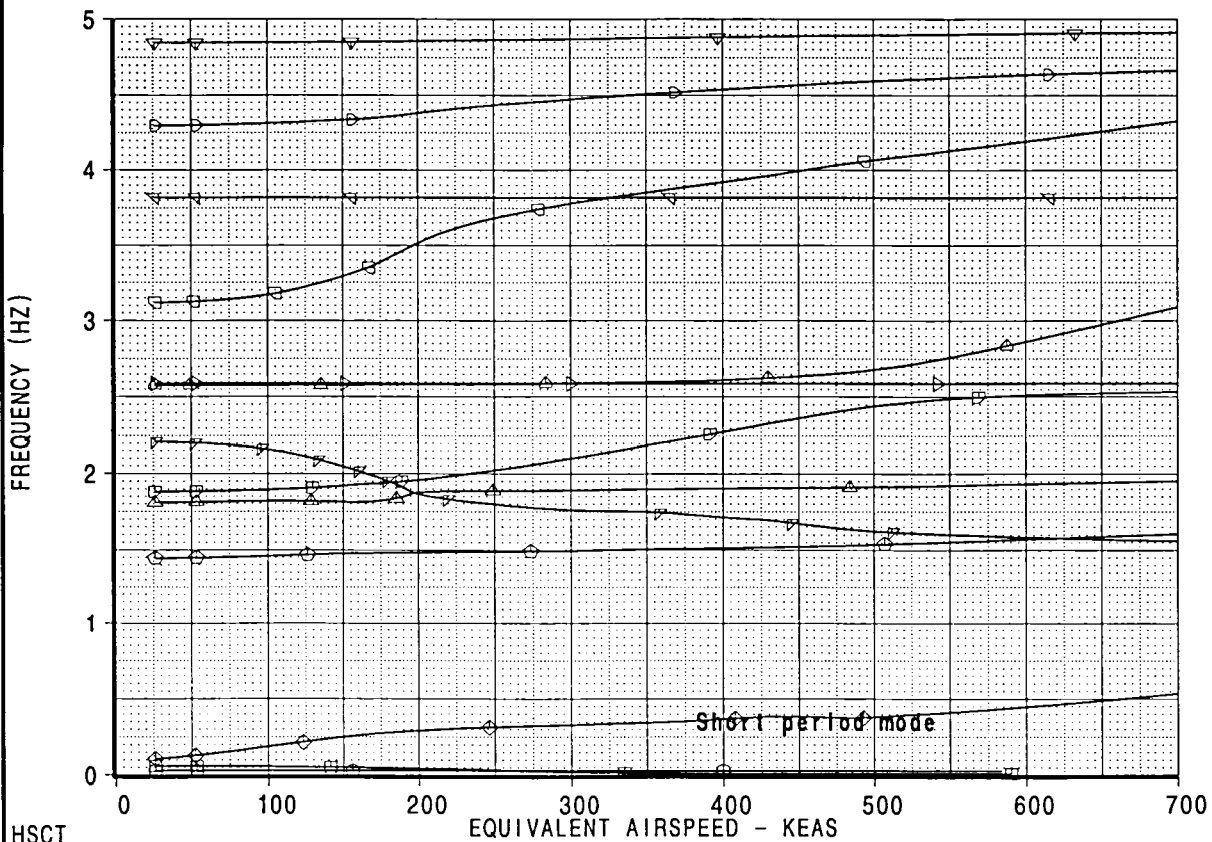


CALC	K.S.NAGARAJA	27Mar98	REVISED	DATE	CONTROL SYSTEM EFFECTS STRENGTH+FLUTTER SIZED AIRPLANE DITS MODEL TCAY BOEING	HSCT
CHECK						FIGURE 16
APPD.						PAGE 22
APPD.						

HSCT MODEL TCAY, SYMMETRIC FLUTTER ANALYSIS, M=2.60
GAMMA-DOT V CONTROLLER , MASS:M02



- mode001
- mode002
- ◇ mode003
- mode004
- △ mode005
- ▽ mode006
- ▽ mode007
- △ mode008
- ▷ mode009
- ▽ mode010
- ▷ mode011
- ▷ mode012
- ▽ mode013
- △ mode014
- △ mode015



[A]: /acct/ksn8042/ASE/PLOTS/VGLOTS/mach26.esb
 [B]: /acct/ksn8042/ASE/M26/M02/DOC/b59515a6bC1.esb

HSCT

CALC	K.S.NAGARAJA	26Mar98	REVISED	DATE
CHECK				
APPD.				
APPD.				
PLOT				

CONTROL SYSTEM EFFECTS
STRENGTH+FLUTTER SIZED AIRPLANE
DITS MODEL TCAY

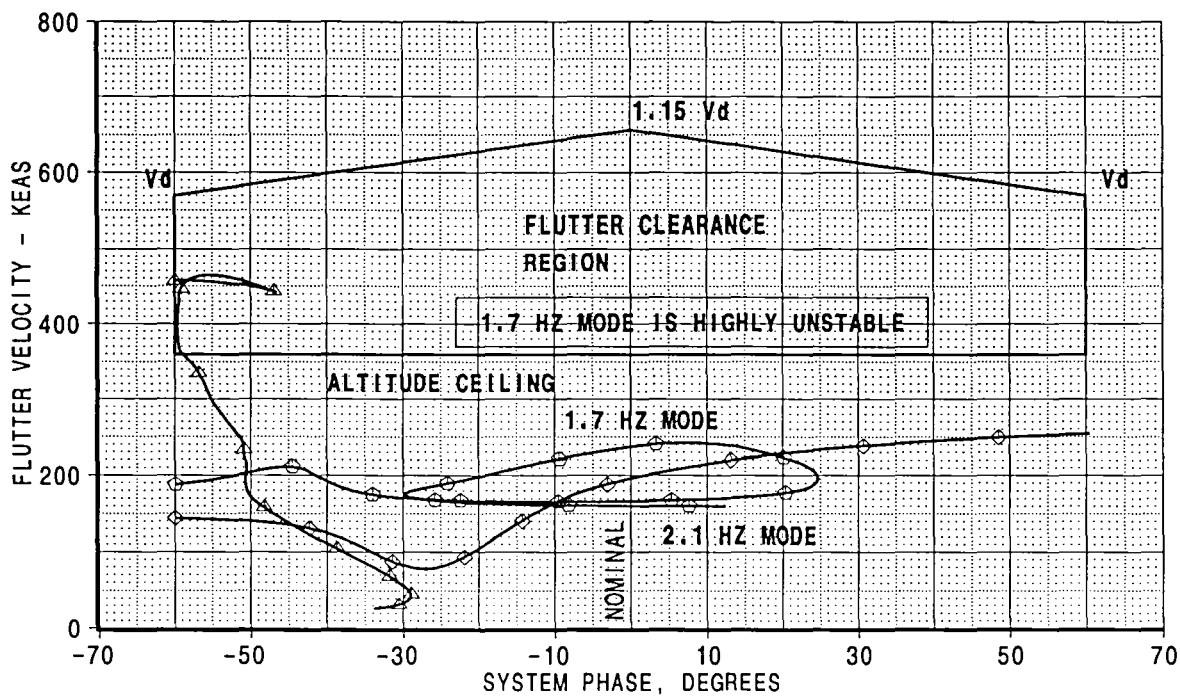
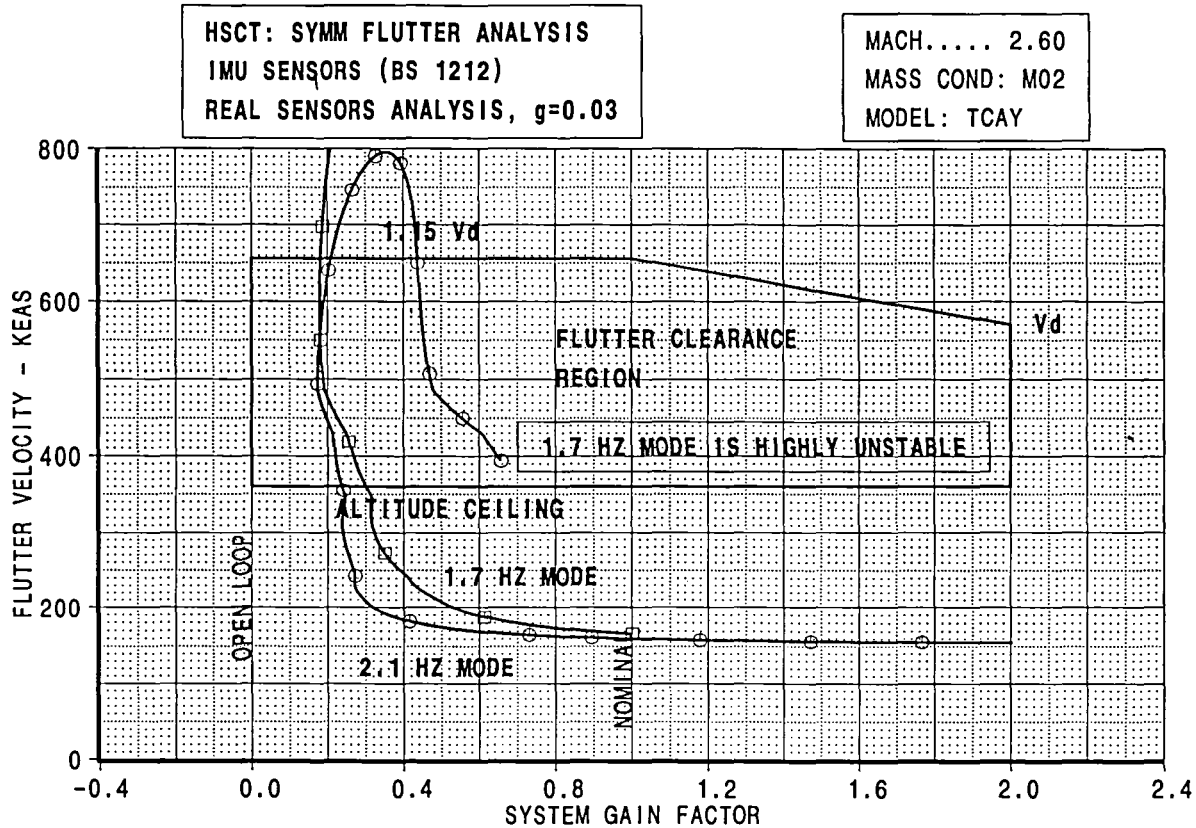
BOEING

HSCT

FIGURE 17

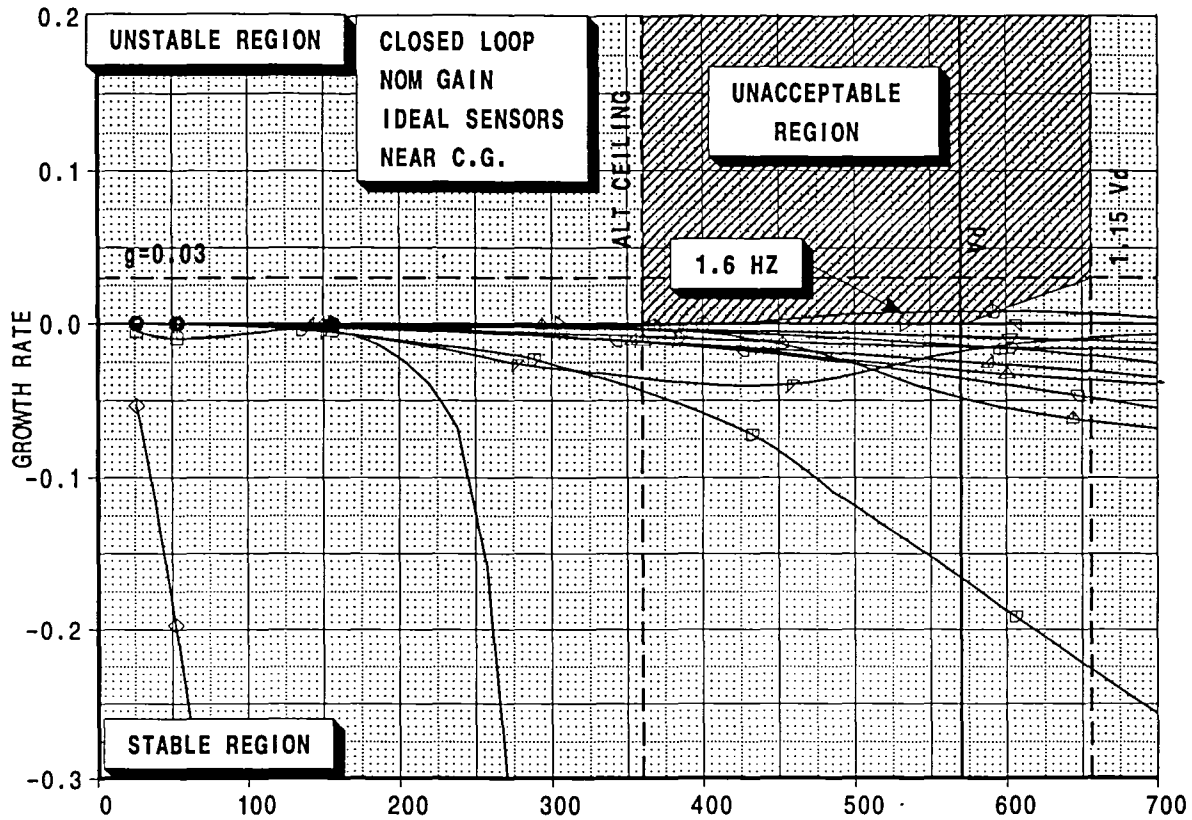
PAGE **23**

A]: /acct/ksn8042/ASE/PLOTS/GV/gvmach26.esb
 [B]: /acct/ksn8042/ASE/M26/M02/DOC/b595t5a6bgv1.esb
 [C]: /acct/ksn8042/ASE/M26/M02/DOC/b595t5a6b1pv1.esb

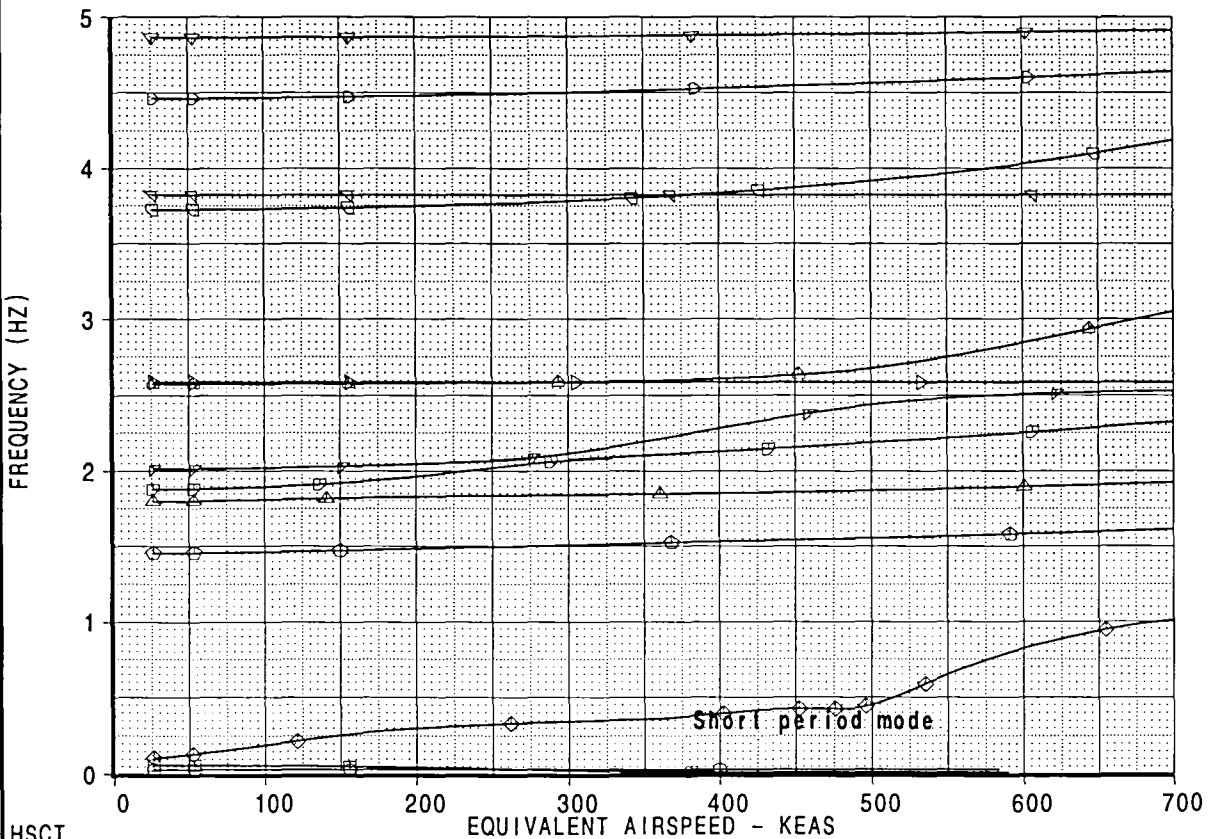


CALC	K.S.NAGARAJA	28Mar98	REVISED	DATE	CONTROL SYSTEM EFFECTS STRENGTH+FLUTTER SIZED AIRPLANE DITS MODEL TCAY BOEING	HSCT
CHECK						FIGURE 18
APPD.						PAGE
APPD.						24

HSCT MODEL TCAY, SYMMETRIC FLUTTER ANALYSIS, M=2.60
GAMMA-DOT V CONTROLLER, MASS:M02



- mode001
- mode002
- ◇ mode003
- △ mode004
- ▽ mode005
- ▽ mode006
- ▽ mode007
- △ mode008
- ▷ mode009
- ▽ mode010
- ▽ mode011
- ▷ mode012
- ▽ mode013
- △ mode014
- △ mode015



HSCT

CALC	K.S.NAGARAJA	26Mar98	REVISED	DATE
CHECK				
APPD.				
APPD.				
PLOT				

CONTROL SYSTEM EFFECTS
STRENGTH+FLUTTER SIZED AIRPLANE
DITS MODEL TCAY

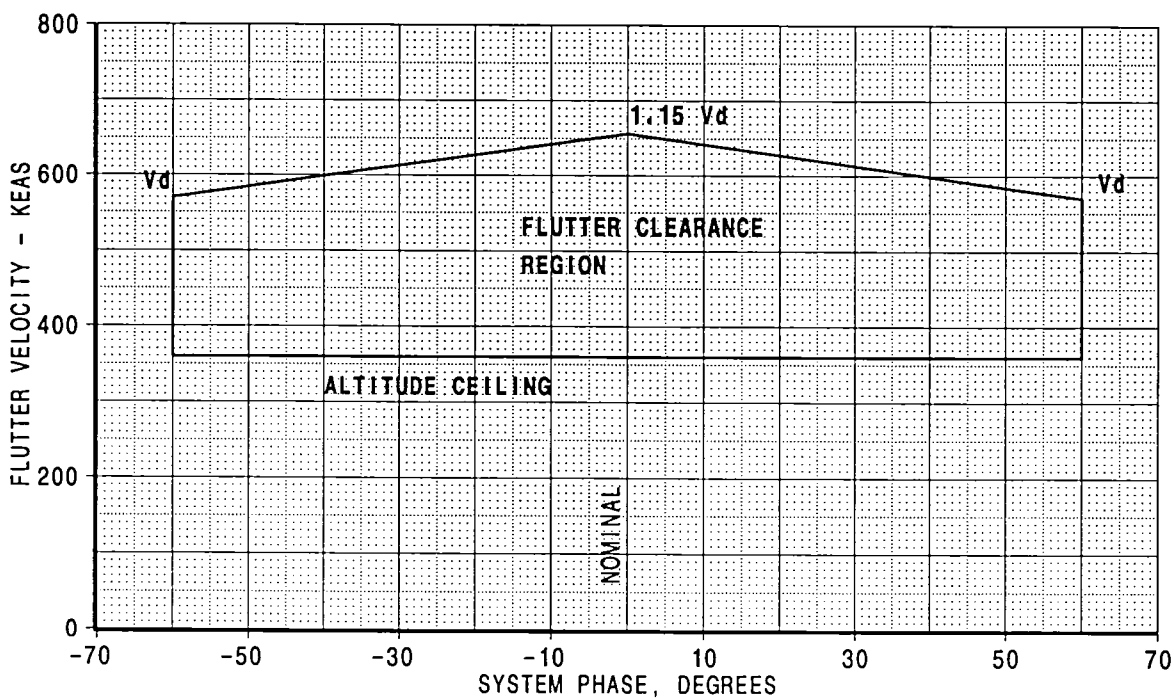
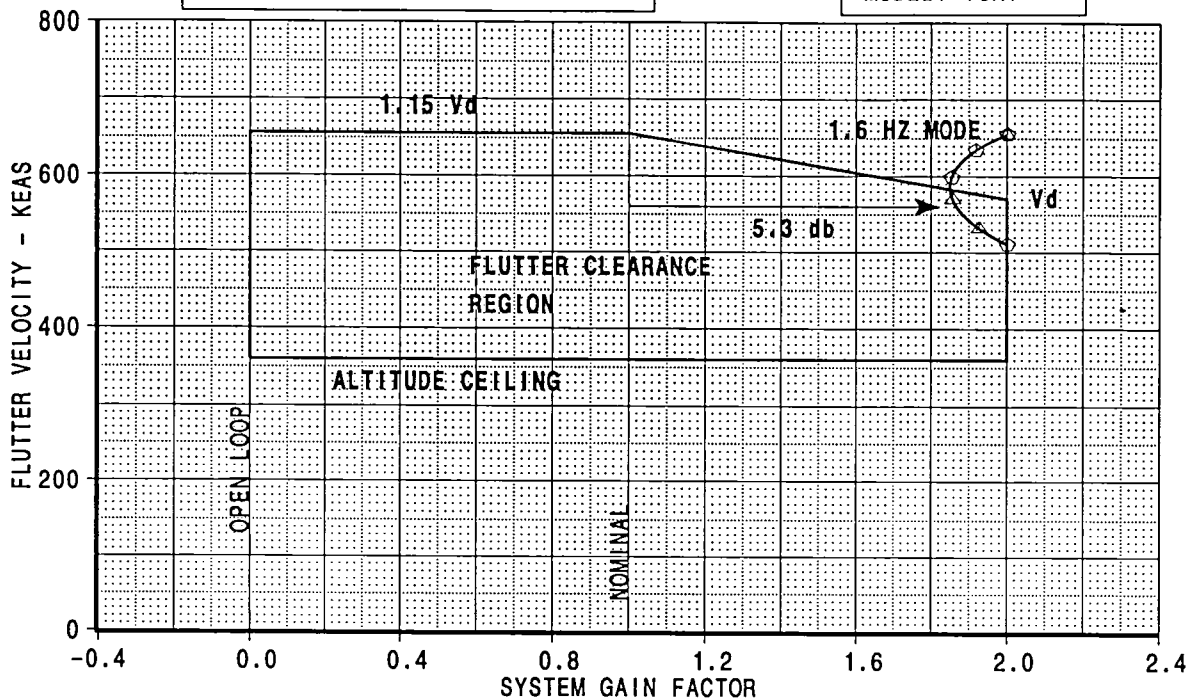
BOEING

HSCT
FIGURE 19
PAGE 25

[A]: /acct/ksn8042/ASE/PLOTS/VG/PLOTS/mach26.esb
[B]: /acct/ksn8042/ASE/M26/M02/DOC/b595t5a6dC1.esb

HSCT: SYMM FLUTTER ANALYSIS
SENSORS NEAR C.G. (BS 2323)
IDEAL SENSORS ANALYSIS, $g=0.03$

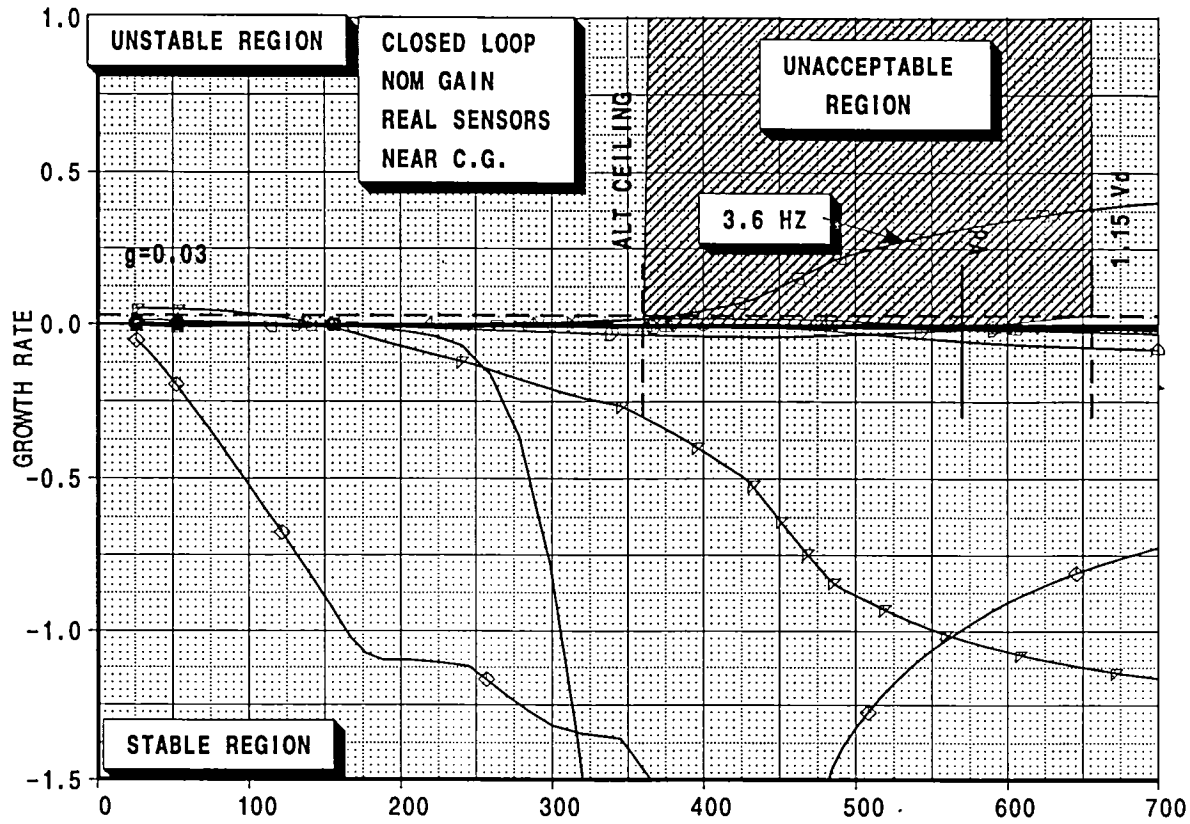
MACH..... 2.60
MASS COND: M02
MODEL: TCAY



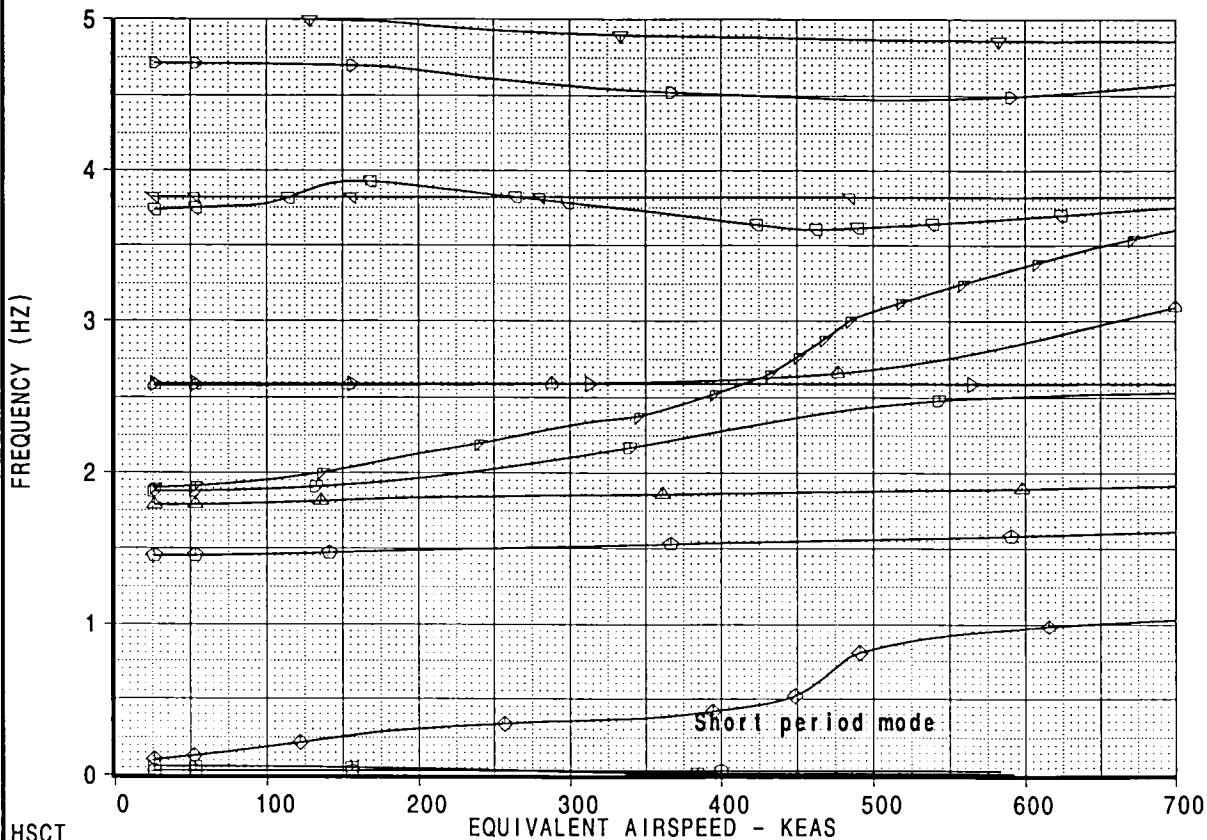
CALC	K.S.NAGARAJA	27Mar98	REVISED	DATE	CONTROL SYSTEM EFFECTS STRENGTH+FLUTTER SIZED AIRPLANE DITS MODEL TCAY BOEING	HSCT
CHECK						FIGURE 20
APPD.						PAGE
APPD.						26

[A]: /acct/ksn8042/ASE/M26/M02/DOC/b595t5a6dgv1.esb
[B]: /acct/ksn8042/ASE/M26/M02/DOC/b595t5a6dgv2.esb
[C]: /acct/ksn8042/ASE/M26/M02/DOC/b595t5a6dgv1.esb
[D]: /acct/ksn8042/ASE/PLOTS/GV/gvmach26.esb

HSCT MODEL TCAY, SYMMETRIC FLUTTER ANALYSIS, M=2.60
GAMMA-DOT V CONTROLLER, MASS:M02



- mode001
- mode002
- ◇ mode003
- mode004
- △ mode005
- ▽ mode006
- ▽ mode007
- △ mode008
- ▷ mode009
- ▽ mode011
- ▷ mode012
- ▽ mode013
- △ mode014
- △ mode015
- ▽ mode010



[.] /acct/ksn8042/ASE/PLOTS/VGPLOTS/mach26.esb
[B]: /acct/ksn8042/ASE/M26/M02/DOC/b595t5a6fC1.esb
[C]: /acct/ksn8042/ASE/M26/M02/DOC/b595t5a6faC1.esb

HSCT

CALC	K.S.NAGARAJA	26Mar98	REVISED	DATE
CHECK				
APPD.				
APPD.				
PLOT				

CONTROL SYSTEM EFFECTS
STRENGTH+FLUTTER SIZED AIRPLANE
DITS MODEL TCAY

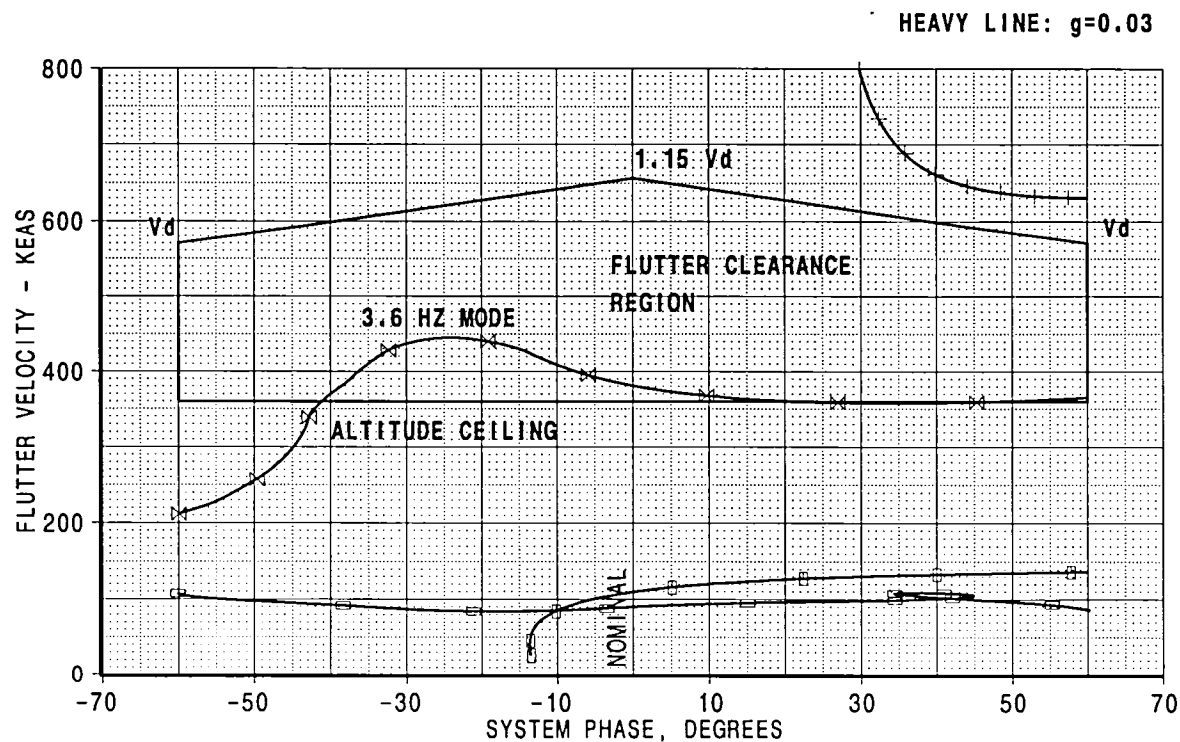
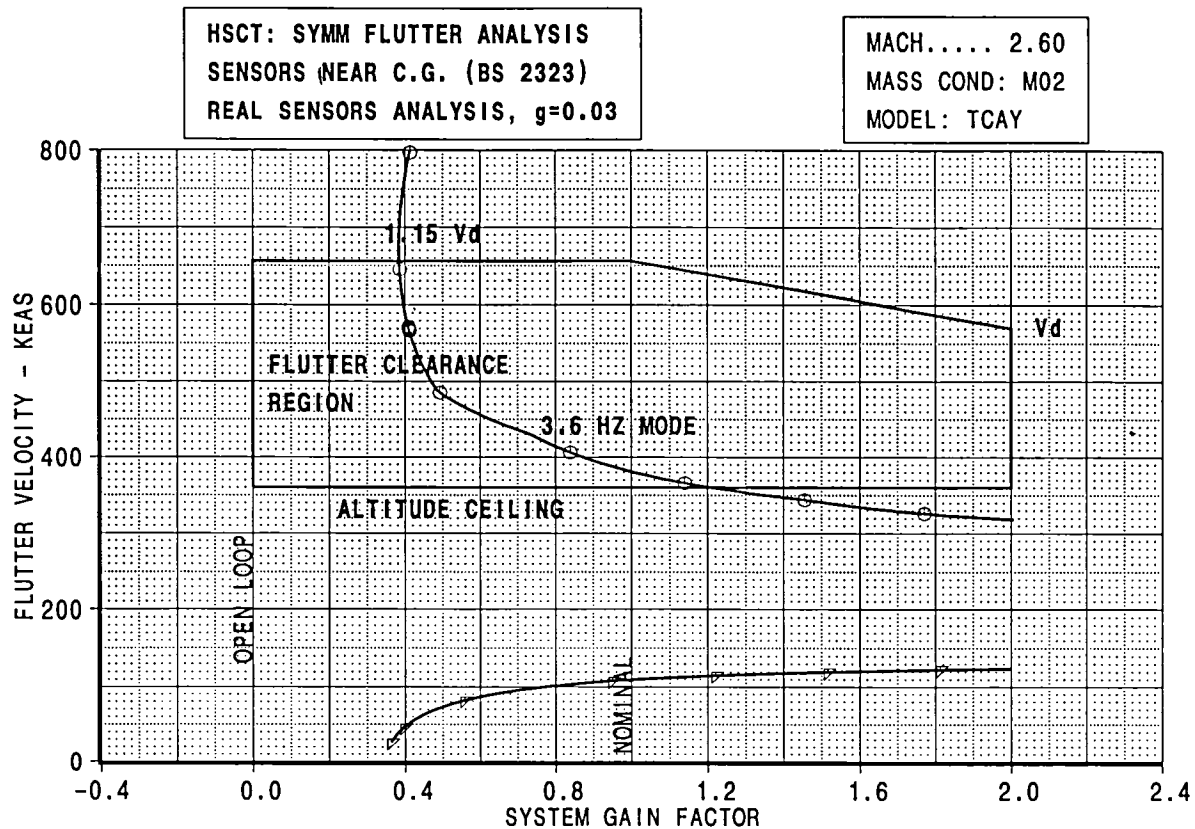
BOEING

HSCT

FIGURE 21

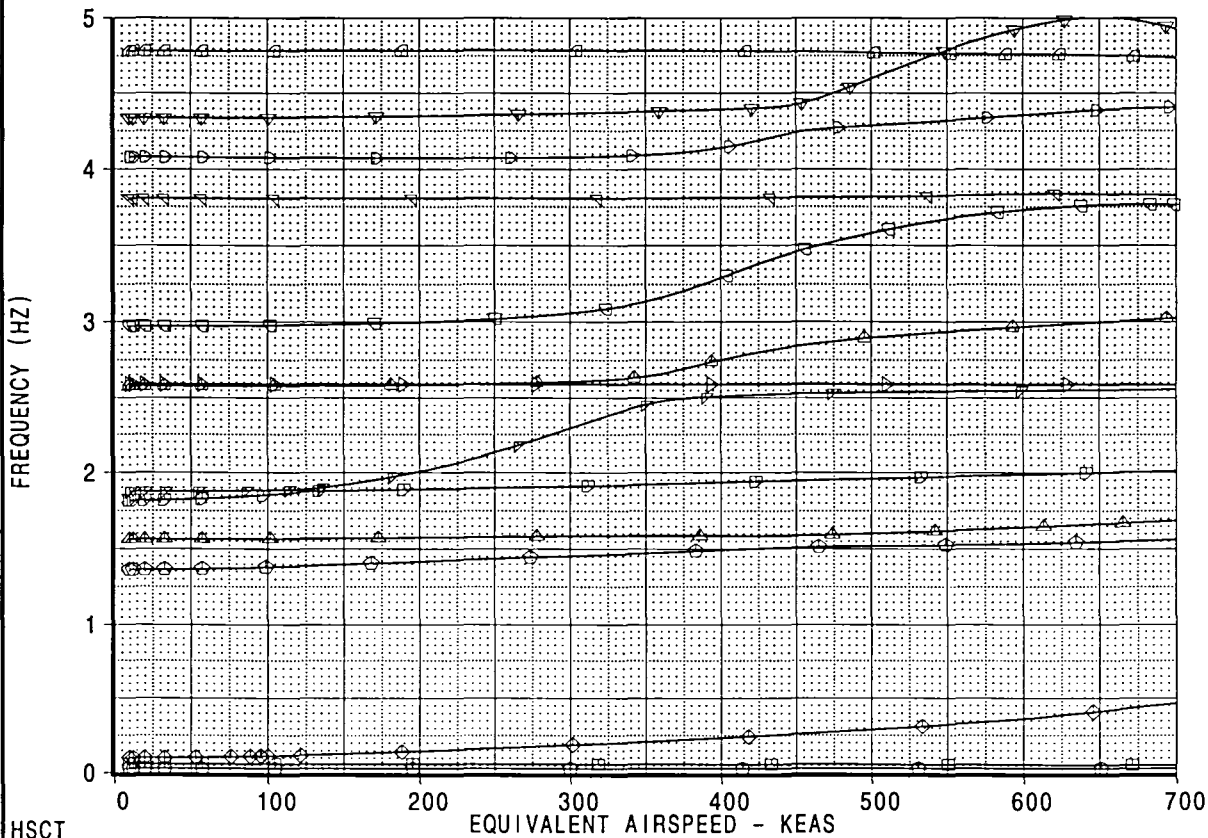
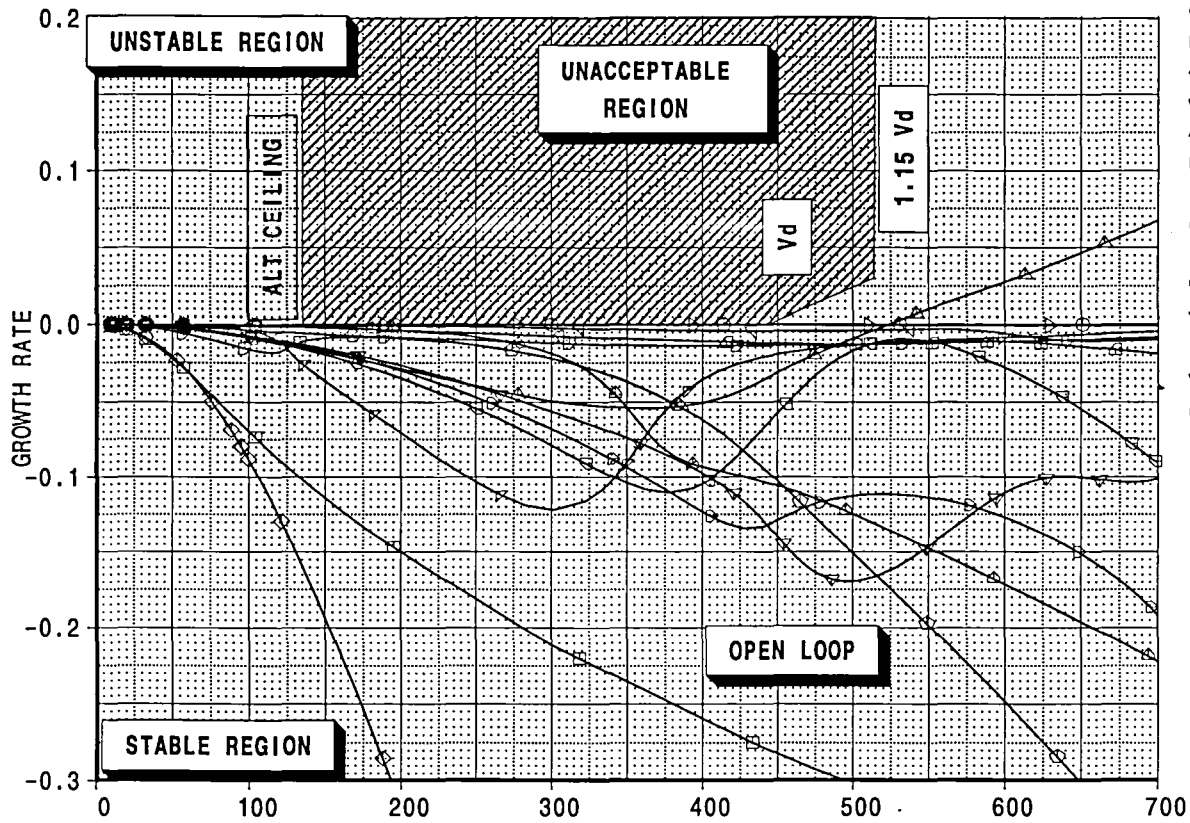
PAGE 27

[D]: /acct/ksn8042/ASE/M26/M02/DOC/b595t5a6fgy1.esb
 [E]: /acct/ksn8042/ASE/M26/M02/DOC/b595t5a6fgy2.esb
 [F]: /acct/ksn8042/ASE/M26/M02/DOC/b595t5a6fpy1.esb
 [G]: /acct/ksn8042/ASE/M26/M02/DOC/b595t5a6fpy1.esb



CALC	K.S.NAGARAJA	28Mar98	REVISED	DATE	CONTROL SYSTEM EFFECTS STRENGTH+FLUTTER SIZED AIRPLANE DITS MODEL TCAY BOEING	HSCT
CHECK						FIGURE 22
APPD.						PAGE
APPD.						28

HSCT MODEL TCAY, SYMMETRIC FLUTTER ANALYSIS, M=0.95
MASS:MT1



HSCT

CALC	LRF	27Mar98	REVISED	DATE
CHECK				
APPD.				
APPD.				
PLOT				

CONTROL SYSTEM EFFECTS
STRENGTH+FLUTTER SIZED AIRPLANE
DITS MODEL TCAY

BOEING

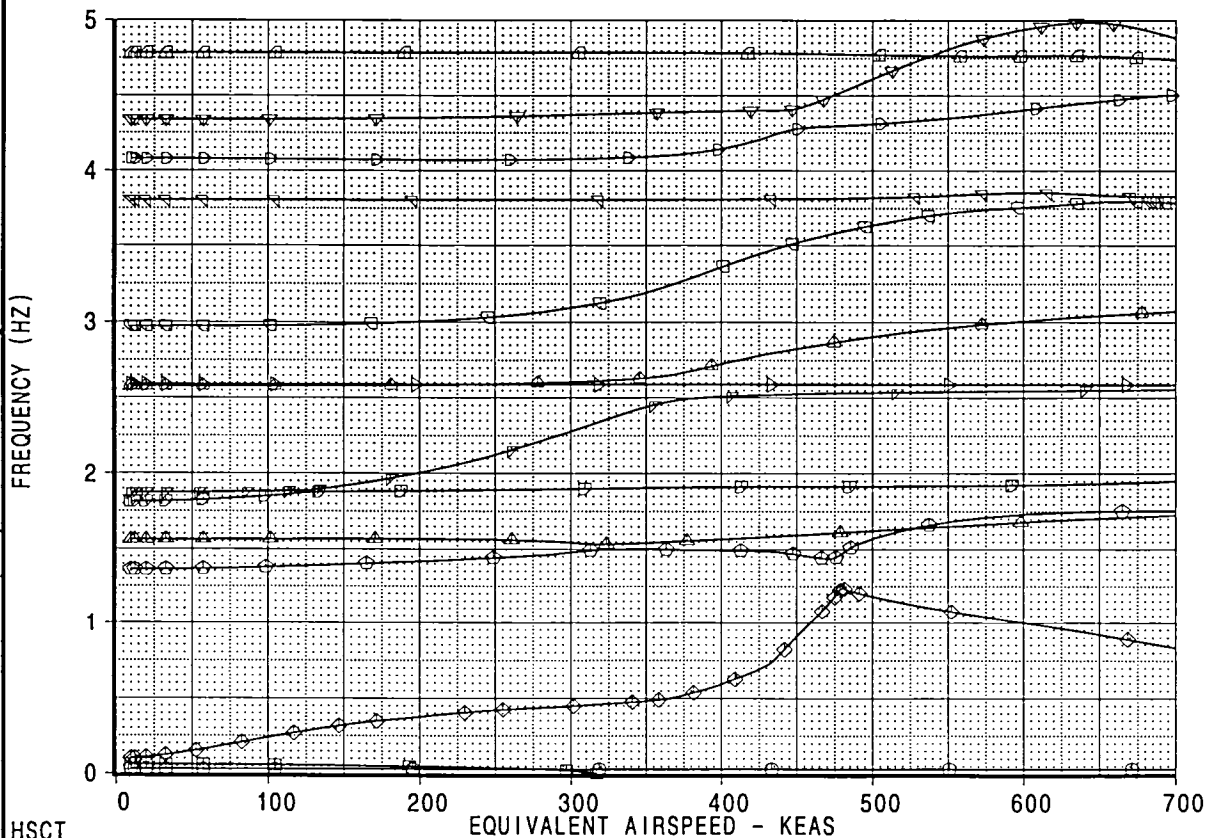
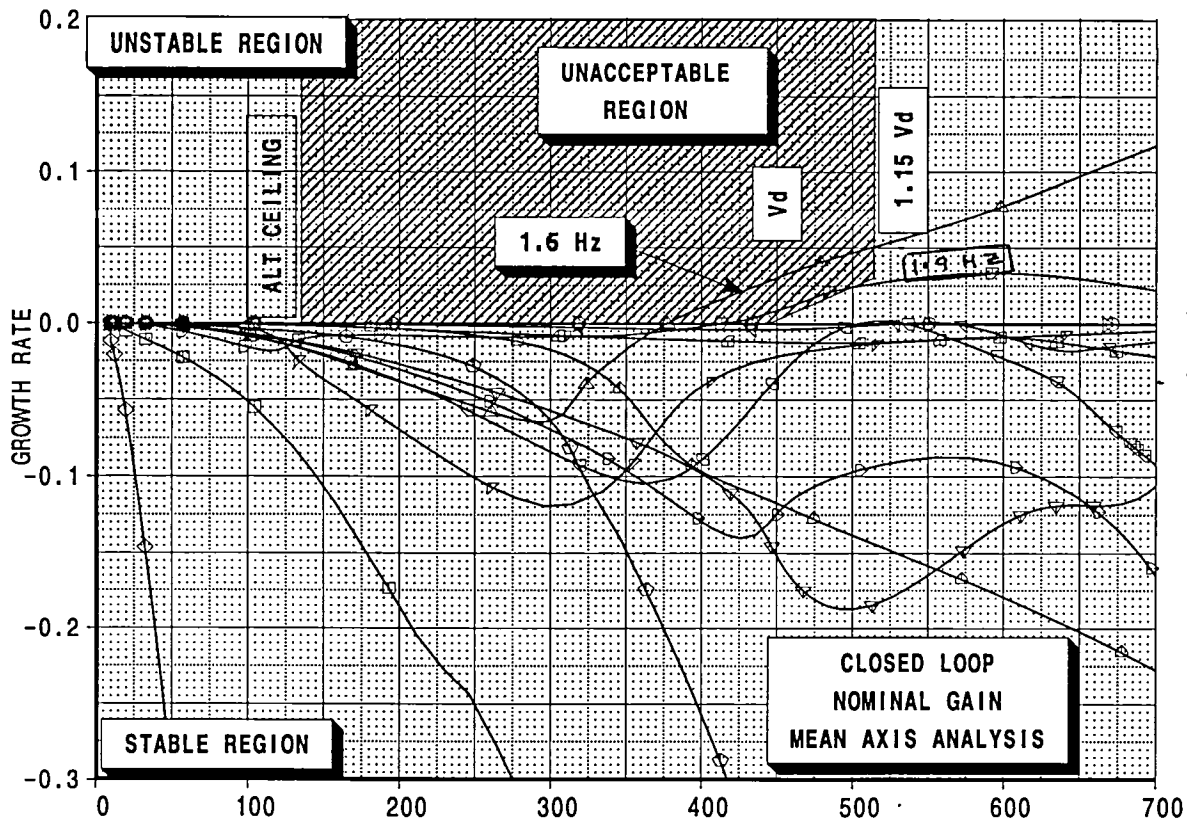
HSCT

FIGURE 23

PAGE 29

[A]: /acct/lrf0076/projects/fm/mt1/mt1.esb
[B]: /acct/lrf0076/projects/fm/mt1/gvmach95.esb

HSCT MODEL TCAY, SYMMETRIC FLUTTER ANALYSIS, M=0.95
GAMMA-DOT V CONTROLLER , MASS:MT1

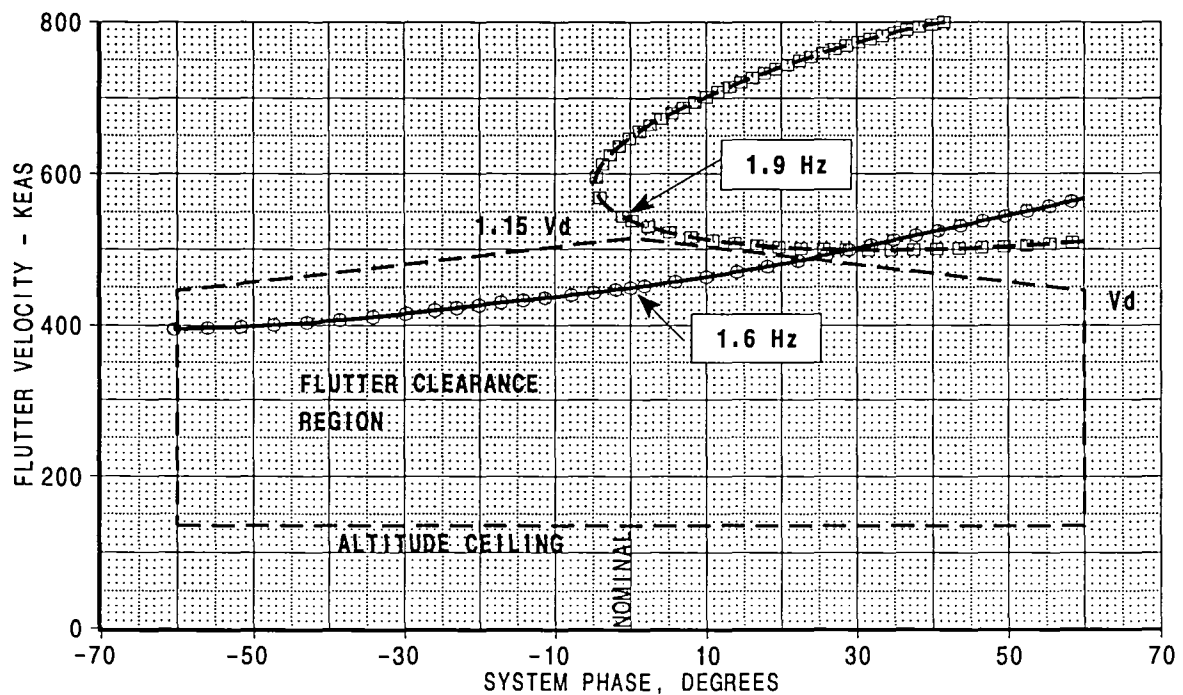
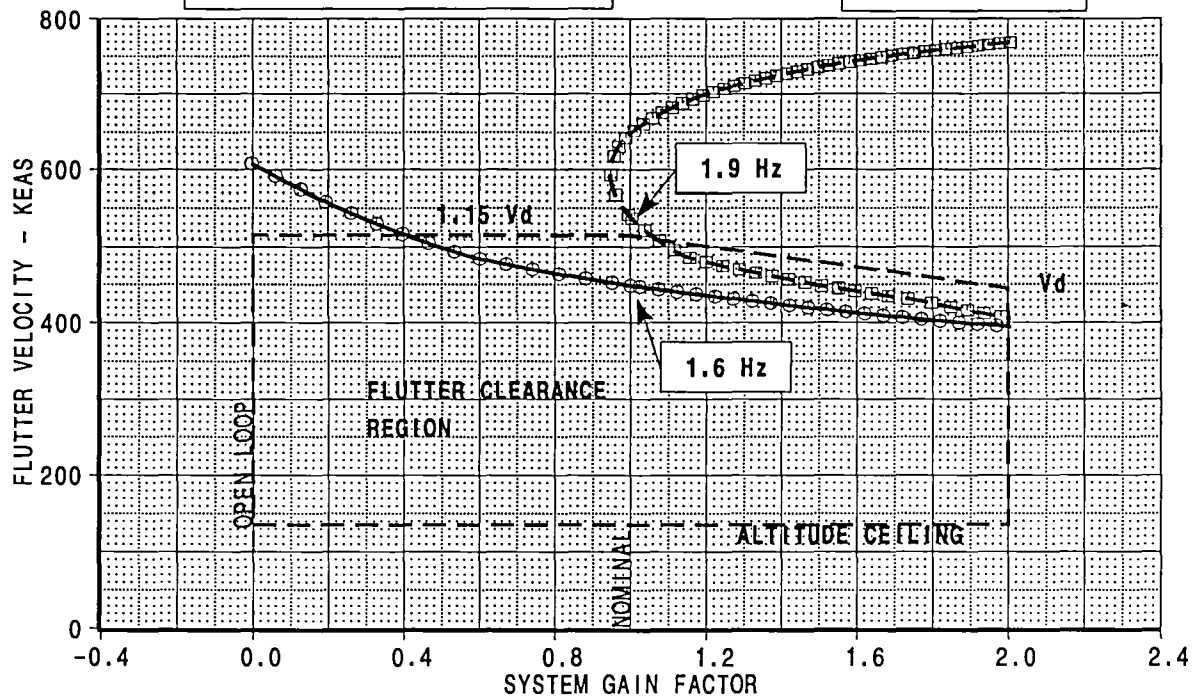


HSCT	CALC	LRF	27Mar98	REVISED	DATE	CONTROL SYSTEM EFFECTS STRENGTH+FLUTTER SIZED AIRPLANE DITS MODEL TCAY BOEING	HSCT
	CHECK						FIGURE 24
	APPD.						PAGE 30
	APPD.						
	PLOT						

[A]: /acct/lrf0076/projects/ffm/mt1/mt1.esb
[B]: /acct/lrf0076/projects/ffm/mt1/gvmach95.esb

HSCT: SYMM FLUTTER ANALYSIS
 IMU SENSORS AT BS 1211
 MEAN AXIS ANALYSIS, $g=0.03$

MACH..... 0.95
 MASS COND: MT1
 MODEL: TCAY



CALC	LRF	27Mar98	REVISED	DATE
CHECK				
APPD.				
APPD.				

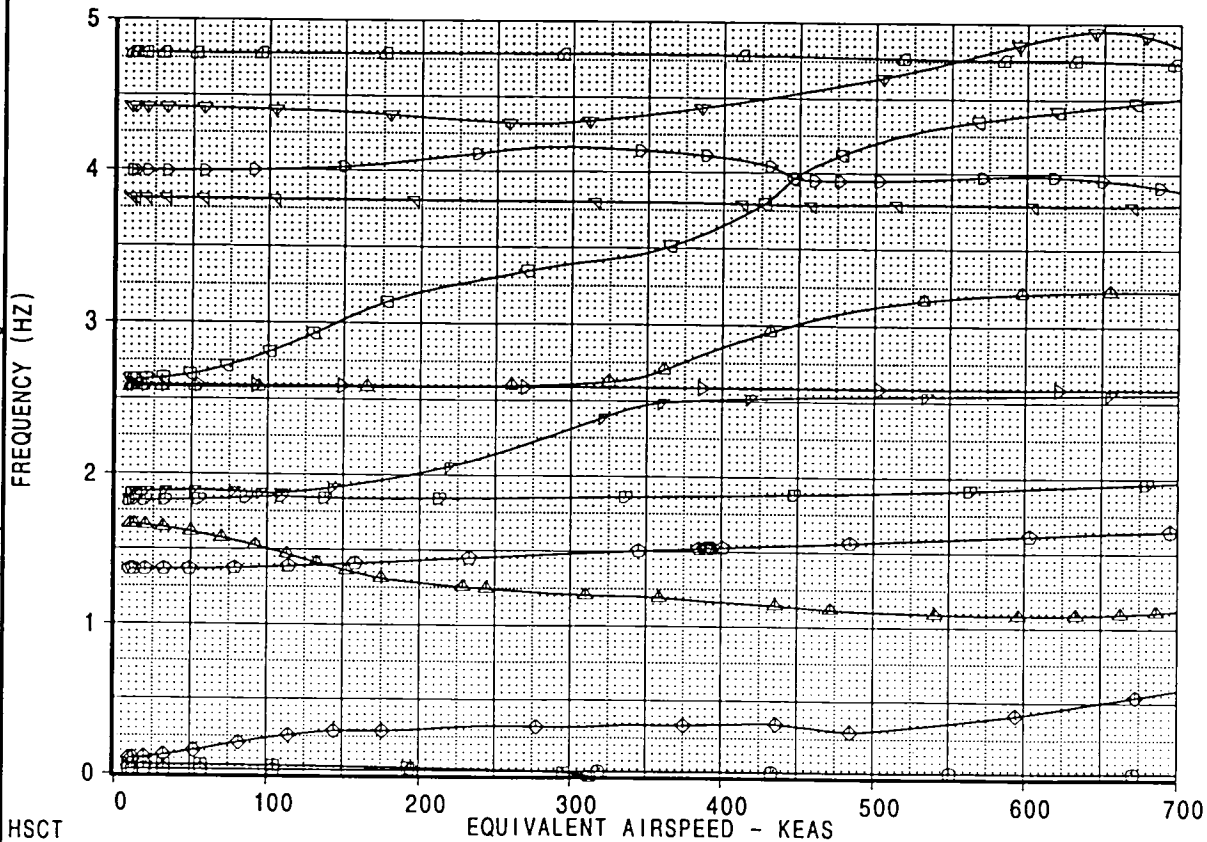
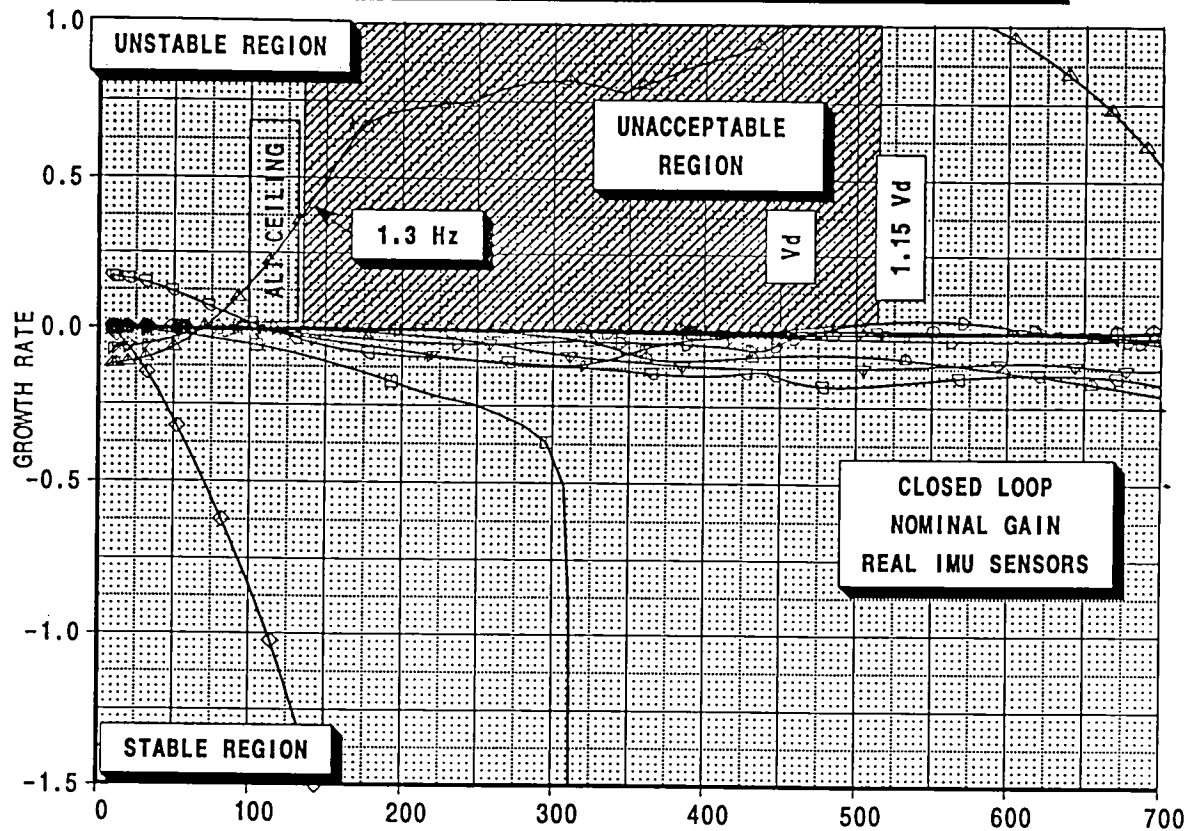
CONTROL SYSTEM EFFECTS
 STRENGTH+FLUTTER SIZED AIRPLANE
 DITS MODEL TCAY

BOEING

FIGURE 25

PAGE 31

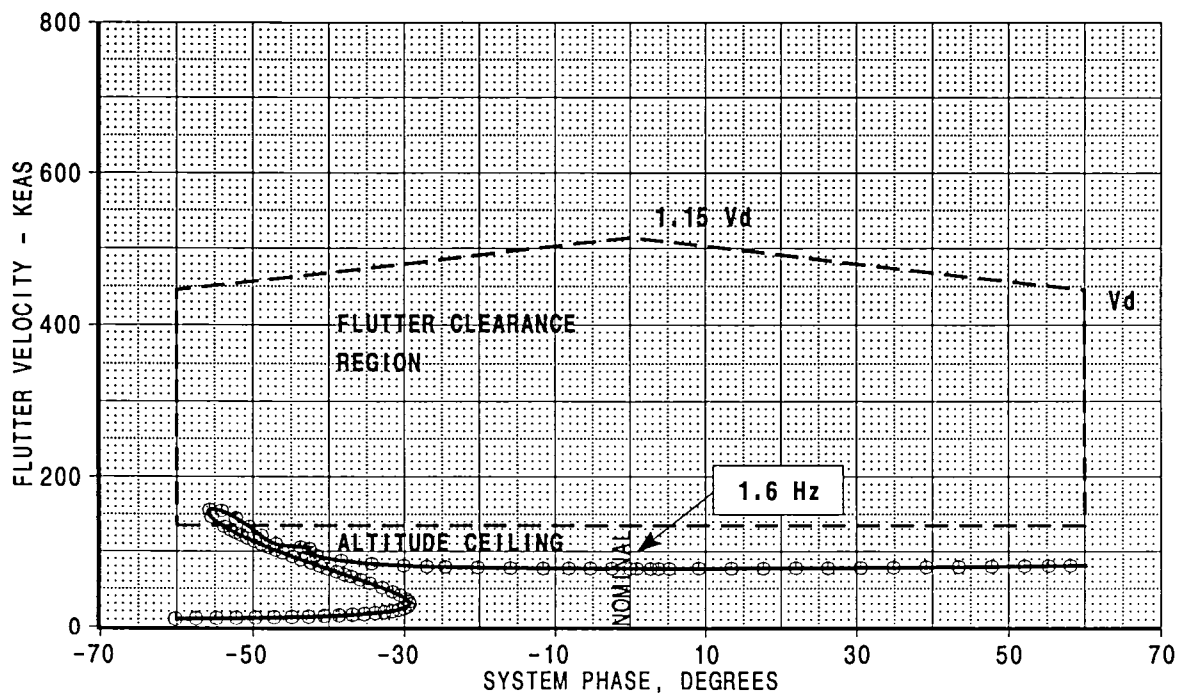
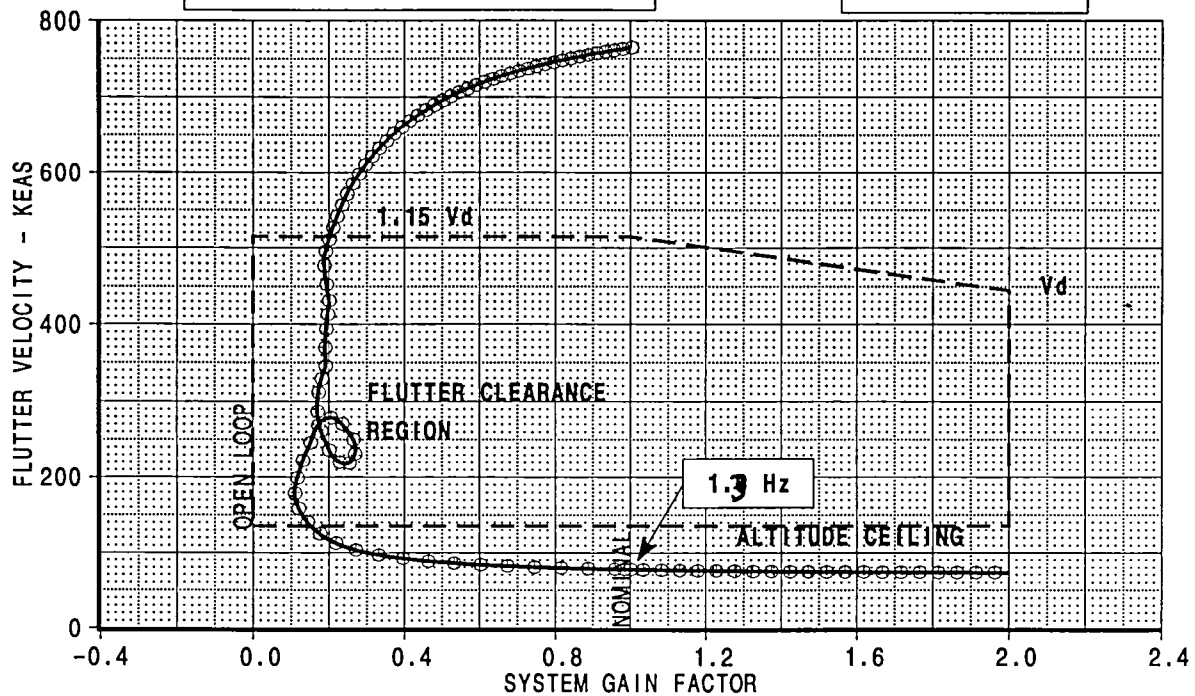
HSCT MODEL TCAY, SYMMETRIC FLUTTER ANALYSIS, M=0.95
GAMMA-DOT V CONTROLLER , MASS:MT1



HSCT	ALC	LRF	25Mar98	REVISED	DATE	CONTROL SYSTEM EFFECTS STRENGTH+FLUTTER SIZED AIRPLANE DITS MODEL TCAY BOEING	HSCT
CHECK							FIGURE 26
APPD.							PAGE 32
PLOT							

HSCT: SYMM FLUTTER ANALYSIS
IMU SENSORS AT BS 1211
FULL FEEDBACK ANALYSIS, $g=0.03$

MACH..... 0.95
MASS COND: MT1
MODEL: TCAY



CALC	LRF	27Mar98	REVISED	DATE	CONTROL SYSTEM EFFECTS STRENGTH+FLUTTER SIZED AIRPLANE DITS MODEL TCAY BOEING	FIGURE 27 PAGE 33
CHECK						
APPD.						
APPD.						

1
This page will be updated at a later time to include p-k flutter solution for

M=2.60, Mass Condition: MT1, Open Loop Solution

Figure 28

Page 34

This page will be updated at a later time to include p-k flutter solution for

$M=2.60$, Mass Condition: MT1, Mean Axis Solution

Figure 29

Page 35

This page will be updated at a later time to include p-k flutter solution for
M=2.60, Mass Condition: MT1, Gain & Phase Variation for Mean Axis Solution

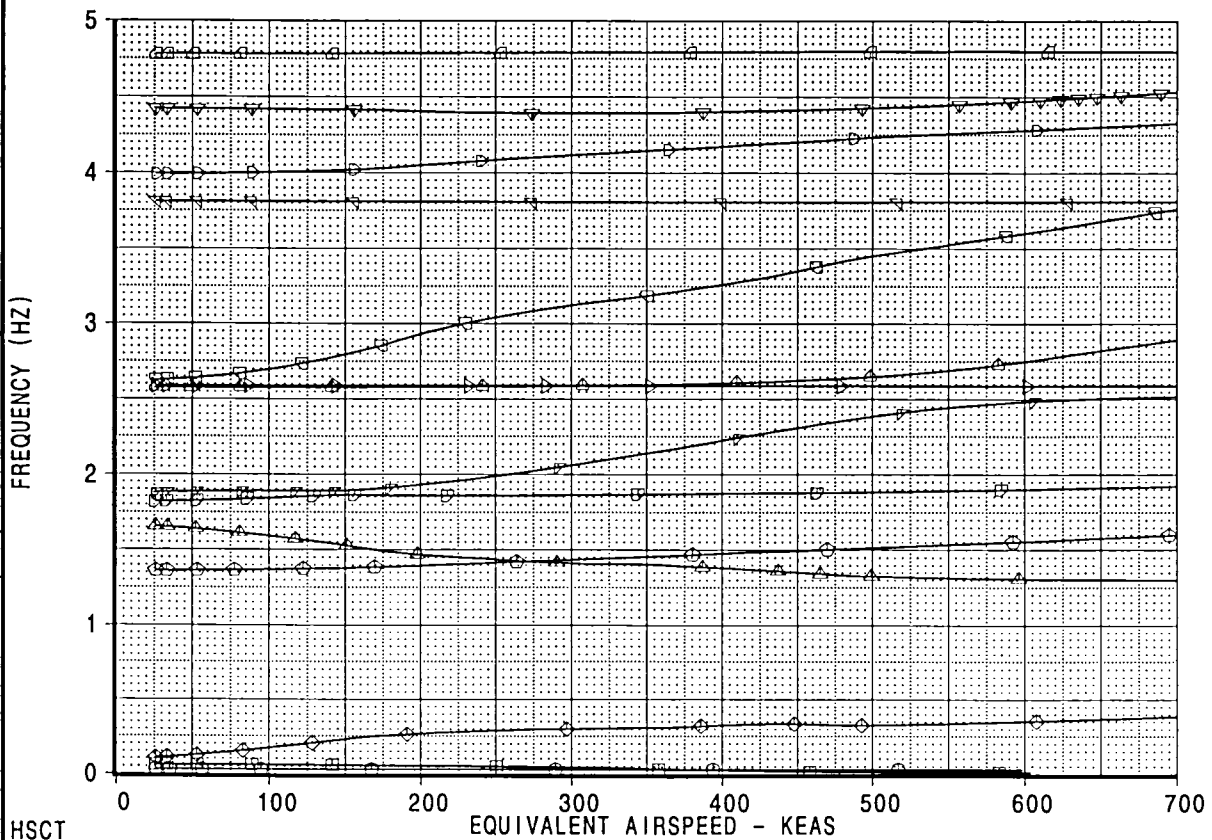
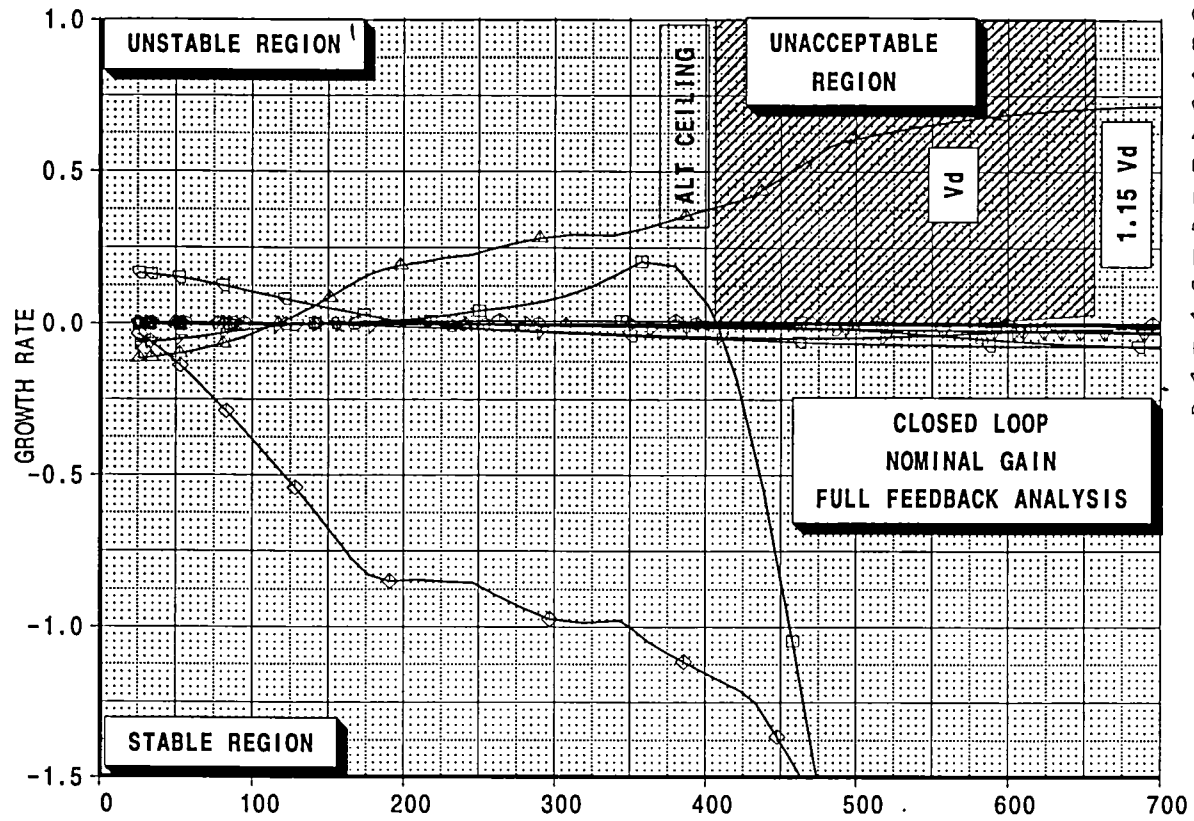
Figure 30

Page 36

SECRET

This information is controlled under the provisions of the Arms Export Control Act (22 U.S.C. 1792) and is not to be released to the public.

**HSCT MODEL TCAY, SYMMETRIC FLUTTER ANALYSIS, M=2.60
GAMMA-DOT V CONTROLLER , MASS:MT1**



HSCT

CALC	LRF	27Mar98	REVISED	DATE
CHECK				
APPD.				
APPD.				
PLOT				

CONTROL SYSTEM EFFECTS
STRENGTH+FLUTTER SIZED AIRPLANE
DITS MODEL TCAY

BOEING

HSCT
FIGURE 31
PAGE 37

[A]: /acct/lrf0076/projects/ffm/mt1/mt1.esb
[B]: /acct/lrf0076/projects/ffm/mt1/gymach95.esb

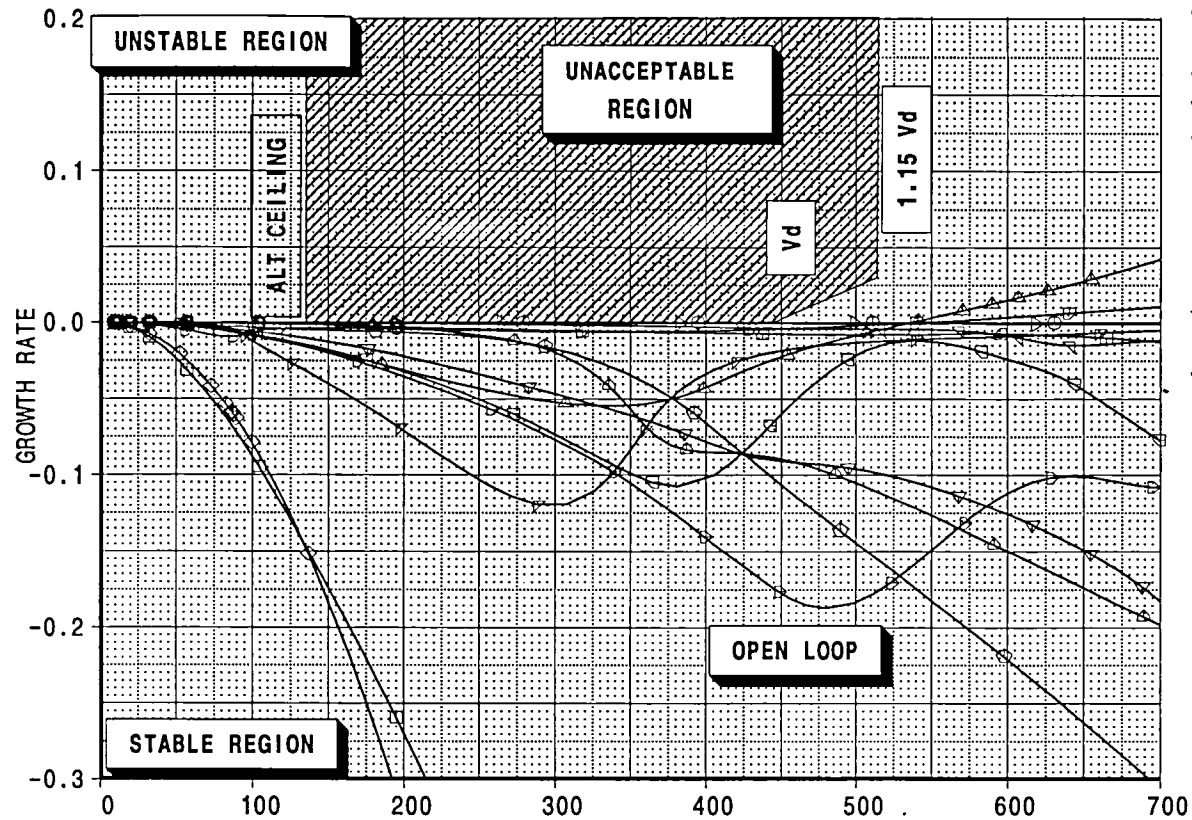
1

This page will be updated at a later time to include p-k flutter solution for
M=2.60, Mass Condition: MT1, Gain & Phase Variation for Full Feed Back
Solution

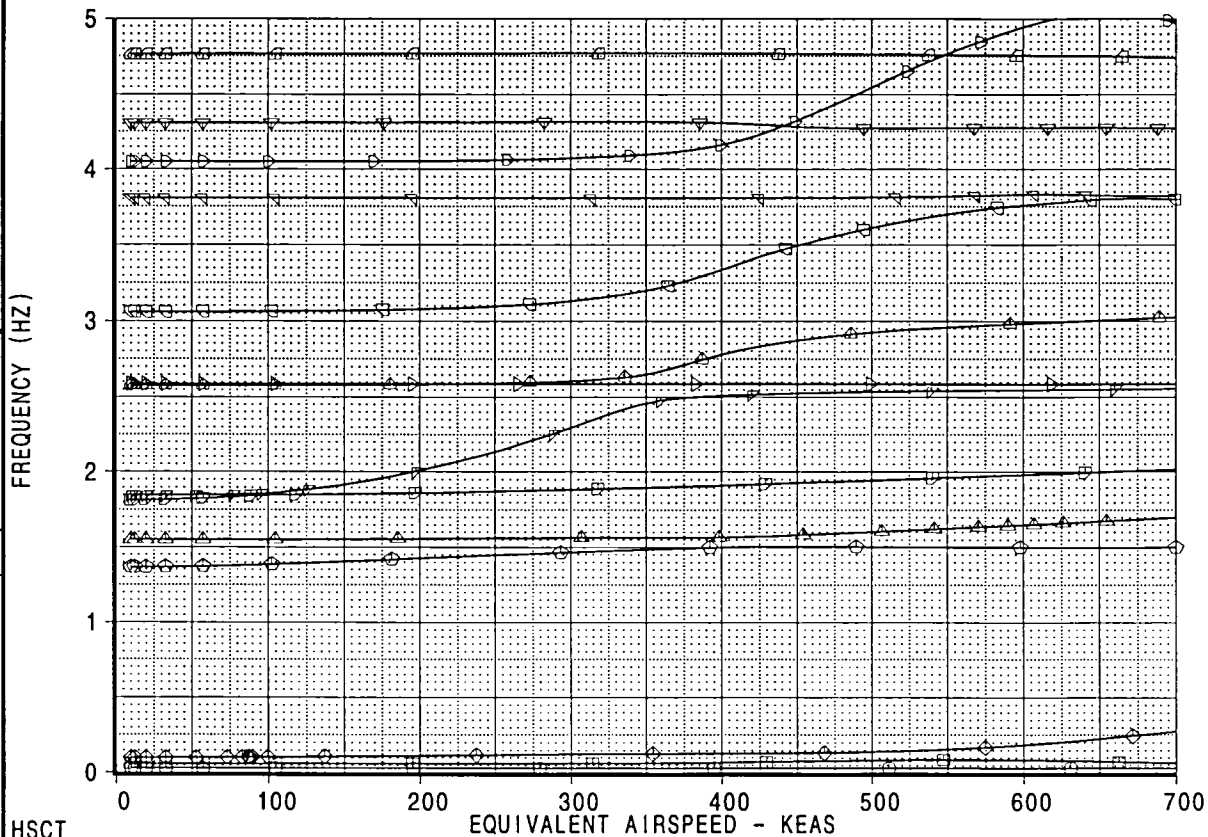
Figure 32

Page 38

HSCT MODEL TCAY, SYMMETRIC FLUTTER ANALYSIS, M=0.95
MASS:MT4



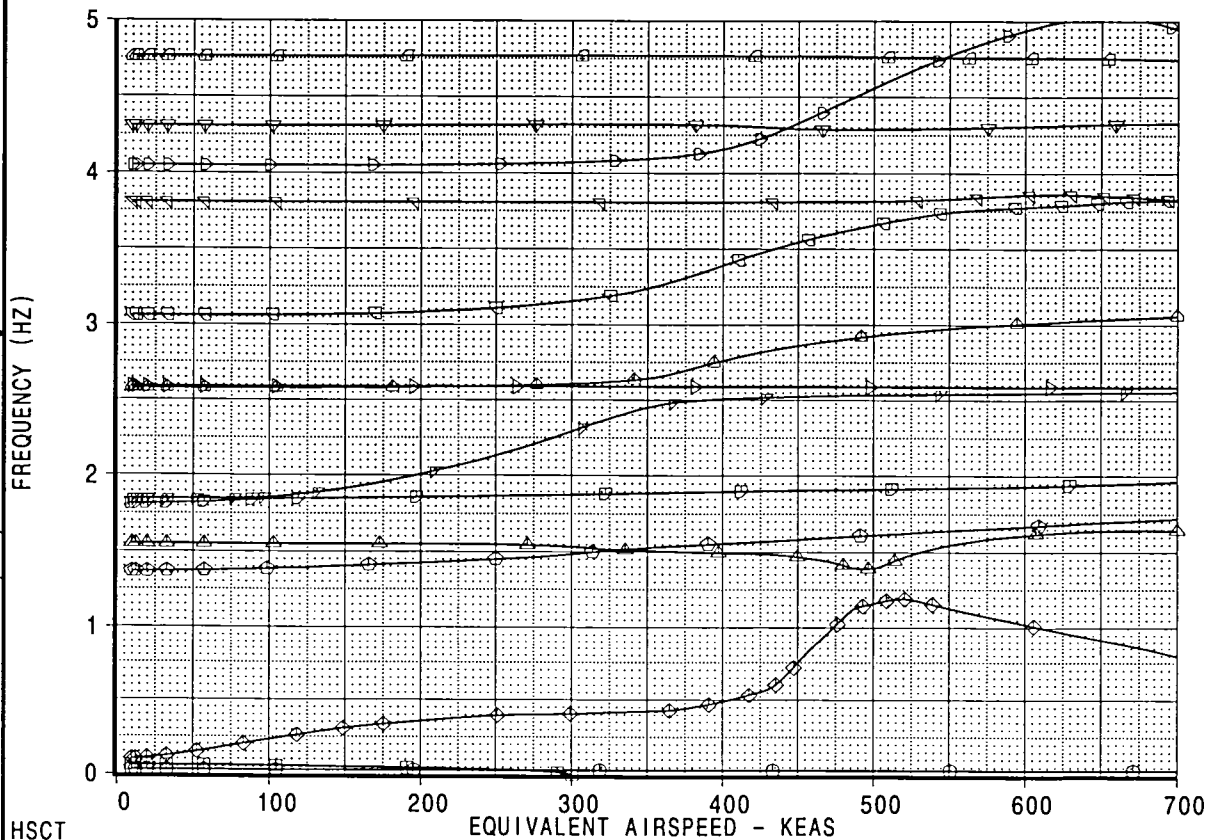
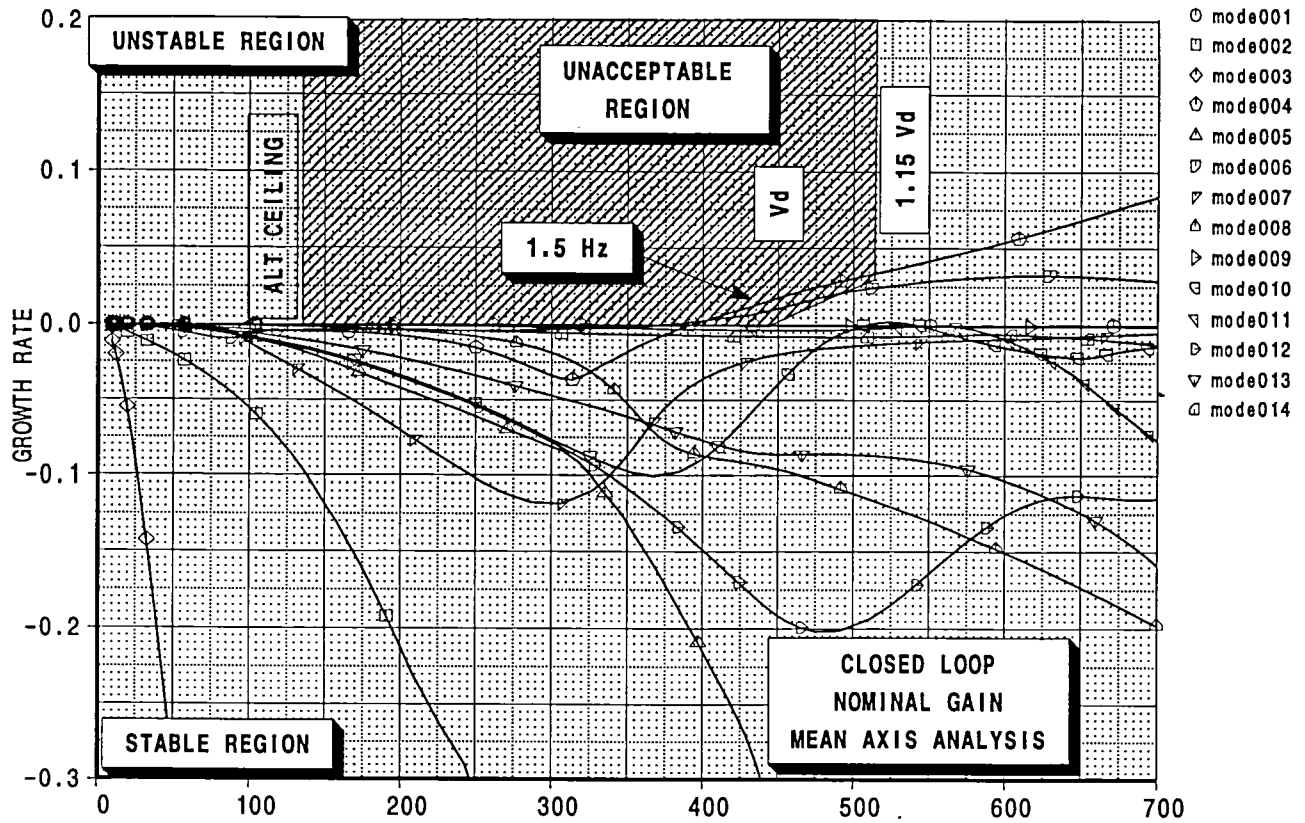
- mode001
- mode002
- ◇ mode003
- ◊ mode004
- △ mode005
- ▽ mode006
- ▽ mode007
- △ mode008
- ▷ mode009
- ◊ mode010
- ▽ mode011
- ▷ mode012
- ▽ mode013
- ◊ mode014



[A]: /acct/lrf0076/projects/ffm/mt4/mt4.esb
 [B]: /acct/lrf0076/projects/ffm/mt4/gvmach95.esb

HSCT					CONTROL SYSTEM EFFECTS STRENGTH+FLUTTER SIZED AIRPLANE DITS MODEL TCAY BOEING	HSCT
CALC	LRF	27Mar98	REVISED	DATE		FIGURE 33
CHECK						
APPD.						
APPD.						PAGE 39
PLOT						

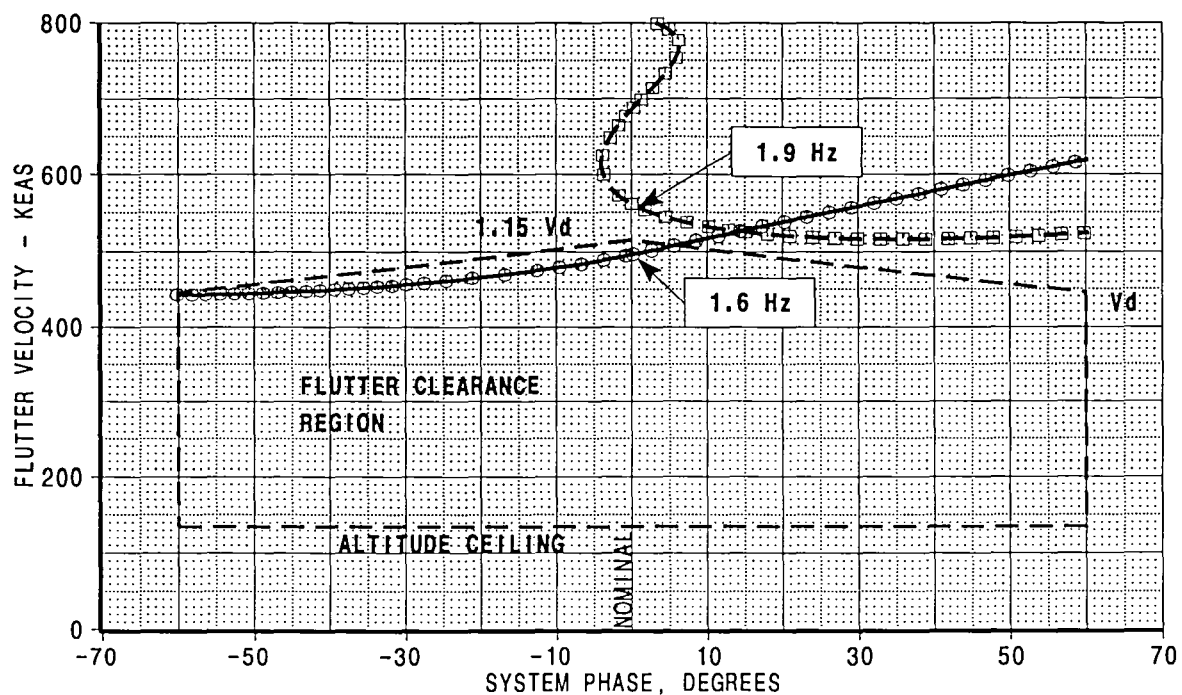
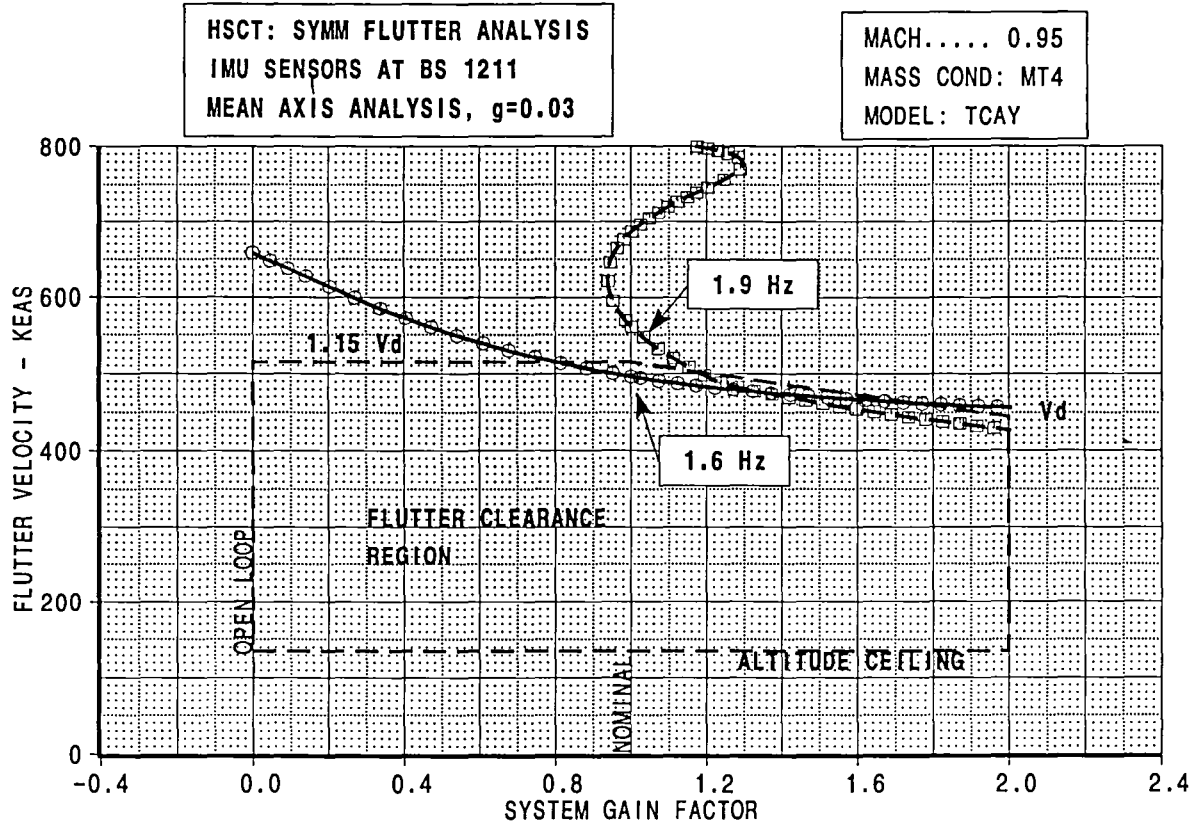
**HSCT MODEL TCAY, SYMMETRIC FLUTTER ANALYSIS, M=0.95
GAMMA-DOT V CONTROLLER , MASS:MT4**



HSCT

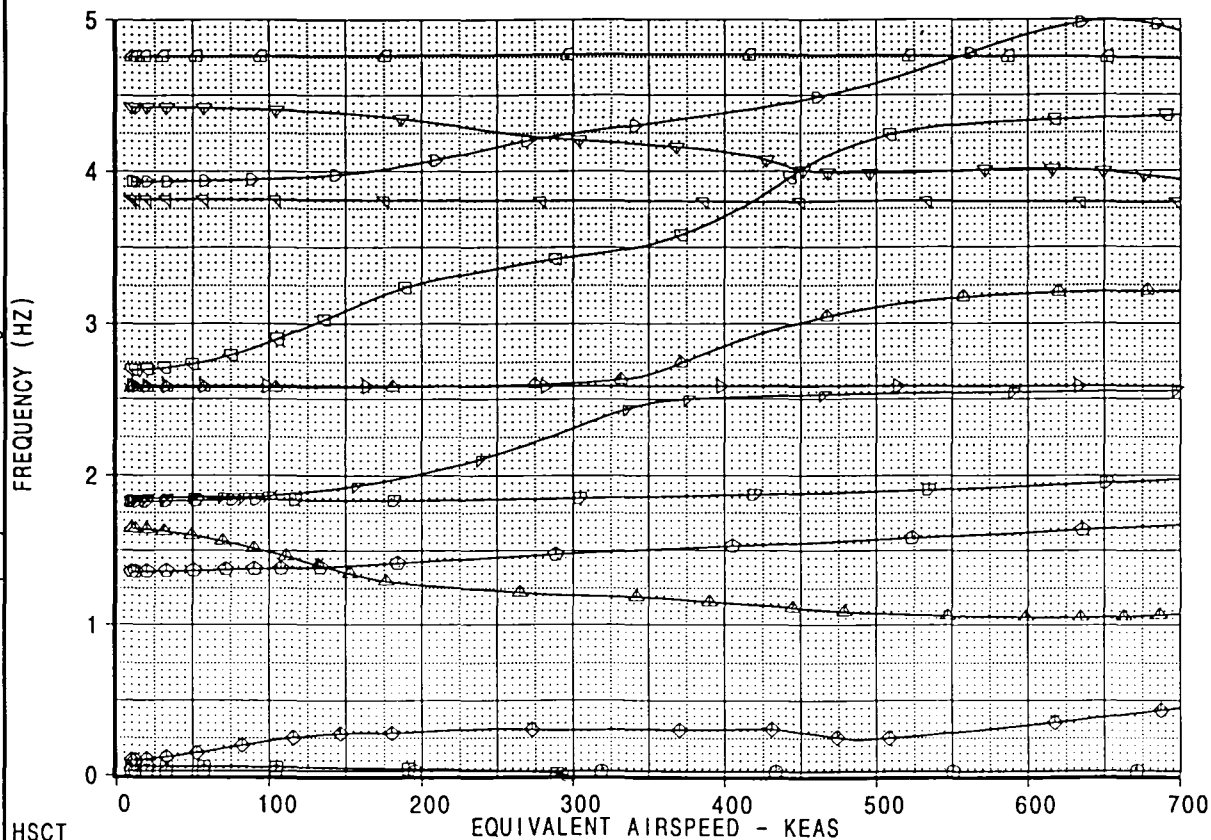
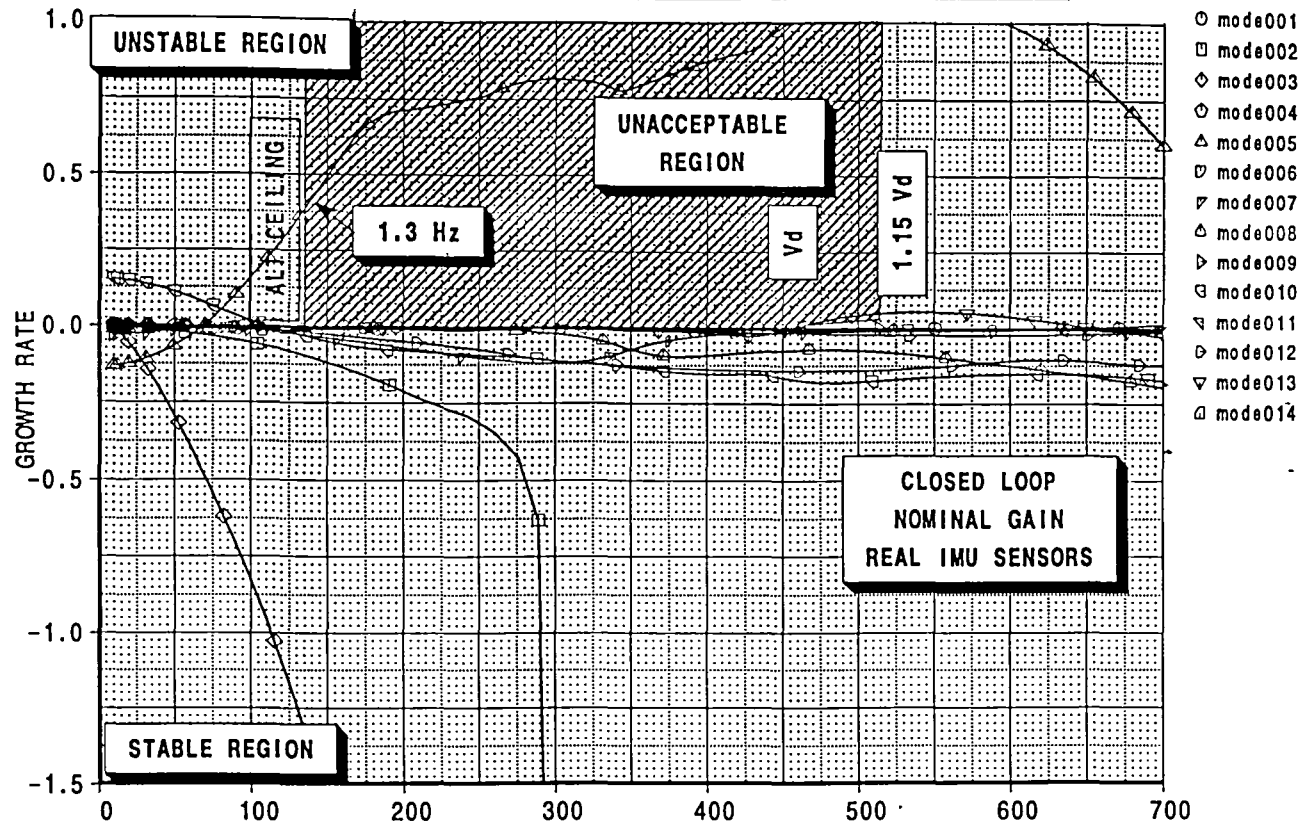
CALC	LRF	27Mar98	REVISED	DATE	CONTROL SYSTEM EFFECTS STRENGTH+FLUTTER SIZED AIRPLANE DITS MODEL TCAY BOEING	HSCT
CHECK						FIGURE 34
APPD.						PAGE
APPD.						4.0
PLOT						

[A]: /acct/lrf0076/projects/ffm/mt4/mt4.esb
[B]: /acct/lrf0076/projects/ffm/mt4/gvmach95.esb



CALC	LRF	27Mar98	REVISED	DATE	CONTROL SYSTEM EFFECTS STRENGTH+FLUTTER SIZED AIRPLANE DITS MODEL TCAY BOEING	FIGURE 35
CHECK						
APPD.						
APPD.						PAGE 41

HSCT MODEL TCAY, SYMMETRIC FLUTTER ANALYSIS, M=0.95
GAMMA-DOT V CONTROLLER , MASS:MT4



HSCT

CALC	LRF	26Mar98	REVISED	DATE
CHECK				
APPD.				
APPD.				
PLOT				

CONTROL SYSTEM EFFECTS
STRENGTH+FLUTTER SIZED AIRPLANE
DITS MODEL TCAY

BOEING

HSCT

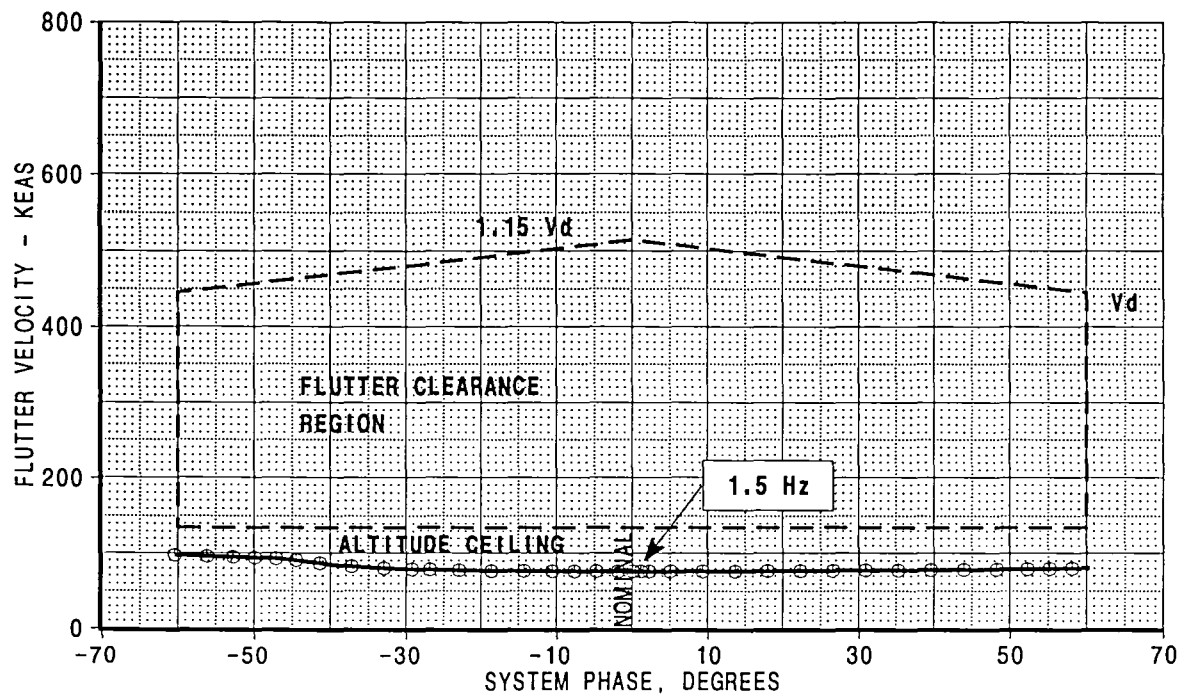
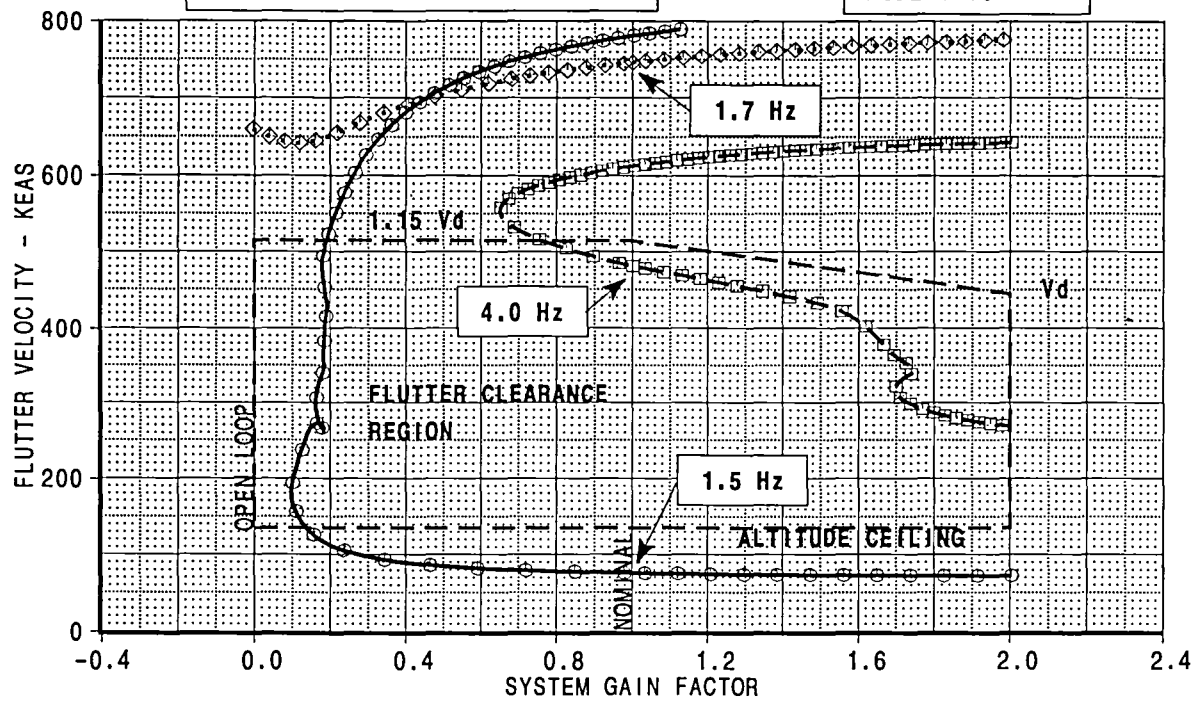
FIGURE 36

PAGE 42

[A]: /acct/lrf0076/projects/fm/mt4/mt4.esb
[B]: /acct/lrf0076/projects/fm/mt4/gvmach95.esb

HSCT: SYMM FLUTTER ANALYSIS
 IMU SENSORS AT BS 1211
 FULL FEEDBACK ANALYSIS, $g=0.03$

MACH..... 0.95
 MASS COND: MT4
 MODEL: TCAY



CALC	LRF	27Mar98	REVISED	DATE	CONTROL SYSTEM EFFECTS STRENGTH+FLUTTER SIZED AIRPLANE DITS MODEL TCAY BOEING	FIGURE 37 PAGE 43
CHECK						
APPD.						
APPD.						

M=2.60, Mass Condition: MT4, Open Loop Solution

Page 44

This page will be updated at a later time to include p-k flutter solution for

$M=2.60$, Mass Condition: MT4, Mean Axis Solution

Figure 39

Page 45

SECRET

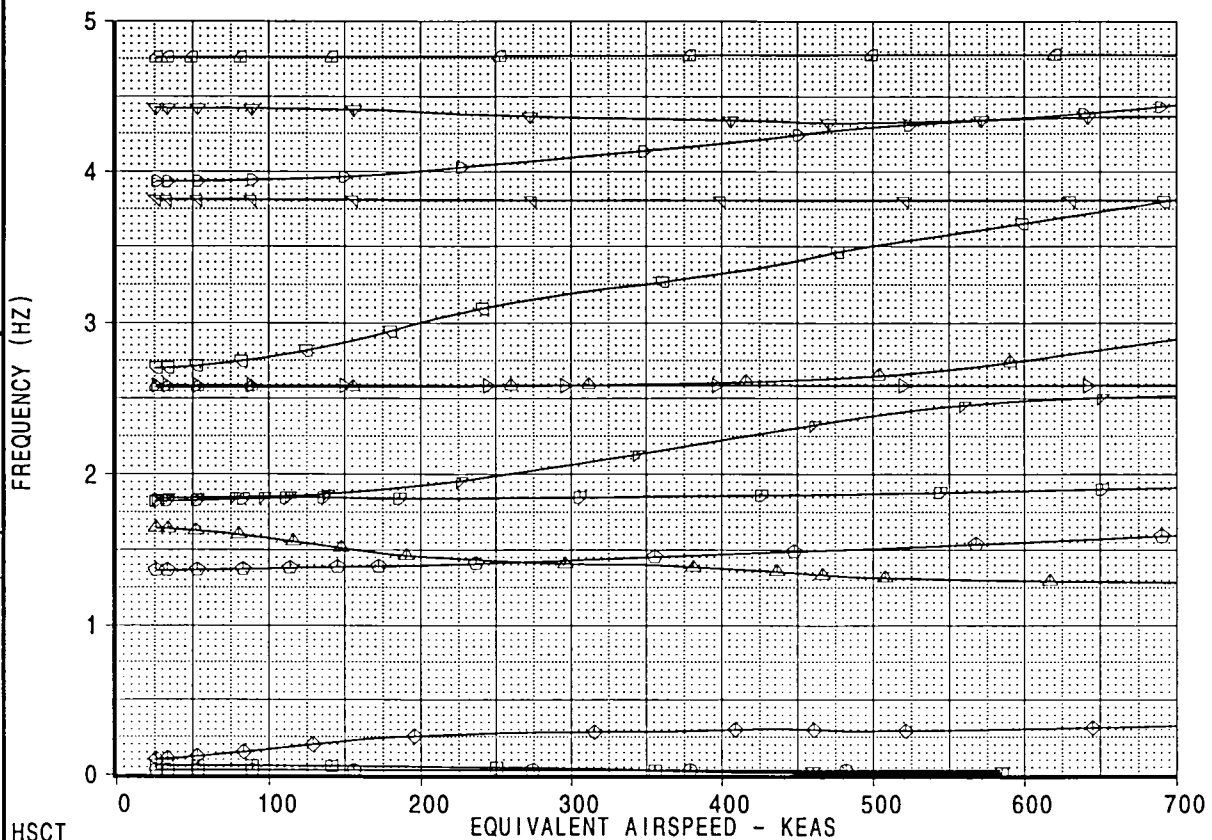
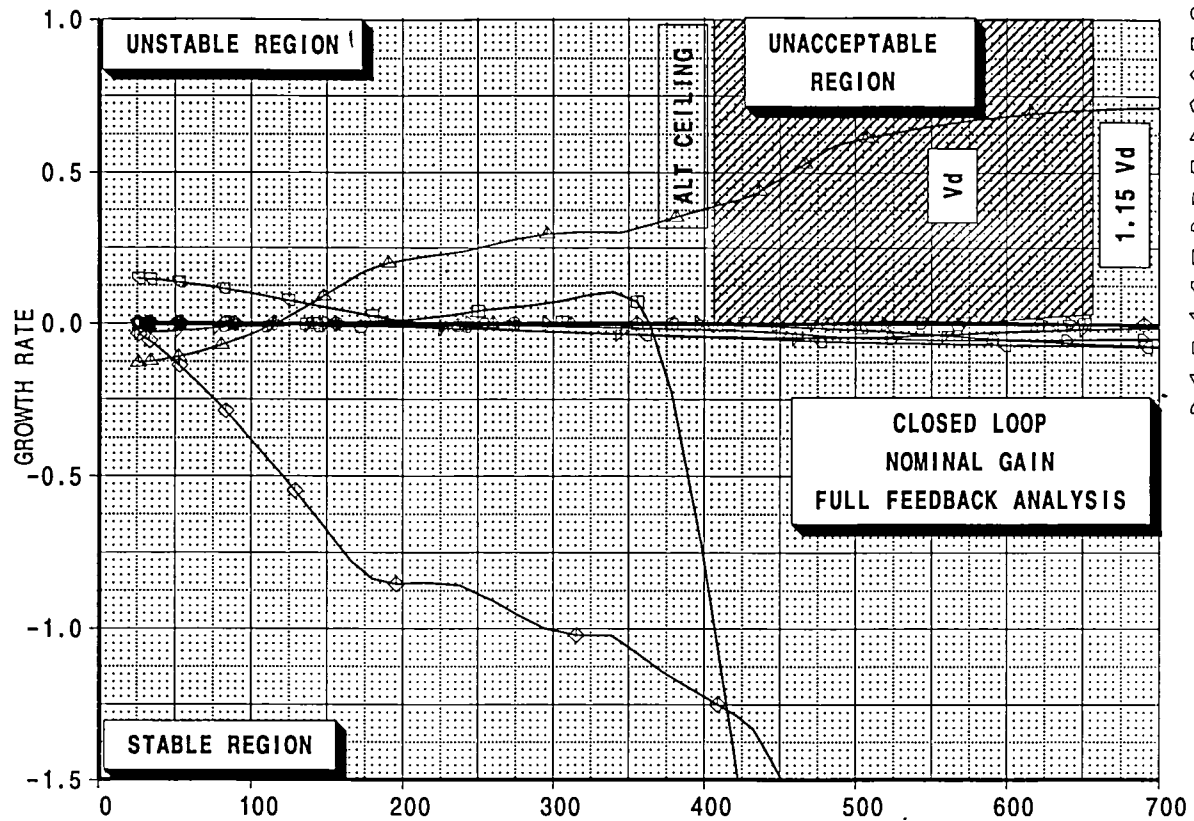
SECRET - This document is sensitive. It is subject to limited distribution and is not to be released to the public.

This page will be updated at a later time to include p-k flutter solution for
M=2.60, Mass Condition: MT4, Gain & Phase Variation (Mean Axis) Solution

Figure 40

Page 46

HSCT MODEL TCAY, SYMMETRIC FLUTTER ANALYSIS, M=2.60
GAMMA-DOT V CONTROLLER , MASS:MT4



HSCT

CALC	LRF	27Mar98	REVISED	DATE
CHECK				
APPD.				
APPD.				
PLOT				

CONTROL SYSTEM EFFECTS
STRENGTH+FLUTTER SIZED AIRPLANE
DITS MODEL TCAY

BOEING

HSCT

FIGURE 4-1

PAGE 47

[A]: /acct/lrf0076/projects/ffm/mt4/mt4.esb
[B]: /acct/lrf0076/projects/ffm/mt4/gvmach95.esb

This page will be updated at a later time to include p-k flutter solution for

M=2.60, Mass Condition: MT4, Gain & Phase Variation Solution

Figure 42

Page 48

M02 Eigenvalues, Mach 0.95

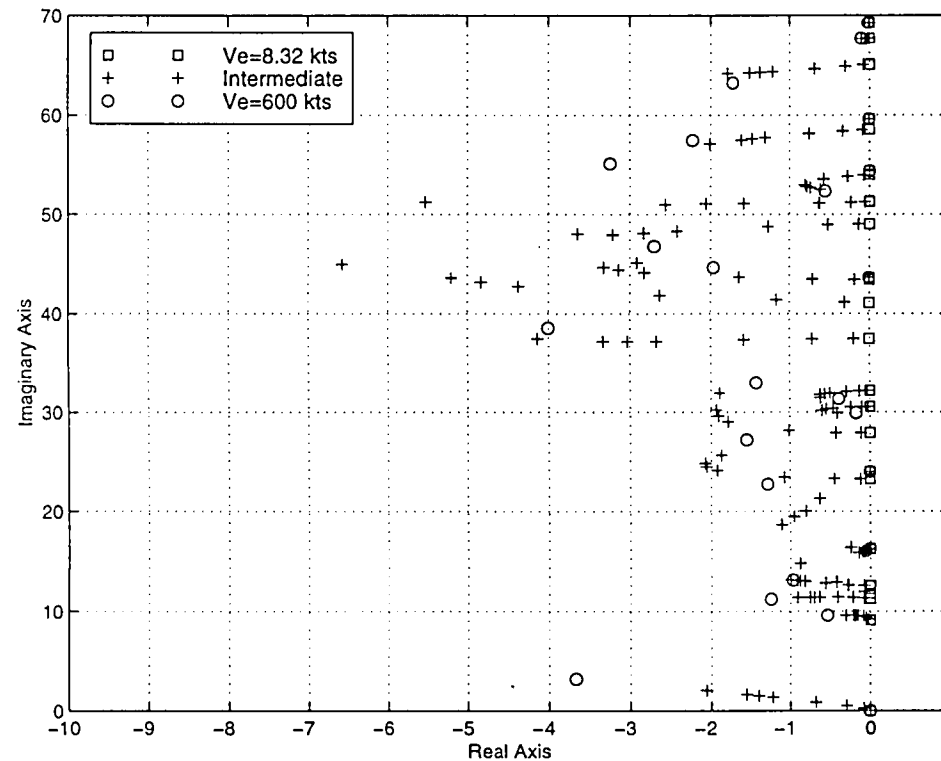


Figure 43: Open Loop Root Locus for: 60 Flex, 2 RB, 2 Assumed, 8 lags

M02 Eigenvalues, Mach 2.6

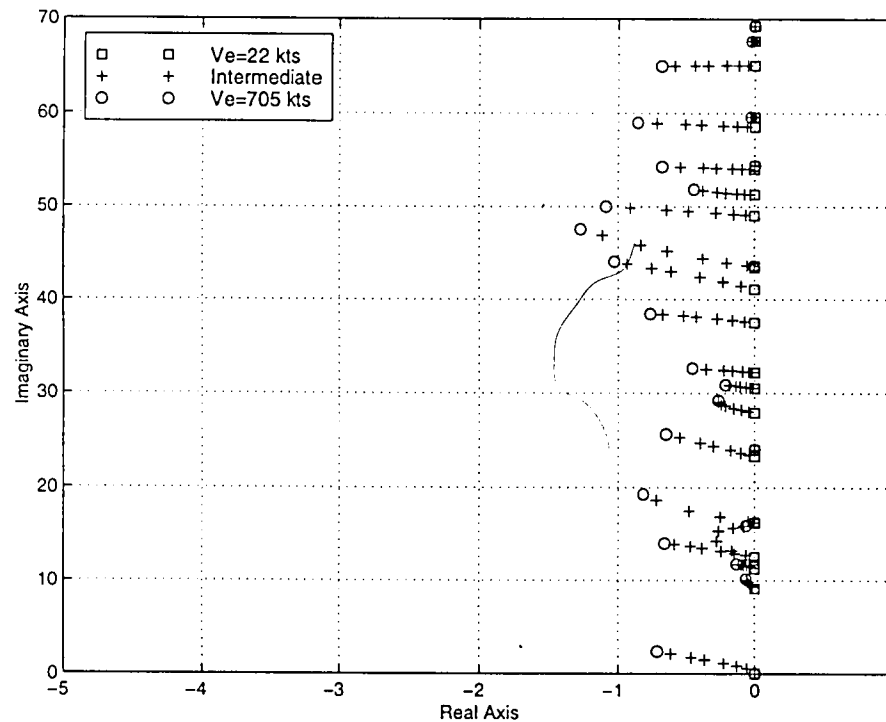


Figure 44: Open Loop Root Locus for: 60 Flex, 2 RB, 2 Assumed, 8 lags

MT1 Eigenvalues, Mach 0.95

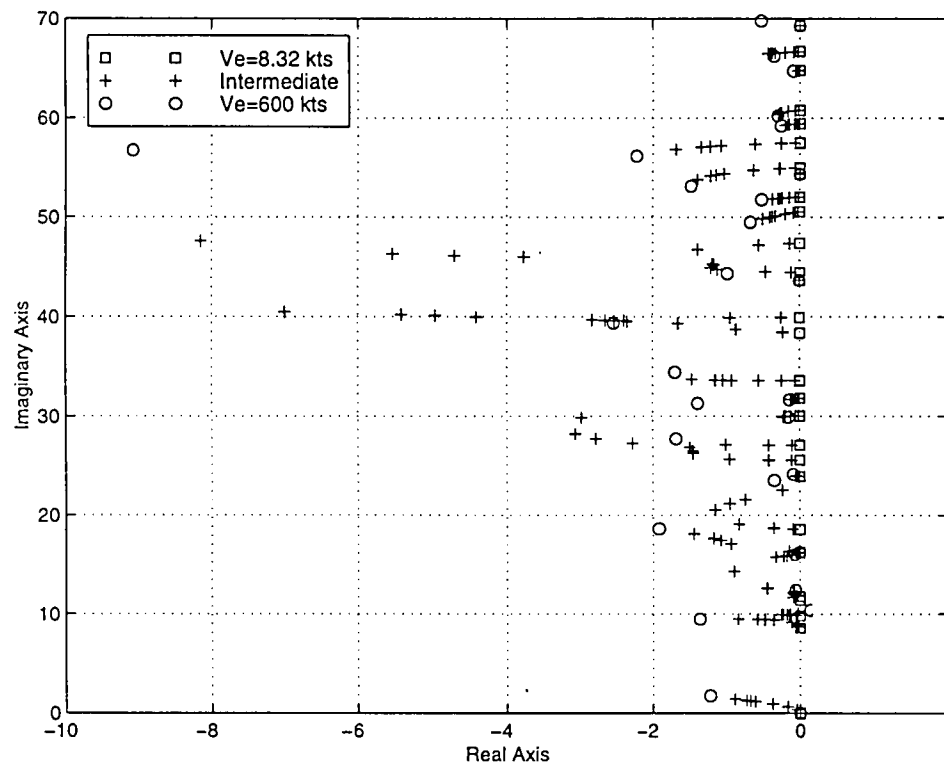


Figure 45: Open Loop Root Locus for: 60 Flex, 2 RB, 2 Assumed, 8 lags

MT1 Eigenvalues, Mach 2.6

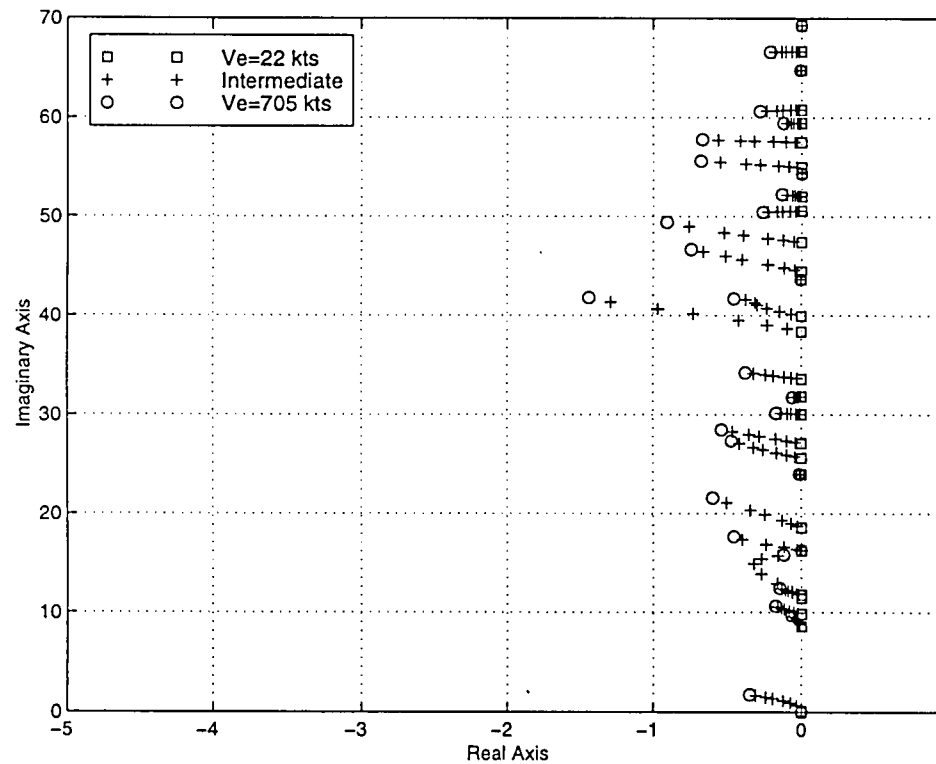


Figure 46: Open Loop Root Locus for: 60 Flex, 2 RB, 2 Assumed, 8 lags

M02 Eigenvalues, Mach 0.95

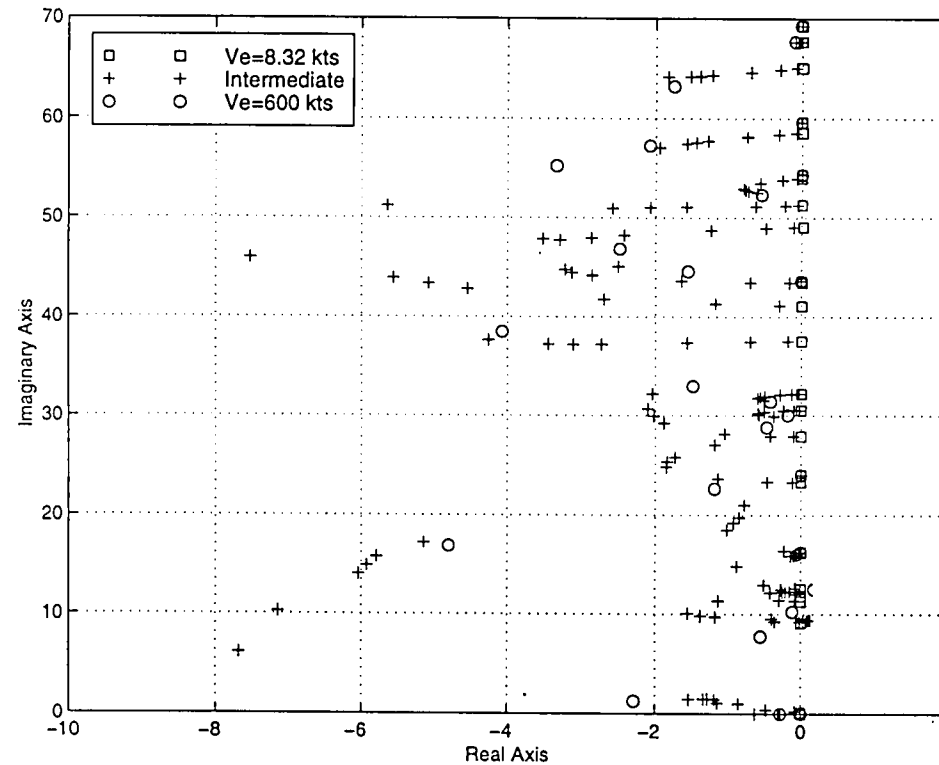


Figure 41: Mean Axis Closed Loop Root Locus for: 60 Flex, 2 RB, 2 Assumed, 8 lags

MT1 Eigenvalues, Mach 0.95

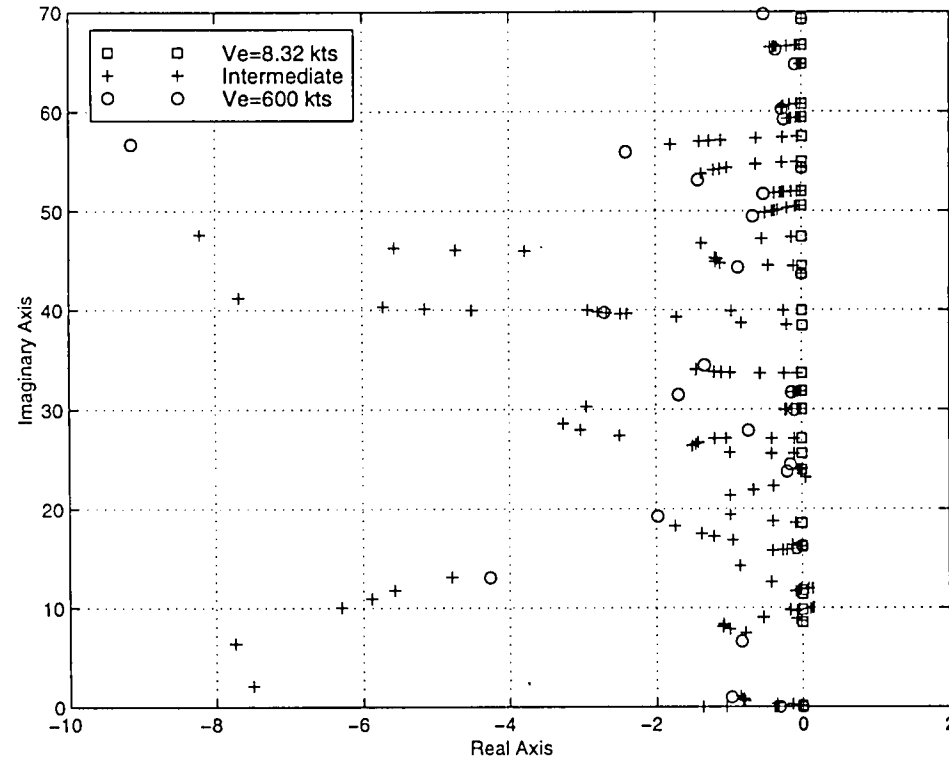


Figure 48: Mean Axis Closed Loop Root Locus for: 60 Flex, 2 RB, 2 Assumed, 8 lags

Closed Loop Eigenvalues

$$M = 0.95$$

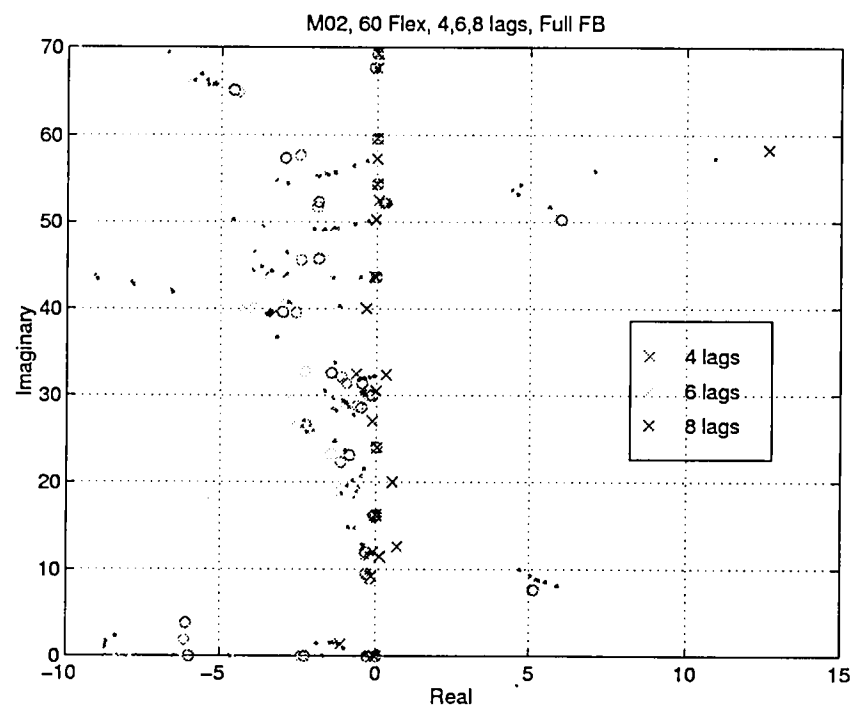


Figure 49: Another View of Closed Loop Root Locus for: M02, 60 Flex, 2 RB, 2 Assumed, 4, 6, & 8 lags, Full Structural IMU Feedback

M02 Eigenvalues, Mach 2.6

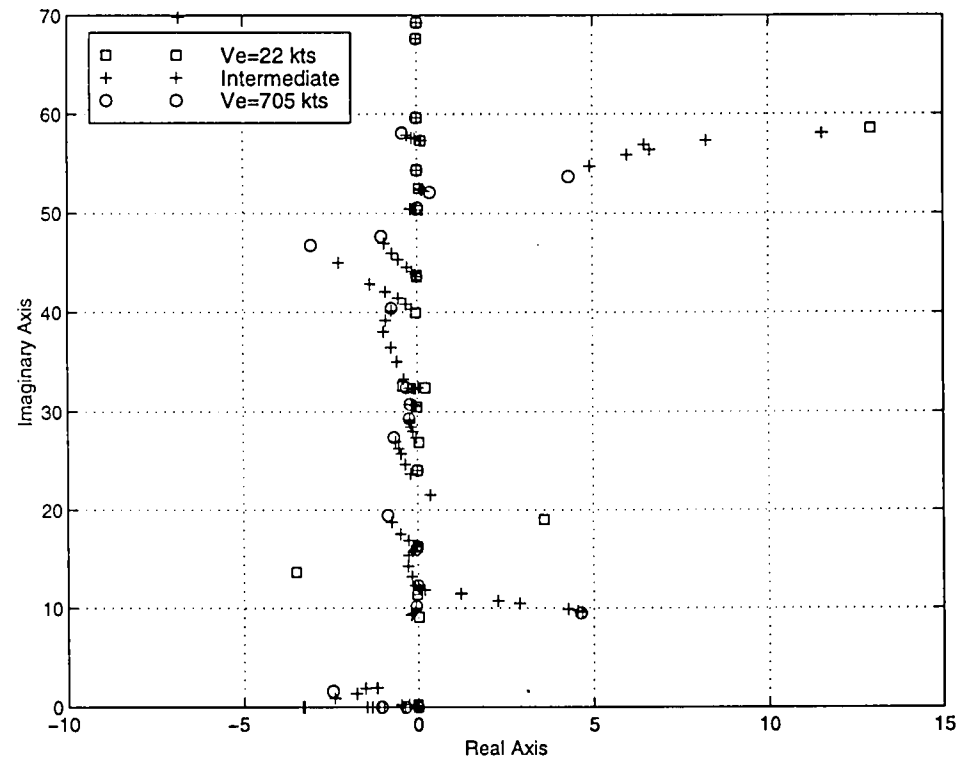


Figure 50: Full Feedback Closed Loop Root Locus for: 60 Flex, 2 RB, 2 Assumed, 8 lags

MT1 Eigenvalues, Mach 0.95

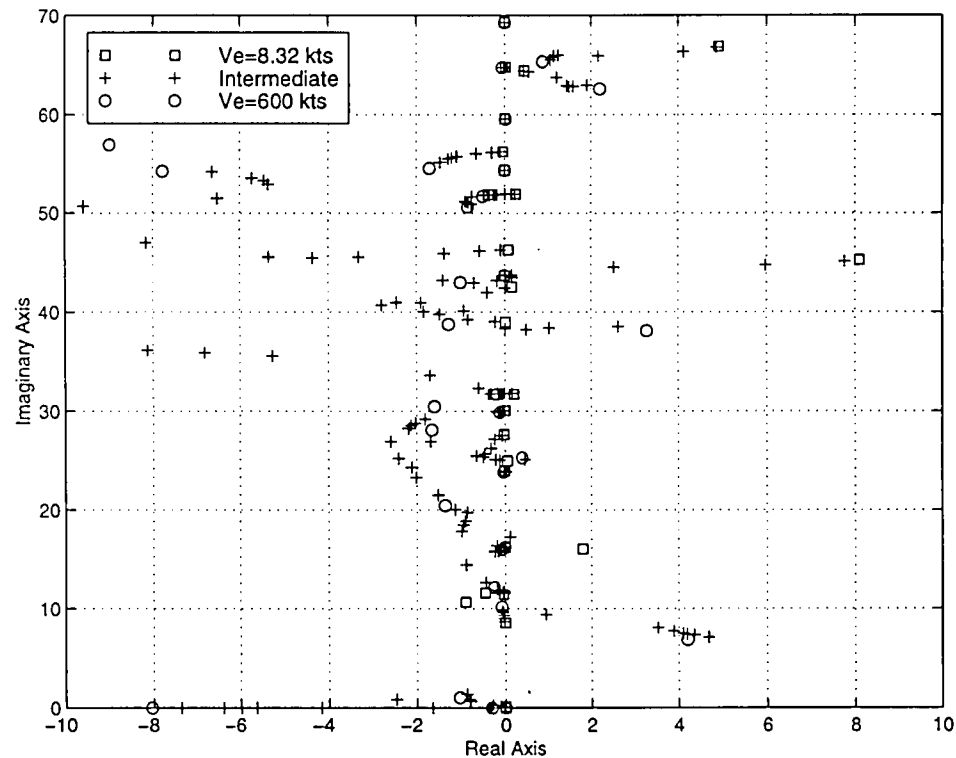


Figure 51: Full Feedback Closed Loop Root Locus for: 60 Flex, 2 RB, 2 Assumed, 8 lags

MT1 Eigenvalues, Mach 2.6

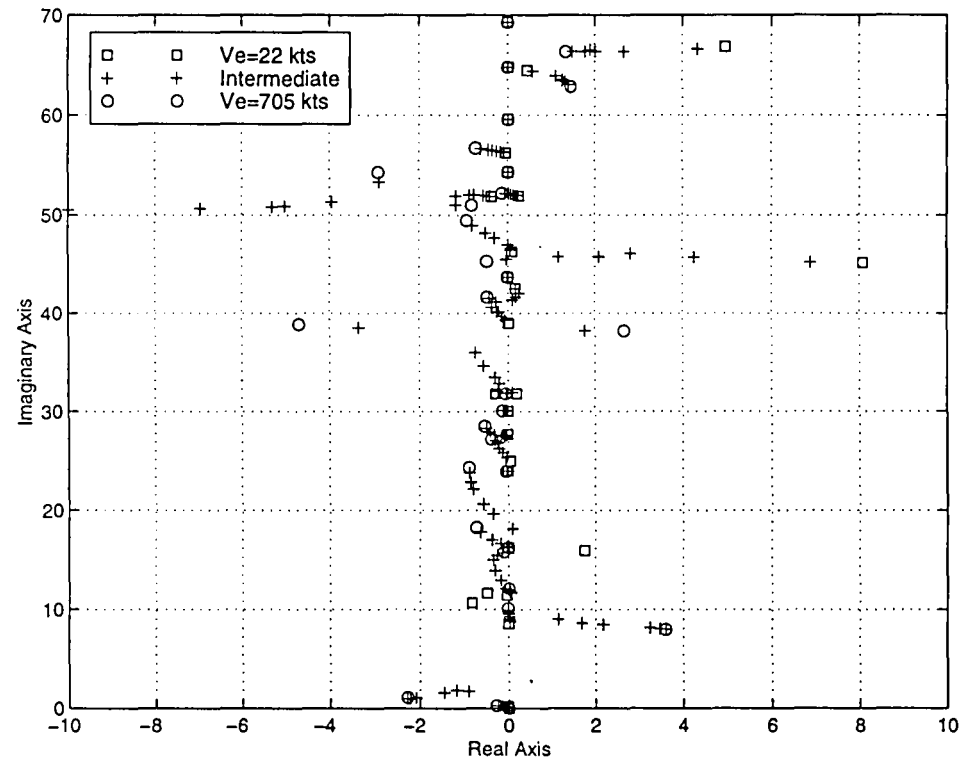
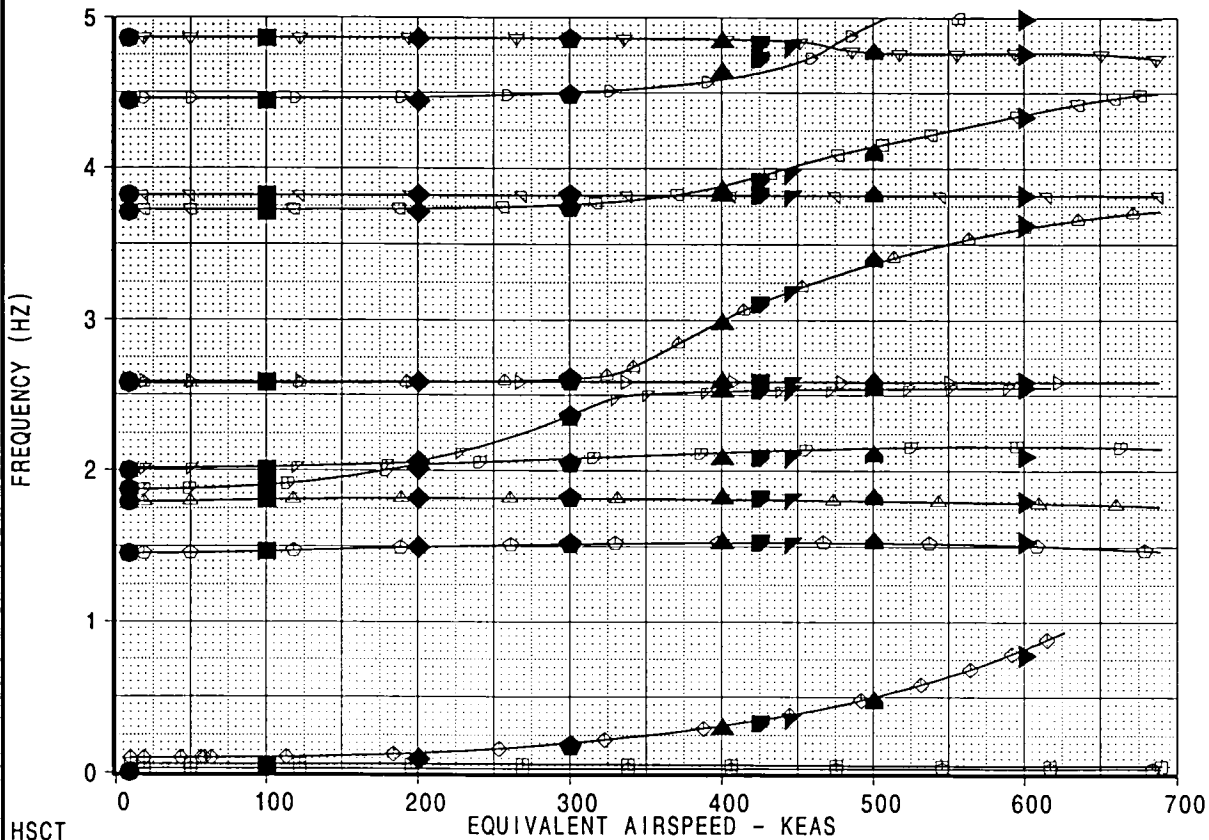
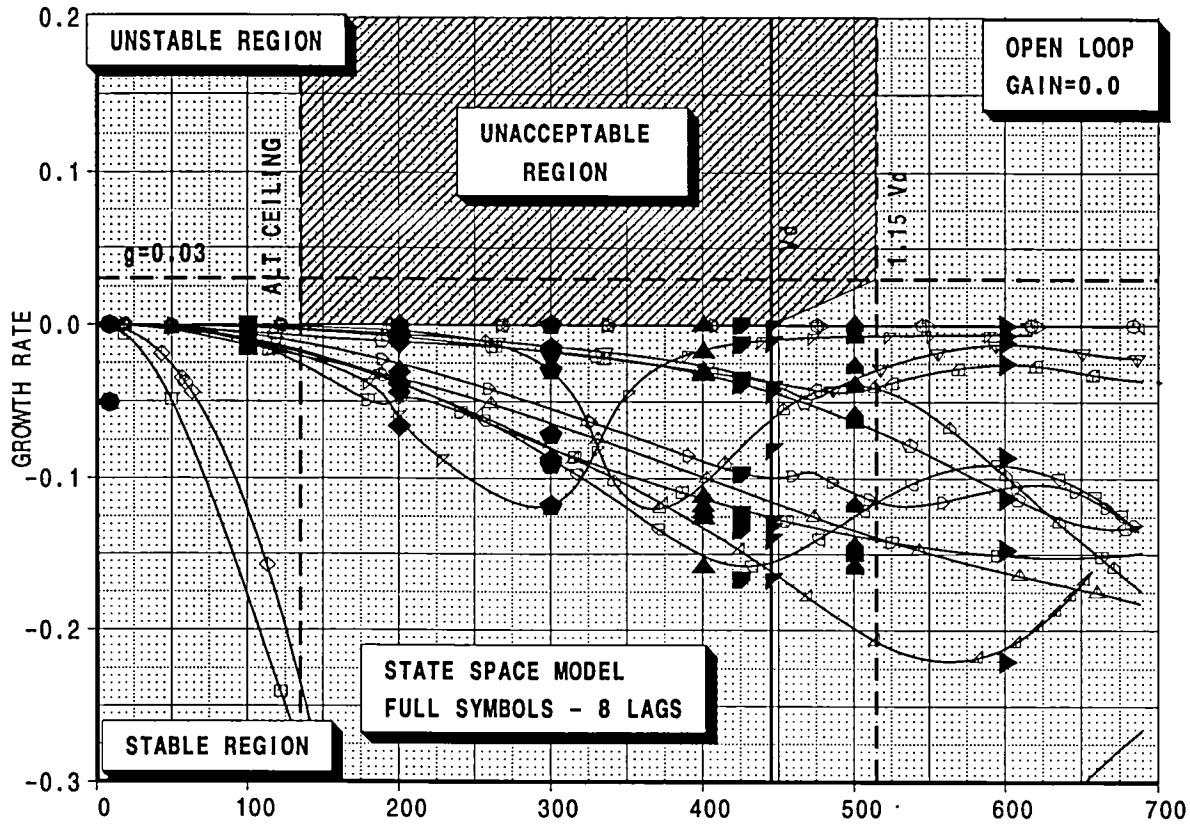


Figure 52: Full Feedback Closed Loop Root Locus for: 60 Flex, 2 RB, 2 Assumed, 8 lags

HSCT MODEL TCAY, SYMMETRIC FLUTTER ANALYSIS, M=0.95
GAMMA-DOT V CONTROLLER, MASS:M02



HSCT

CALC	K.S.NAGARAJA	27Mar98	REVISED	DATE
CHECK				
APPD.				
APPD.				
PLOT				

COMARISON BETWEEN PK & STATE SPACE MODELS
STRENGTH+FLUTTER SIZED AIRPLANE
DITS MODEL TCAY

BOEING

HSCT

FIGURE 53

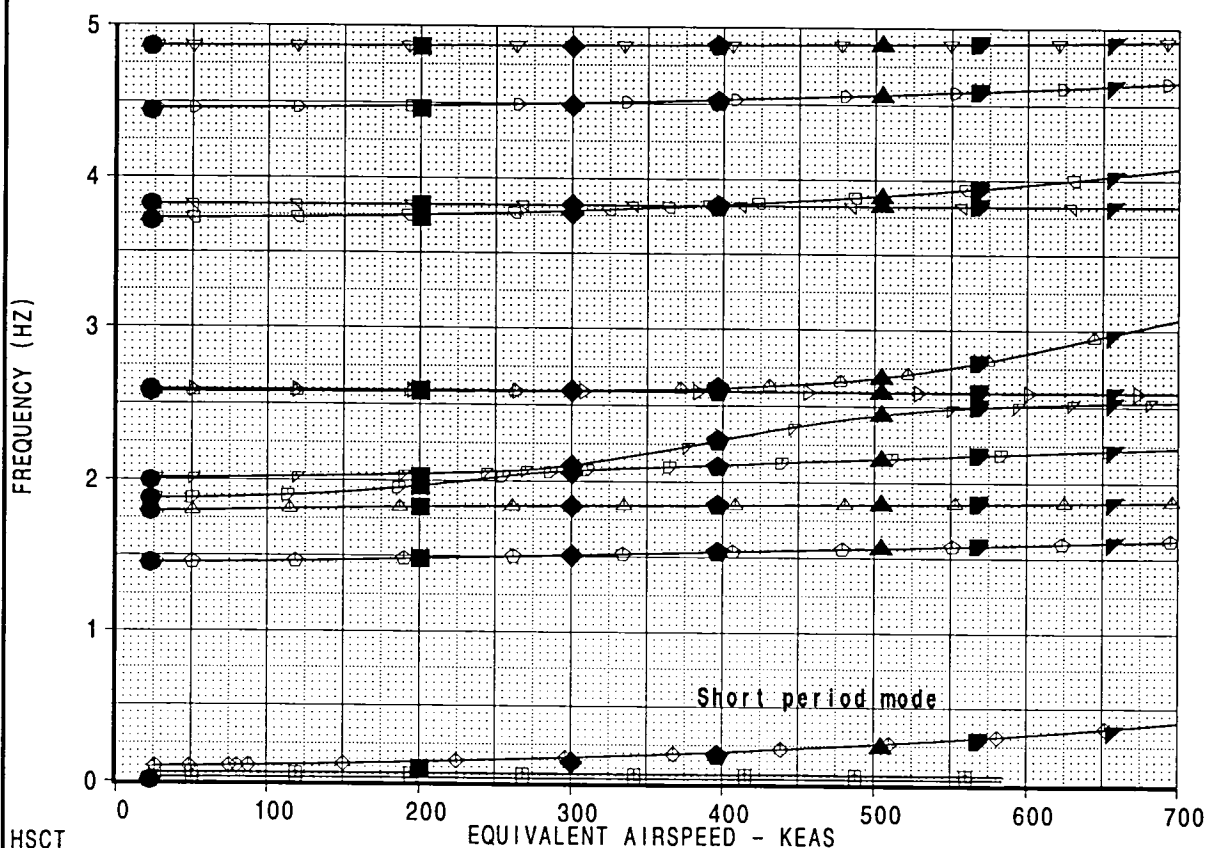
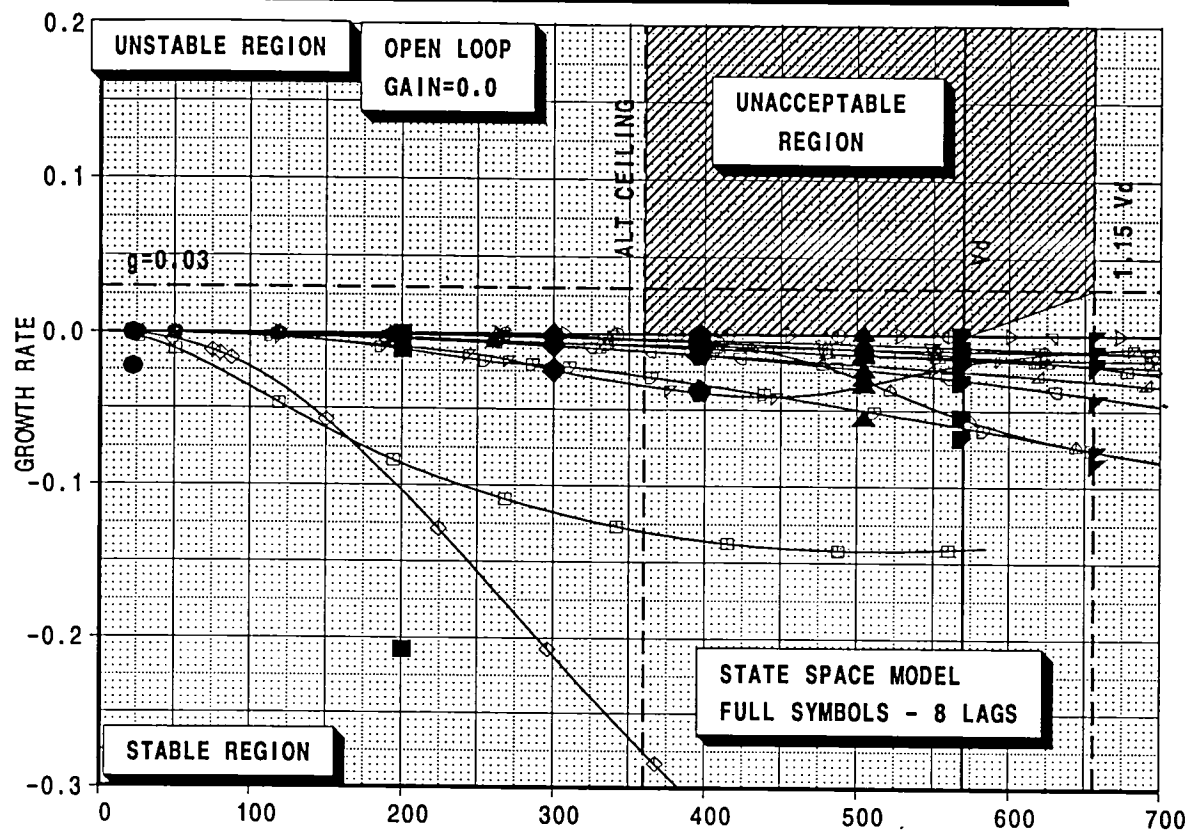
PAGE 59

1) : /acct/ksn8042/ASE/PLOTS/VGPLOTS/mach95.esb

[B] : /acct/ksn8042/ASE/M02/DOC/b595t5a6b1C0.esb

[C] : /acct/ksn8042/ASE/PLOTS/VGPLOTS/M95/FILES/m02m95o11.esb

HSCT MODEL TCAY, SYMMETRIC FLUTTER ANALYSIS, M=2.60
GAMMA-DOT V CONTROLLER, MASS:M02



HSCT

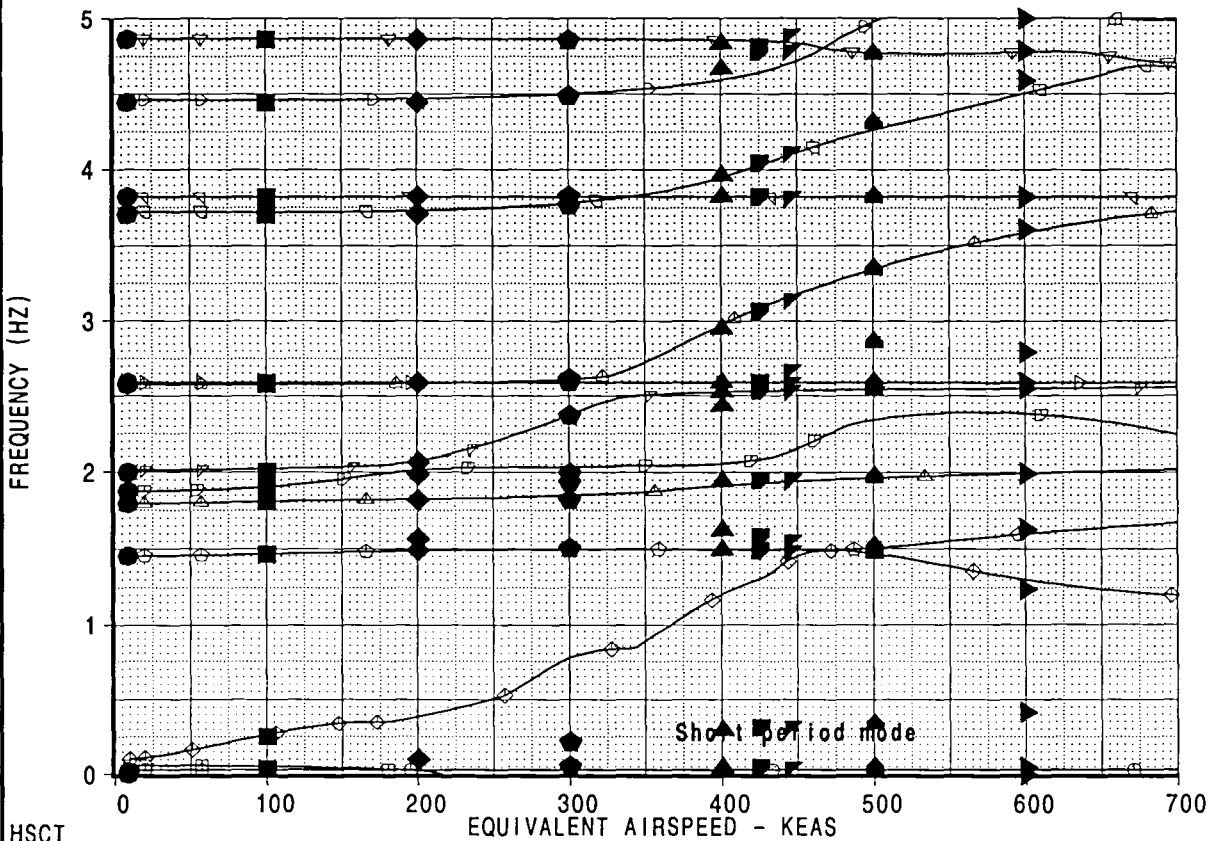
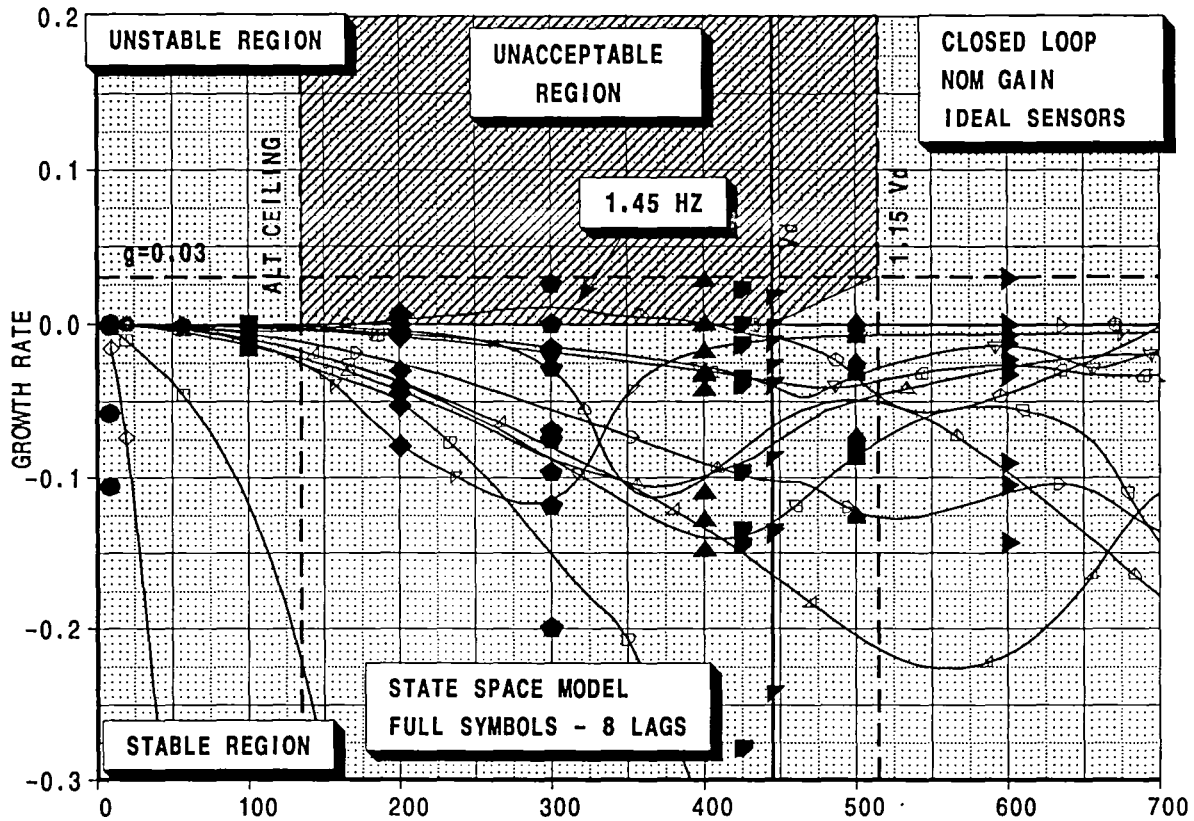
CALC	K.S.NAGARAJA	27Mar98	REVISED	DATE	COMPARISON BETWEEN PK & STATE SPACE MODELS	HSCT
CHECK					STRENGTH+FLUTTER SIZED AIRPLANE	FIGURE 54
APPD.					DITS MODEL TCAY	
APPD.						
PLOT						

BOEING

PAGE 60

[A]: /acct/ksn8042/ASE/PLOTS/VGPLOTS/mach26.esb
[B]: /acct/ksn8042/ASE/M02/DOC/b59515a6a100.esb
[C]: /acct/ksn8042/ASE/PLOTS/VGPLOTS/M95/FILES/m02m26o11.esb

HSCT MODEL TCAY, SYMMETRIC FLUTTER ANALYSIS, M=0.95
GAMMA-DOT V CONTROLLER, MASS:M02



HSCT

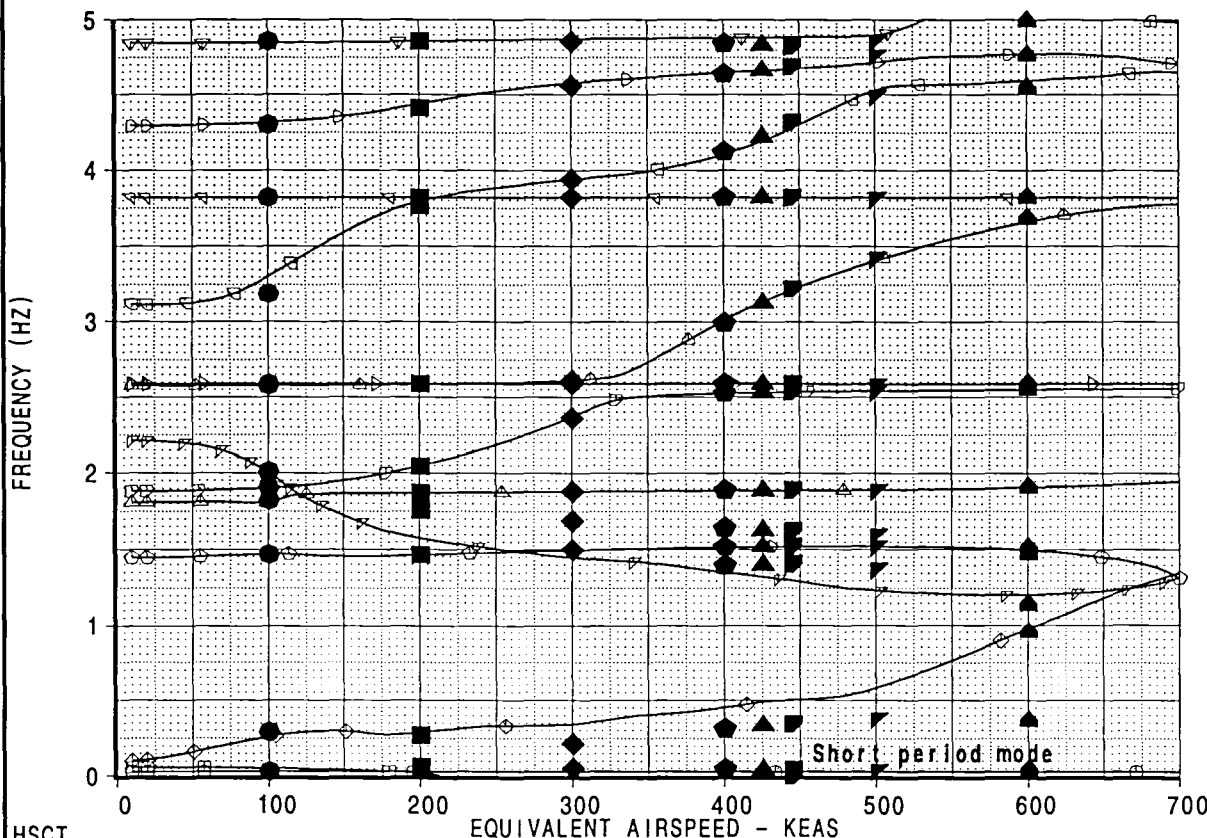
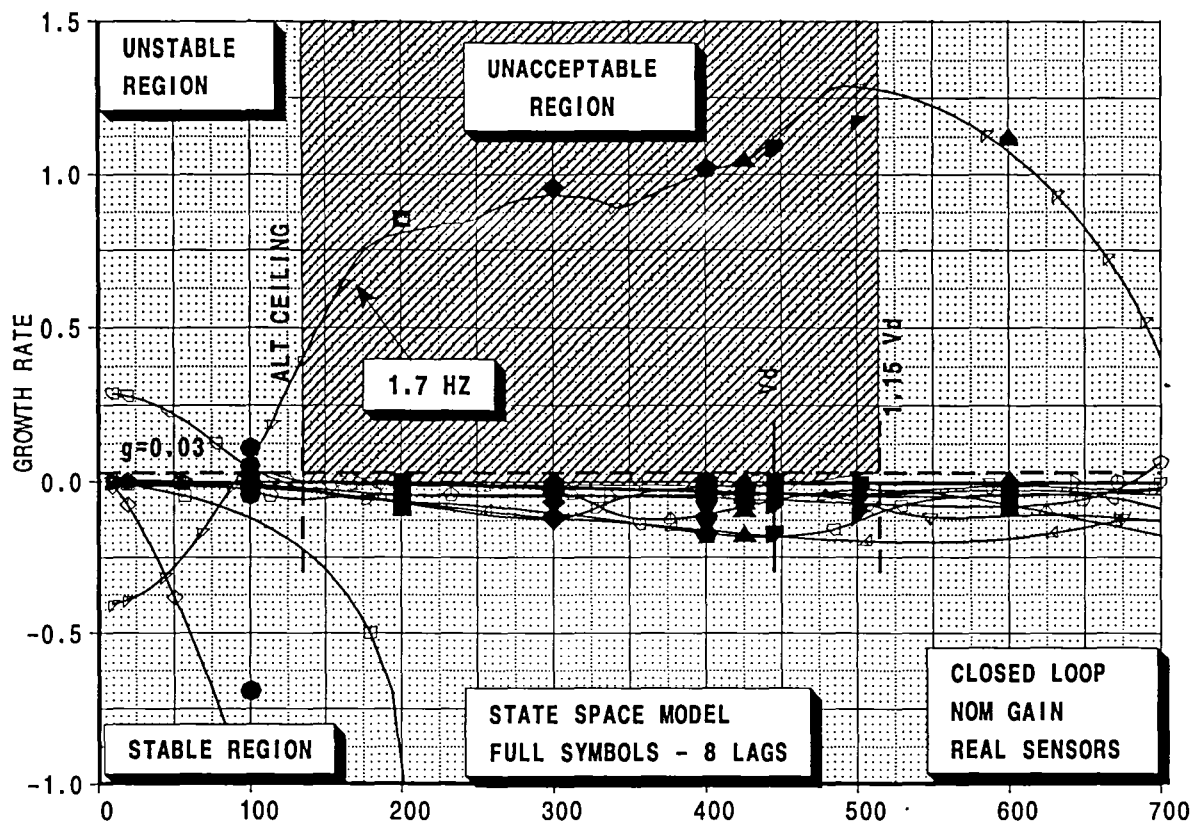
CALC	K.S.NAGARAJA	27Mar98	REVISED	DATE	COMPARISON BETWEEN PK & STATE SPACE MODELS STRENGTH+FLUTTER SIZED AIRPLANE DITS MODEL TCAY BOEING	HSCT
CHECK						FIGURE 55
APPD.						
APPD.						PAGE
PLOT						61

A]: /acct/ksn8042/ASE/PLOTS/VGPLOTS/mach95.esb

[B]: /acct/ksn8042/ASE/M95/M02/DOC/b59515a6aC1.esb

[C]: /acct/ksn8042/ASE/PLOTS/VGPLOTS/M95/FILES/m02m95ma1.esb

HSCT MODEL TCAY, SYMMETRIC FLUTTER ANALYSIS, M=0.95
GAMMA-DOT V CONTROLLER , MASS:M02



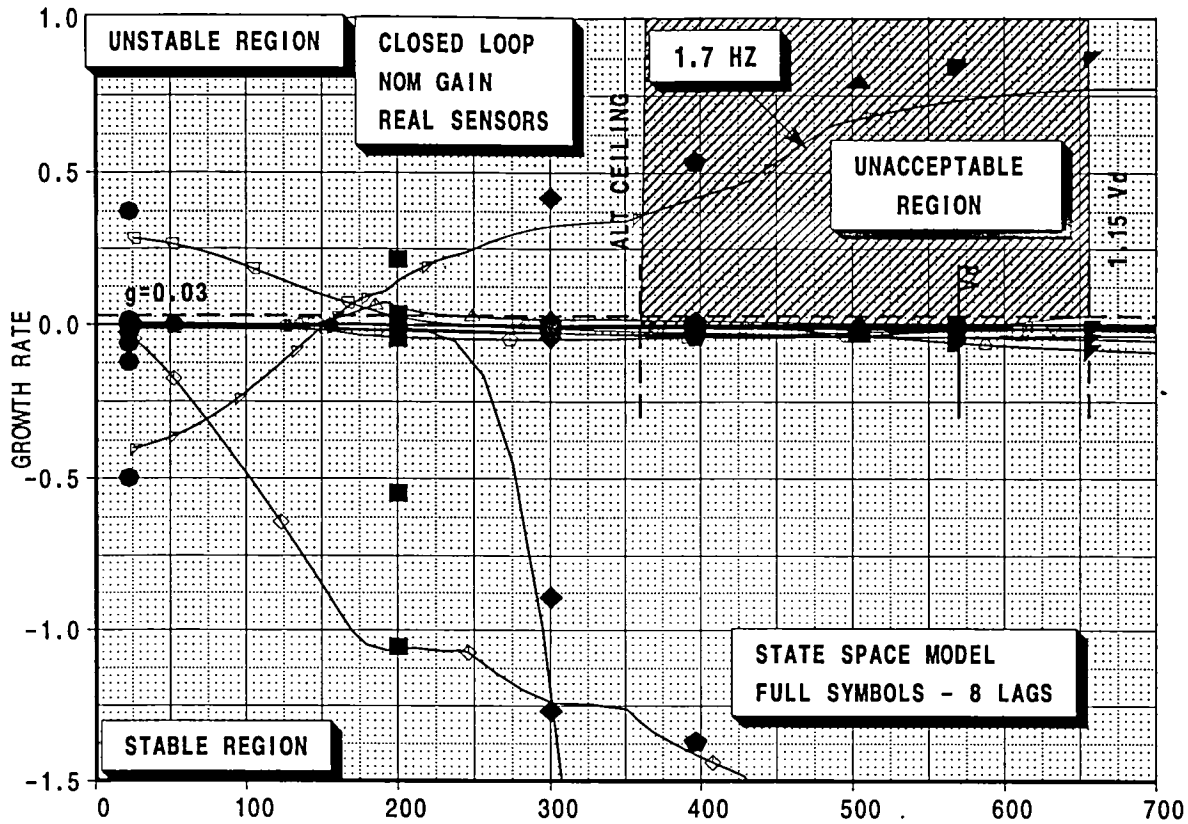
HSCT	ALC	K.S.NAGARAJA	27Mar98	REVISED	DATE	COMPARISON BETWEEN PK AND STATE SPACE MODEL	HSCT
	CHECK						FIGURE 56
	APPD.					DITS MODEL TCAY	PAGE 62
	APPD.					BOEING	
	PLOT						

A): /acct/ksn8042/ASE/PLOTS/VGPLOTS/mach95.esb

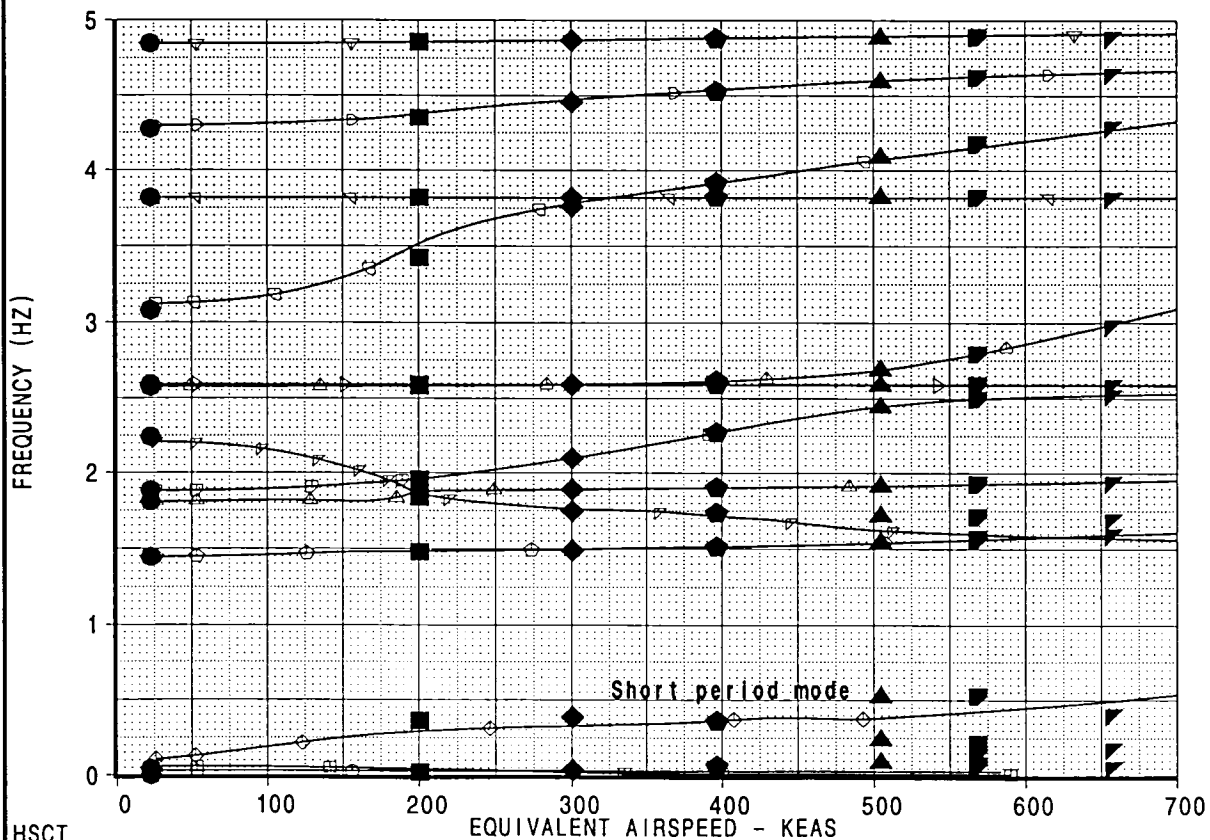
[B]: /acct/ksn8042/ASE/M02/DOC/b59515a6bC1.esb

[C]: /acct/ksn8042/ASE/PLOTS/VGPLOTS/M95/FILES/eigvals_60_8_2_c1f3.esb

HSCT MODEL TCAY, SYMMETRIC FLUTTER ANALYSIS, M=2.60
GAMMA-DOT V CONTROLLER, MASS:M02



- speed22
- speed200
- ◆ speed300
- ◆ speed396
- ▲ speed504
- ▼ speed568
- ▼ speed656
- ▲ speed705
- mode001
- mode002
- ◇ mode003
- ◇ mode004
- △ mode005
- ▽ mode006
- ▽ mode007
- △ mode008
- ▷ mode009
- ▽ mode010
- ▽ mode011
- ▷ mode012
- ▽ mode013
- ◇ mode014
- △ mode015



HSCT	CALC	K.S.NAGARAJA	27Mar98	REVISED	DATE	COMPARISON BETWEEN PK & STATE SPACE MODELS STRENGTH+FLUTTER SIZED AIRPLANE DITS MODEL TCAY	HSCT
	CHECK						FIGURE 57
	APPD.						PAGE
	APPD.						63
	PLOT						

BOEING

APPENDIX A

Analytical Approach for Closed Loop Flutter Analysis

Task 20: Sub Task 7 - Aeroservoelastic Design Studies

High Speed Civil Transport



ANALYSIS PROCESS

- STRUCTURAL DYNAMIC MODEL : DITS TCAY MODEL WITH STIFFENED ACTUATOR SPRINGS FOR STABILIZER AND ELEVATORS
- PITCH CONTROL LAWS (GAMMA DOT - V CONTROLLER) DEFINED BY GFC BASED ON QSAE MODELS
- INCORPORATED THE CONTROLLER IN DYNAMIC EQUATIONS OF MOTION IN TO THE BOEING (SEATTLE) P-K FLUTTER ANALYSIS PROCESS
- ESTABLISHED OPEN LOOP AND CLOSED LOOP FLUTTER SOLUTIONS FOR THE PITCH CONTROLLER
- ESTABLISHED WITH FLIGHT CONTROLS TO VERIFY CONCURRENCE BETWEEN P-K FLUTTER SOLUTION RESULTS & STATE-SPACE MODEL RESULTS

Task 20: Sub Task 7 - Aeroservoelastic Design Studies

High Speed Civil Transport

DYNAMICS MODEL

- DITS TCAY MODEL OPTIMIZED FOR STRENGTH AND FLUTTER
- MASS CONDITIONS CONSIDERED - M1, M02, ML2, MCF, MCI, MT1, MT4
- UNSTEADY AERODYNAMICS
 - DOUBLET LATTICE TYPE METHOD FOR $M = .24, .40, .65, .80, .90, .95$
 - A502 AERO FOR $M = 1.20, 2.0, 2.6$
 - REDUCED FREQUENCIES 'k' FROM 0.0 TO .0127 (21 VALUES)
- COMMON MODEL FOR ALL OF THE FOLLOWING
 - DESIGN INTEGRATION TRADE STUDIES
 - AEROELASTIC DESIGN STUDIES
 - AEROSERVOELASTIC DESIGN STUDIES

Task 20 - Sub Task 7 - Aeroservoelastic Design Studies

Boeing, Seattle



High Speed Civil Transport

TCA Finite Element Model (FEM)

Strength and Flutter Discretized Sizing with Stiffened Actuators

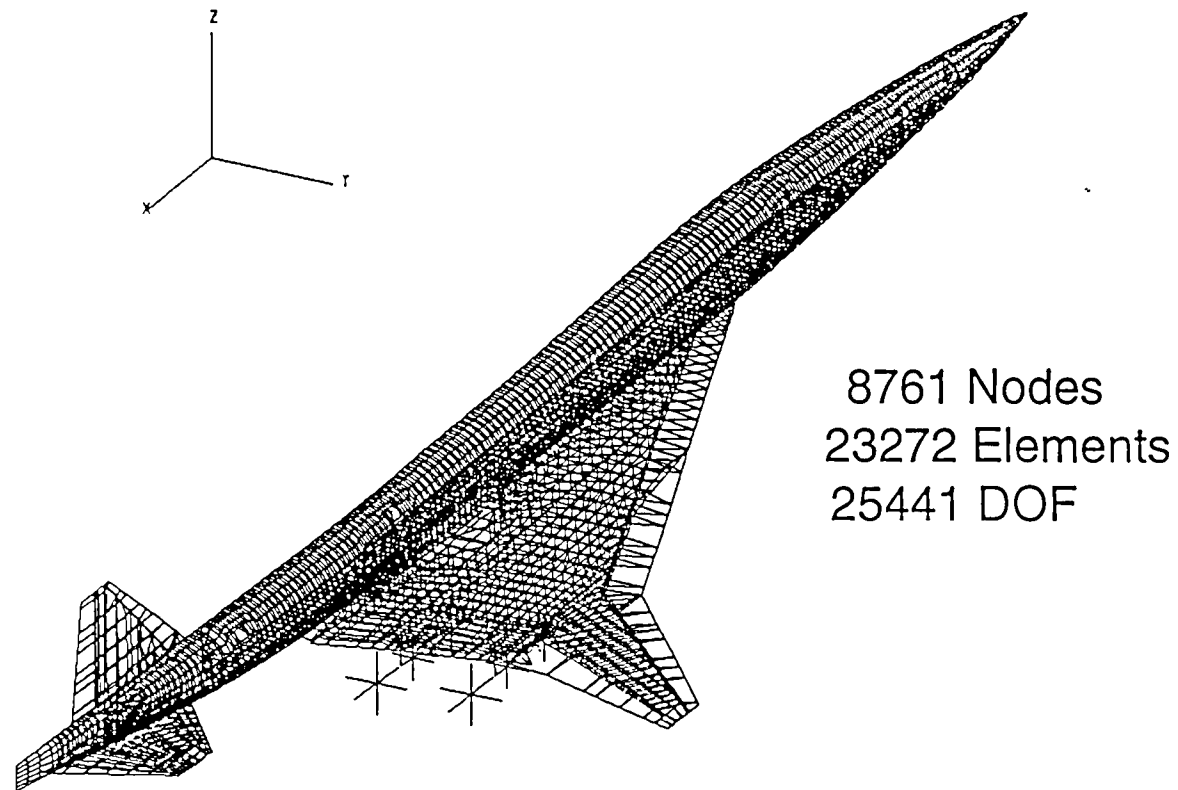



FIGURE A3: TCA FINITE ELEMENT MODEL

~~NOTICE: This is a preliminary drawing.~~

~~This drawing is not to be used for manufacturing purposes without the approval of Boeing.~~

TCA Elfini Flutter Aerodynamic Meshes

Elfini Singularity
Subsonic Mach numbers
0.65, 0.80, 0.90, 0.95



A502
Supersonic Mach numbers
1.2, 2.0, 2.6




FIGURE A4: TCA ELFINI FINITE AERODYNAMIC MESHES



TCA Elfini Flutter Computational Grid

Shaded regions denote zones within which the Elfini basis deformation shapes are defined

Coincident zones are defined on each aerodynamic mesh

An unsteady aero Cp distribution is solved for each basis shape and projected to the grid

Generalized airforces are computed in terms of basis shapes

FEM modal displacements are approximated in terms of basis shapes by least squares fit

Modal gaf's are computed

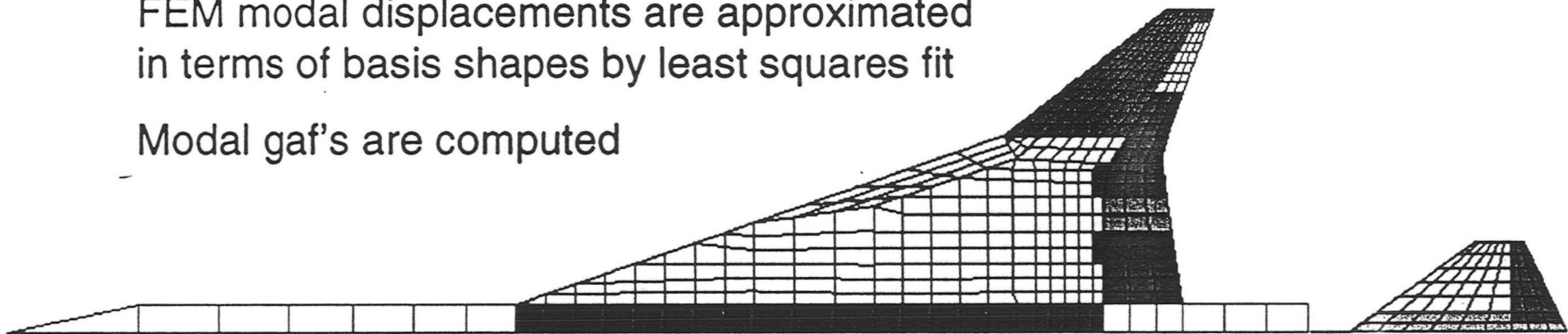


FIGURE A5: TCA ELFINI FLUTTER COMPUTATIONAL GRID

NOTICE: Limited Exclusive Rights Data

This information is sensitive. It is subject to Limited Exclusive Rights provision under NASA Contract No. NAS1-60220.

Task 20: Sub Task 7 - Aeroservoelastic Design Studies

High Speed Civil Transport



TCA Gross Weight vs CG Diagram
All Mass Cases

WEIGHT/C.G.
DIAGRAM

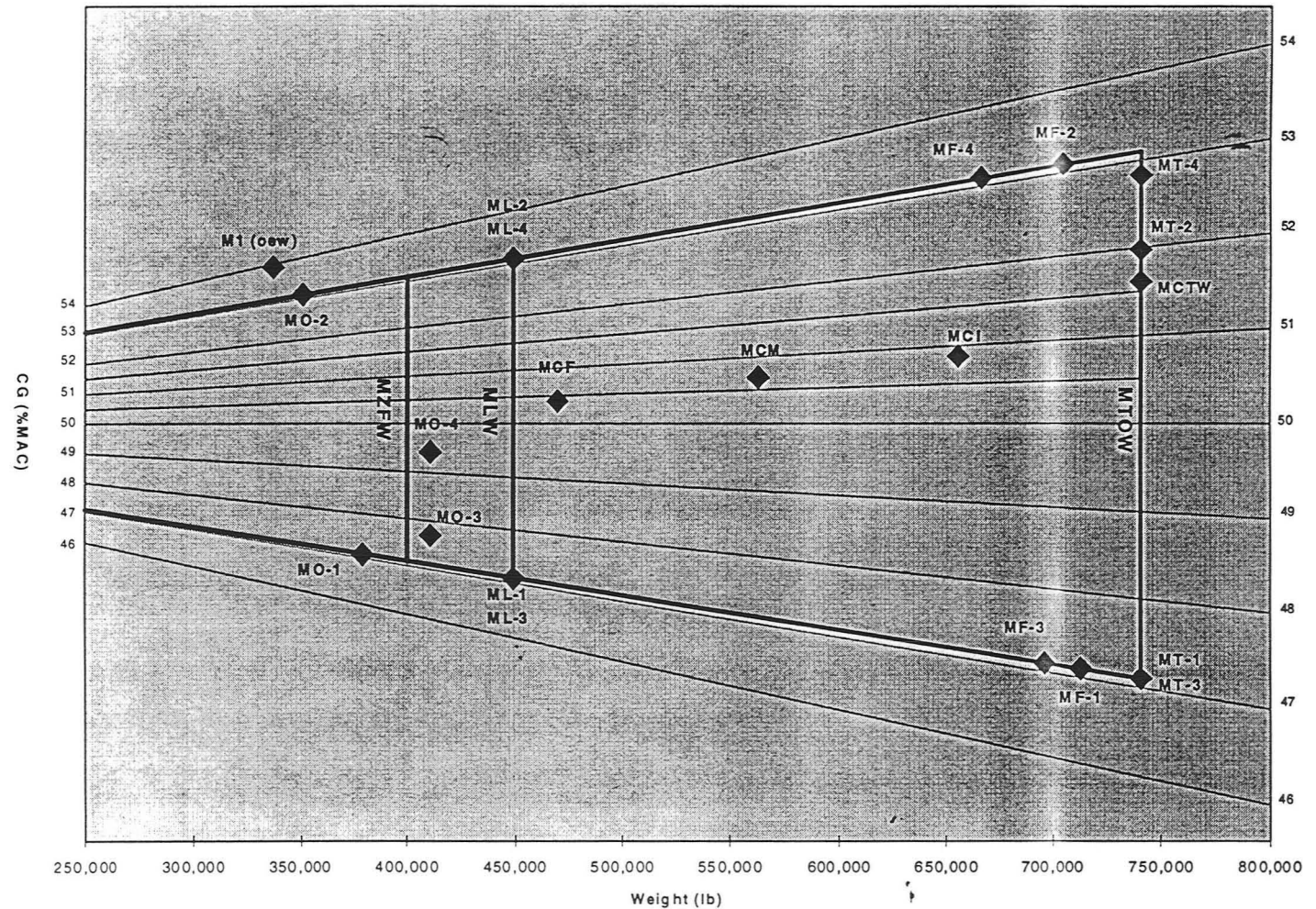


FIGURE A6: WEIGHT/C.G. DIAGRAM

Task 20: Sub Task 7 - Aeroservoelastic Design Studies

High Speed Civil Transport

FLUTTER EQUATIONS OF MOTION (APEX P-K PROGRAM):

$$Du = [s^2 M + sG + (1 + ig)K + iS - qA(p, M_n) + C]u = 0$$

M ~ Mass Matrix, q ~ Dynamic pressure
 K ~ Stiffness Matrix, M_n ~ Mach Number
 A ~ Aerodynamic Matrix, G ~ Gyroscopic Matrix
 C ~ Control Law Matrix, S ~ Damping Matrix, p ~ Reduced frequency, g ~ structural Damping

Control Law
Equations

PITCH CONTROL LAWS (SIMPLIFIED GAMMA DOT- V CONTROLLER):

$$\delta_{STABc} = \underbrace{\left\{ \frac{k_{ei}}{s} + k_{sp} \right\}}_{\text{Outer Loop}} \underbrace{k_{\theta} \gamma_m + k_{\theta} \theta_m + k_{\alpha} \alpha_m + k_q q_m}_{\text{PSAS Inner Loop}}$$

Pitch Rate at IMU

$\gamma_m = z/v$ Flight Path Angle
 θ_m Euler Pitch Angle
 $\alpha_m = \theta_m - z/v$ Angle of Attack
 q_m Pitch Rate

$$\delta_{ELEVc} = 2\delta_{STABc}$$

SENSOR EQNS: $\dot{z} = -s \sum_{i=1}^{i=N} q_i \phi_i T_z$ $q_m = s \sum_{i=1}^{i=N} q_i \phi R_y$

$k_{ei}, k_{sp}, k_{\theta}, k_{\alpha}, k_q$ are function of q

SIMPLIFIED ACTUATOR MODEL:

$$ACTTF = \left(\frac{20}{s + 20} \right) \left(\frac{6400}{s^2 + 113.12s + 6400} \right)$$



FIGURE A7: EQUATIONS USED FOR ^{P-K FLUTTER} CLOSED LOOP ANALYSIS

Task 20: Sub Task 7 - Aeroservoelastic Design Studies

High Speed Civil Transport

FLIGHT ENVELOPE

MACH .65 AND .95
FOR INITIAL ASSEMENT

REQUIREMENTS FOR FLUTTER:

To V_D and $1.15 V_D$ CLEARANCES
FOR NOMINAL GAIN &
To V_D : 6DB GAIN MARGIN
60 DEG PHASE MARGIN

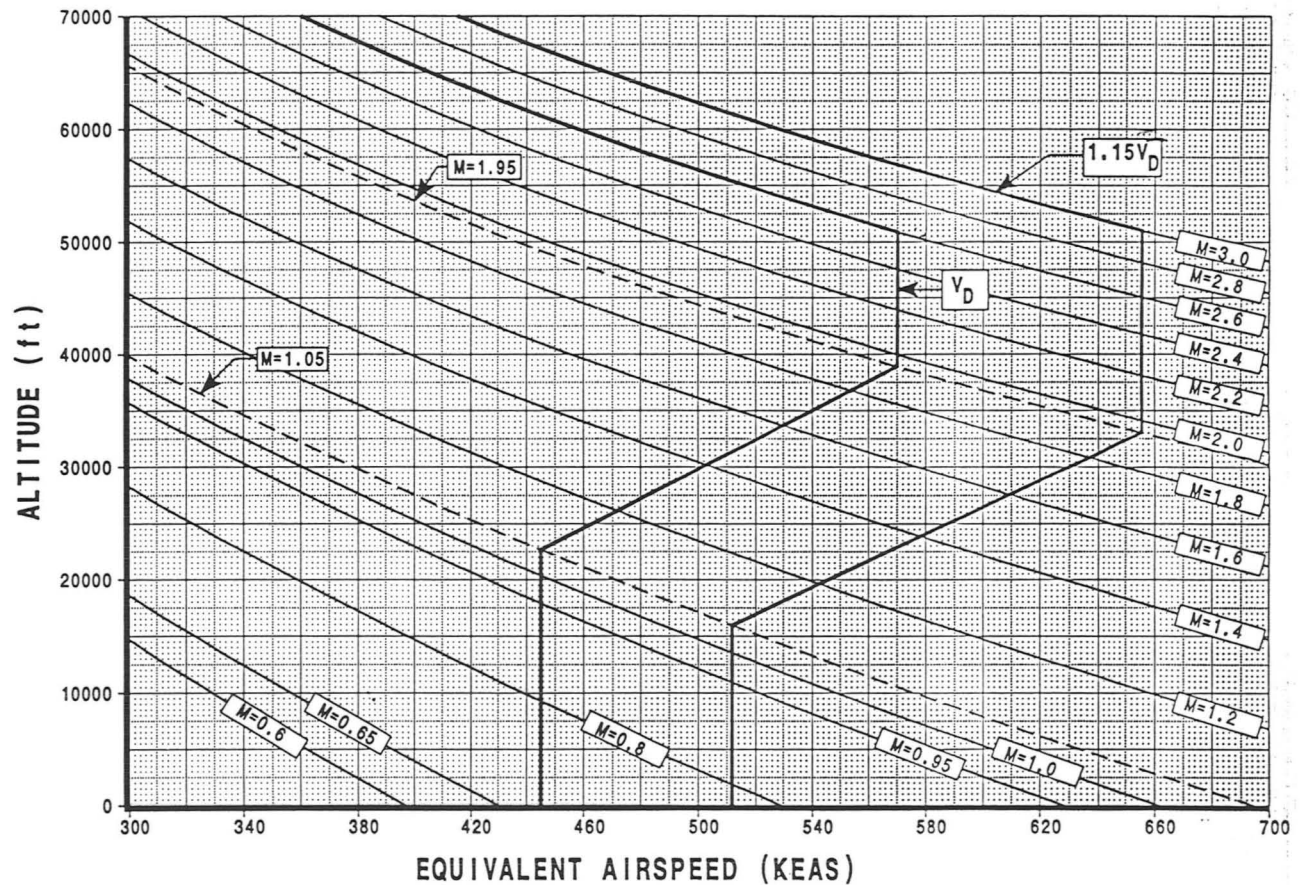


FIGURE A9: FLUTTER CLEARANCE ENVELOPE AND REQUIREMENTS

APPENDIX B

Longitudinal Control Law Overview

Longitudinal Control Law Overview: $\dot{\gamma}V$

- Present Control Laws
 - The throttle controls speed.
 - The elevator controls flight path.
- $\dot{\gamma}V$ Control Law
 - The throttle controls the total energy.
 - The elevator controls how the energy is split between flight path and speed.

FIGURE B1: LONGITUDINAL CONTROL LAW OVERVIEW



~~NOTICE: This information is sensitive. It is subject to~~
~~Limited Exclusive Rights provisions under NASA Contract No. NAS1-20210.~~

Longitudinal Control Law Overview: $\dot{\gamma}V$ (Cont.)

- Basic concept of $\dot{\gamma}/V$ is to control total energy
- Total energy is sum of potential and kinetic

$$e_t = mgh + \frac{1}{2}mV^2 \quad (1)$$

- Specific energy rate (normalized by weight and velocity):

$$\dot{E}_t = \frac{T - D}{mg} = \gamma + \frac{\dot{V}}{g} \quad (2)$$



FIGURE B 2 : LONGITUDINAL CONTROL LAW OVERVIEW (CONT.)

~~NOTICE: This information is sensitive and is subject to
limited Exclusive Rights provisions under NASA Contract No. NAS1-28220.~~

Longitudinal Control Law Overview: $\dot{\gamma}V$ (Cont.)

- Along flight path, required trim thrust is:

$$T_{\text{req}} = mg\dot{E}_t + D \quad (3)$$

- Assuming drag variation is slow, T_{req} is proportional to specific energy rate (i.e. throttles control rate of energy addition)
- Use throttle feedback law:

$$\frac{\delta_T}{mg} \triangleq \left(K_{\text{TP}} + \frac{K_{\text{TI}}}{s} \right) \dot{E}_{te} = \left(K_{\text{TP}} + \frac{K_{\text{TI}}}{s} \right) \left(\gamma_E + \frac{\dot{V}_E}{g} \right) \quad (4)$$

FIGURE B3: LONGITUDINAL CONTROL LAW OVERVIEW (CONT.)



~~NOTICE: This information is sensitive and is subject to the Limited Exclusive Rights provisions under NASA Contract No. NAS1-20220.~~

Longitudinal Control Law Overview: $\dot{\gamma}V$ (Cont.)

- Forces resulting from elevator movement are essentially conservative \rightarrow no net change in total energy.
- Elevators do *not* significantly change aircraft's total energy state.
- Elevators serve mainly to redistribute energy between potential and kinetic.
- Use elevator to control energy distribution error $\frac{\dot{E}_{de}}{V} \triangleq \frac{\dot{V}}{g} - \gamma$.
- Elevator feedback law:

$$\delta_E \triangleq \left(K_{SP} + \frac{K_{EI}}{s} \right) \dot{E}_{de} = \left(K_{SP} + \frac{K_{EI}}{s} \right) \left(\frac{\dot{V}_E}{g} - \gamma_E \right) \quad (5)$$

FIGURE B4: LONGITUDINAL CONTROL LAW OVERVIEW (CONT.)



~~NOTICE: This information is sensitive and its subject is~~

~~limited by the rights provisions under NASA Commons No. NNC1-202201~~

γV Control Law Core

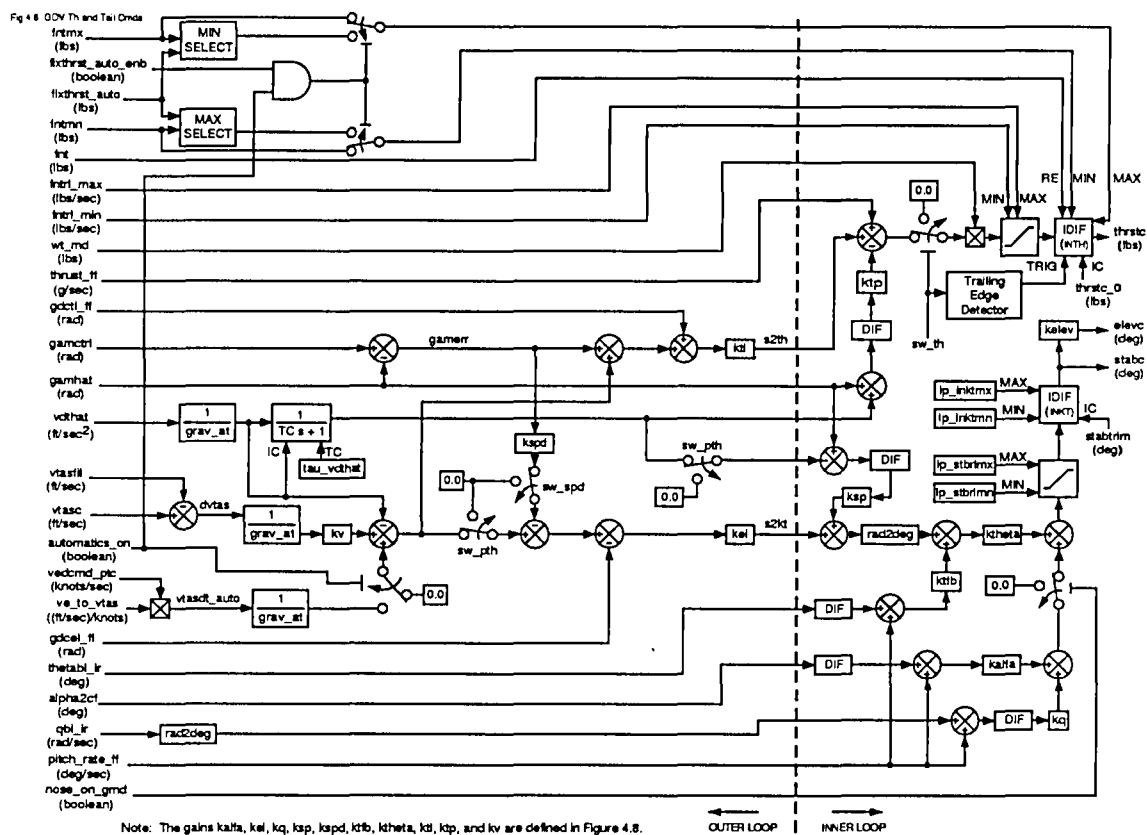


FIGURE B5: γV CONTROL LAW CORE

NOTICE: This information is sensitive. It is subject to

Limited Exclusive Rights provisions under NASA Contract No. NAS1-20220.

FIGURE B6: SIMPLIFIED CONTROL LAW BLOCK DIAGRAM

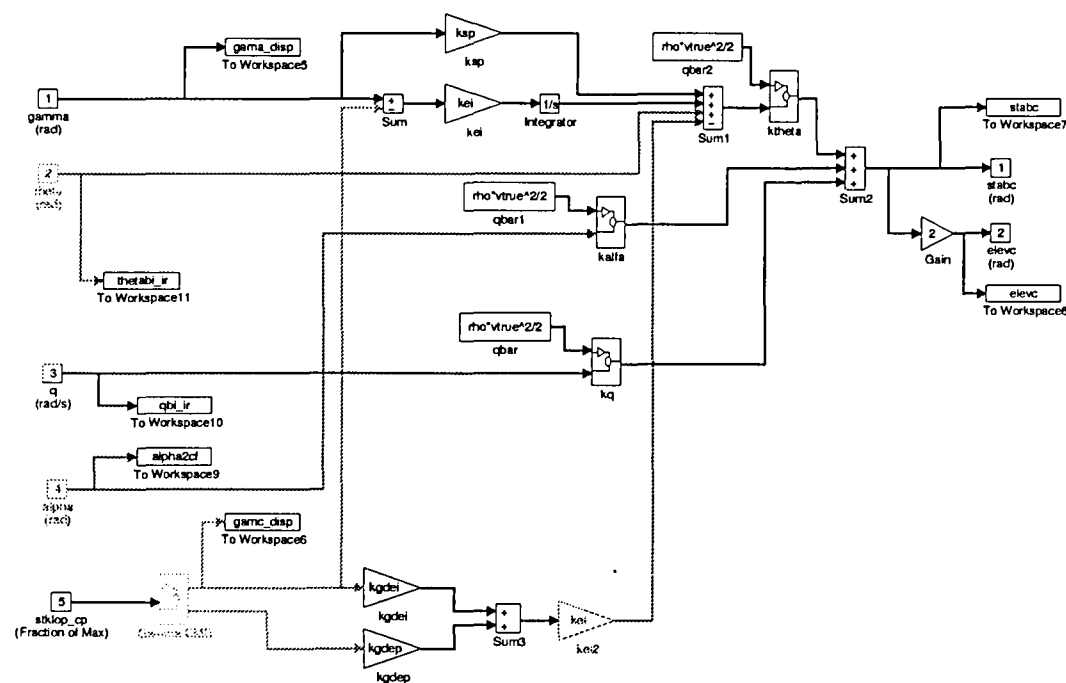


FIGURE B6: SIMPLIFIED CONTROL LAW BLOCK DIAGRAM

~~NOTICE: This information is sensitive, its release is limited by the~~
~~limited Exclusive Rights provisions under NASA Contract No. NAS1-20000-1-220.~~

Simplified $\dot{\gamma}V$ Control Law Equations

$$\delta_{stab_c} = \left\{ \frac{k_{ei}}{s} (\gamma_m - \gamma_c) - k_{col} k_{ei} \left(k_{gdep} + \frac{k_{gdei}}{s} \right) \delta_{stick} + \gamma_m k_{sp} + \theta_m \right\} k_\theta$$

$$+ k_\alpha \alpha_m + k_q q_m \quad (6)$$

$$\delta_{elev_c} = 2\delta_{stab_c} \quad (7)$$

$$\gamma_c = \left(\frac{k_{col}}{s} \right) \delta_{stick} \quad (8)$$

$$\alpha_m \triangleq \alpha_{CM} = \alpha_{IMU} + \left(\frac{l_{IMU}}{V} \right) q_m \quad (9)$$



FIGURE B7: CONTROL LAW EQUATIONS

~~NOTICE: This information is sensitive. It is subject to~~
~~Limited Exclusive Rights provisions under NASA Contract No. NAS1-20220.~~

Total Closed Loop System

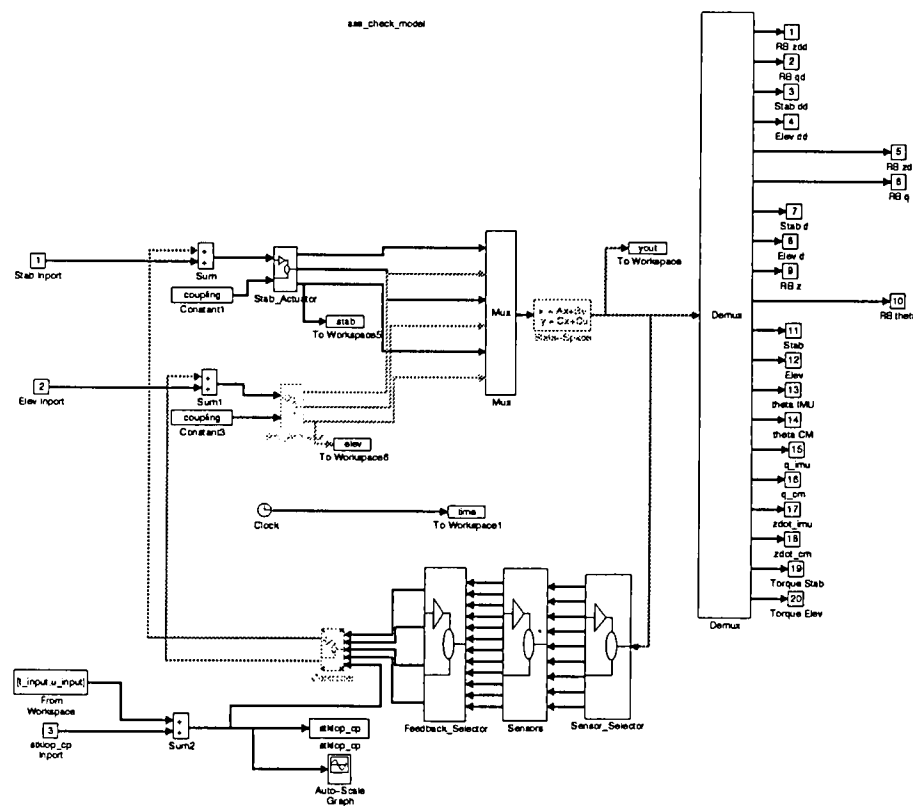


FIGURE B8: AEROSERVOELASTIC STATE-SPACE MODEL

~~NOTICE: This information is sensitive and its disclosure is restricted to the limited Executive Rights provisions under NASA Contract No. NAS1-00000.~~

APPENDIX C

State-Space Modeling Methodology

FC DASE Modeling Methodology

Flutter Equation

$$\left[Ms^2 + Cs + K - qA_{ua}(\hat{s}) \right] X(s) = \Phi^T GU(s) + q \left[Y_g(s) A_{gy}(\hat{s}) + Z_g(s) A_{gz}(\hat{s}) \right] \quad (10)$$

where

$$A_{gy}(\hat{s}) \triangleq \sum_{i=1}^{n_g} A_{igy}(\hat{s}) e^{-\tau_i s} \quad (11)$$

$$A_{gz}(\hat{s}) \triangleq \sum_{i=1}^{n_g} A_{igz}(\hat{s}) e^{-\tau_i s} \quad (12)$$



FC DASE Modeling Methodology

- Flight Controls derives state space models from Structures model (File 41)
 - Automated routine to convert Elfini File 41 to Matlab format.
 - Collection of Matlab m-files used to:
 1. Fit unsteady aero using Roger RFA
 2. Introduce structural viscous damping
 3. Define control inputs
 4. Produce sensor outputs
 5. Return state space A , B , C , D matrices
- Matlab routines also developed to perform:
 1. Frequency domain response analysis
 2. Flutter analysis ($V - g$ diagrams)



~~NO FORN DISSEM. This information is sensitive. It is subject to
Excluded from automatic downgrading and declassification. Rights provisions under NASA Contract No. NAS1-20220.~~

FC DASE Modeling Methodology

Unsteady Aero Approximations

$$A_{ua}(\hat{s}) \approx a_0 \hat{s}^2 - a_1 \hat{s} - a_2 - \left\{ \sum_{i=1}^{n_\beta} a_{i+2} \frac{\hat{s}}{\hat{s} + \hat{\beta}_i} \right\} \quad (13)$$

$$A_{gy}(\hat{s}) \approx a_{0y} \hat{s}^2 - a_{1y} \hat{s} - \left\{ \sum_{i=1}^{n_\beta} a_{i+2y} \frac{\hat{s}}{\hat{s} + \hat{\beta}_i} \right\} \quad (14)$$

$$A_{gz}(\hat{s}) \approx a_{0z} \hat{s}^2 - a_{1z} \hat{s} - \left\{ \sum_{i=1}^{n_\beta} a_{i+2z} \frac{\hat{s}}{\hat{s} + \hat{\beta}_i} \right\} . \quad (15)$$



FC DASE Modeling Methodology

State Space Equations of Motion

$$\dot{x}_{ss} = A_{ss}x_{ss} + B_{ss}u + B_{ssg}w \quad (16)$$

$$x_{ss}^T = \left[\begin{array}{c|cccc} \dot{x} & x & r_1 & r_2 & \dots & r_{n_\beta} \end{array} \middle| \begin{array}{cccc} r_{gy1} & r_{gy2} & \dots & r_{gyn_\beta} \end{array} \middle| \begin{array}{cccc} r_{gz1} & r_{gz2} & \dots & r_{gzr} \end{array} \right] \quad (17)$$

$$w^T = \left[\begin{array}{cccc} \ddot{y}_g & \dot{y}_g & \ddot{z}_g & \dot{z}_g \end{array} \right] \quad (18)$$



FC DASE Modeling Methodology

Torque Inputs vs Prescribed Motion

- Equation (16) uses generalized internal/external forces as driving inputs.
 - Actuator force model required to drive system.
 - Accounts for full two-way coupling of surface-into-vehicle and vehicle-into-surface dynamic coupling.
 - Surface motion is an *output*.
- Prescribed surface motion commonly used when actuator models not well defined.
 - Actuator displacement model required to drive system.
 - Accounts only for surface-into-vehicle dynamic coupling.
 - Equation (16) may be transformed to prescribed motion, making required hinge moment an output.

State-Space Model Generation Process Flight Controls

1. Convert Elfini File 41 data to Matlab format
2. Define State-space Model Build Specification
 - Model file name
 - Added viscous structural damping
 - Flight condition (Mach and altitude)
 - Retained modes
 - Unsteady aero fitting parameters
 - Number of lag states
 - Force fit at zero frequency
 - Use inverse frequency weighting
 - Omit apparent mass term
 - Define sensor and actuator support node numbers
3. Determine true airspeed and density
4. Form basic A , B , C , D representation
 - Calculate viscous damping matrix
 - Determine indices of retained modes
 - Strip-out unretained modes
 - Calculate dynamic pressure
 - Determine frequencies of lag filters
 - Frequencies are evenly spaced between minimum and maximum k -values
 - Form state-space A matrix
 - Fit unsteady aero using linear weighted least squares
 - Combine aero fitting coefficients with mass, stiffness, and damping matrices to form state-space A matrix
 - Correct A matrix for accelerations due to plunge position (should be zero).
 - Correct A matrix such that accelerations due to rigid body plunge velocity agree with accelerations due to rigid body pitch position, the latter being the truth model.
 - Form state-space B matrix
 - Collect mode shapes for assumed modes, or actuator degrees of freedom (Identity matrix)
 - Collect mode shapes for actuator support structure
 - Use finite differencing, if necessary, to obtain modal slopes
 - Calculate difference between mode shapes for the actuator DOFS and the actuator support structure
 - Form state-space B matrix using the mass matrix, apparent aerodynamic mass, and the mode shape differences.

- Form C matrix
 - Include rigid-body mean-axis states
 - Include nodal displacements
 - Include assumed mode deflections
 - Strip out unretained modes
 - Calculate C matrix for \dot{y}
 - Calculate C matrix for \ddot{y}
 - Form total C matrix for y , \dot{y} , and \ddot{y}
 - Form D matrix
 - Include direct feed-through elements from \ddot{y}
 - Convert A , B , C , D representation to sparse arrays
5. Add additional sensors to C and D matrices
- Pitch and pitch rate sensors at various body stations
 - Load factor sensors at various body stations
 - Velocity sensors at various body stations
 - Assemble new combined C and D matrices
6. Transform coordinates and convert units
- Define coordinate transformations
 - Define unit conversions
 - Form transformations matrices for state vector, measurement vector, and control vector.
 - Perform transformation
7. If desired, convert from torque inputs to prescribed motion inputs
8. Done

PART II - Boeing Long Beach Report

Introduction

A closed-loop ASE flutter analysis of the TCA configuration with symmetric boundary condition has been performed using MSC/NASTRAN. While the primary goal of this study was to validate the MSC/NASTRAN ASE analysis process and not to generate ASE stability results for the TCA configuration, several interesting results were nonetheless generated.

MSC/NASTRAN ASE Analysis Process

MSC/NASTRAN is an attractive package for ASE analysis since the control laws can be directly included with the structural and aerodynamic models in a single ASE model, without requiring the intermediate steps of generating vibration modes, generalized AIC's, and the like. In a DITS-type sizing process, the transfer functions could conceivably be included directly in the flutter screening analyses as well as in the flutter constraint calculation in the strength/loads/flutter sizing process.

While MSC/NASTRAN allows the inclusion of control laws directly in the flutter analysis, there are several things that must be kept in mind, and issues that must be overcome.

1. The structural FEM must have rigid-body (i.e. zero frequency) vibration modes for each of the control surfaces to be used in the analysis. For this study, the elevator was the only surface used, so the model had four rigid body modes (pitch, plunge, fore-aft, and elevator pitch).
2. The FEM must have degrees of freedom that directly correspond to the sensors of the ASE model. For example, if an acceleration at the pilot station is a desired input, then a structural node must exist at the pilot station.
3. A structural node must also be created for each actuator, and MPC's defined relating the actuator node deflection to the physical deflection of the associated control surface
4. MSC/NASTRAN has no built-in gain scheduling capability. If gain scheduling is required, then a separate transfer function must be defined for each speed point, and each speed point must be analyzed in a separate subcase.

Addressing these issues required several minor modifications to the finite element model as well as writing a simple preprocessor code to automate the gain scheduling task.

Closed Loop Flutter Analysis Results

In validating the closed loop MSC/NASTRAN flutter analysis two mass conditions, MO-2 and MT-1, were investigated. The open loop flutter results for some of the critical modes of these two mass conditions are presented in Figures 1 and 2. It can be seen that the open-loop aircraft is aeroelastically stable within the flight envelope.

The Gamma dot V control was included in the ASE model for this validation process. That control law, including actuator dynamics, takes the form:

$$\delta_{STAB} = \left[\left(\frac{k_{ei}}{S} + k_{sp} \right) k_{\theta} \gamma_m + k_{\theta} + k_{\alpha} \alpha_m + k_q q_m \right] \left(\frac{20}{S+20} \right) \left(\frac{6400}{S+113.12S+6400} \right)$$

and

$$\delta_{ELEV} = 2\delta_{STAB}$$

The Gamma dot V control law drives both the elevator and the horizontal stabilizer. In the analysis presented in this memo the stabilizer deflection was not included, and the control law only drives the elevator. Since the elevator gain is twice that of the horizontal stabilizer, it is believed this modification would not affect the conclusions of this analysis. The sensor configuration used in these analyses were located near the center of mass of the aircraft.

The closed loop flutter analysis results for mass conditions MO-2 and MT-1 are presented in figures 3 and 4 respectively. It can be seen that both conditions exhibit damping in the unacceptable range.

Raj Nagaraja presented closed loop flutter results for the MO-2 condition at the HSR Airframe Technical Review in February 1998. The results presented in this memo correlate well with those results. This correlation validates the MSC/NASTRAN closed-loop flutter analysis.

Possible Modifications to the "Gamma dot V" Control Law

A further investigation was performed to try and devise a filtering scheme that would reduce the effects of the control law on the flexible aircraft. It was determined that the main cause of the instabilities was the pitch rate feedback (q), and therefore, only this loop was filtered. The control employed in the analysis then became:

$$\delta_{ELEV} = 2 \left[\left(\frac{k_{ei}}{S} + k_{sp} \right) k_{\theta} \gamma_m + k_{\theta} + k_{\alpha} \alpha_m + k_q q_m (NTF) \right] \left(\frac{20}{S+20} \right) \left(\frac{6400}{S+113.12S+6400} \right)$$

Where NTF represents the filter transfer function. Initially a single notch filter was employed at the instability frequency. It was found that such a filter would reduce the initial instability, but would cause sufficient phase shift to drive another mode unstable. Subsequently a double notch configuration was devised that addressed all aeroelastic instabilities. These filters consist of 14db notch filters at 1.8Hz and 3.6Hz and combined to form the transfer function:

$$NTF = \left(\frac{S^2 + 3.164S + 127.69}{S^2 + 15.82S + 127.69} \right) \left(\frac{S^2 + 6.328S + 510.76}{S^2 + 31.64S + 510.76} \right)$$

A bode plot of this filtering scheme is presented in figure 5. Aeroservoelastic analysis results incorporating this filtering scheme are presented in figures 6 and 7 for mass conditions MO-2 and MT-1. It can be seen in Figure 7 that at the low speed end of the flight envelope a humped mode crosses over into the region of unacceptable damping. Further refinements of the notch filters would probably eliminate this instability.

This filtering scheme and the accompanying analyses are presented as a possible solution to the aeroservoelastic instability problem. It is not meant to be the final or only solution. Some further filter refinement and analysis is still required to:

1. Completely eliminate all aeroelastic instabilities within the flight envelope, for all mass and flight conditions
2. Determine the filters' effects on the aircraft's flying qualities.

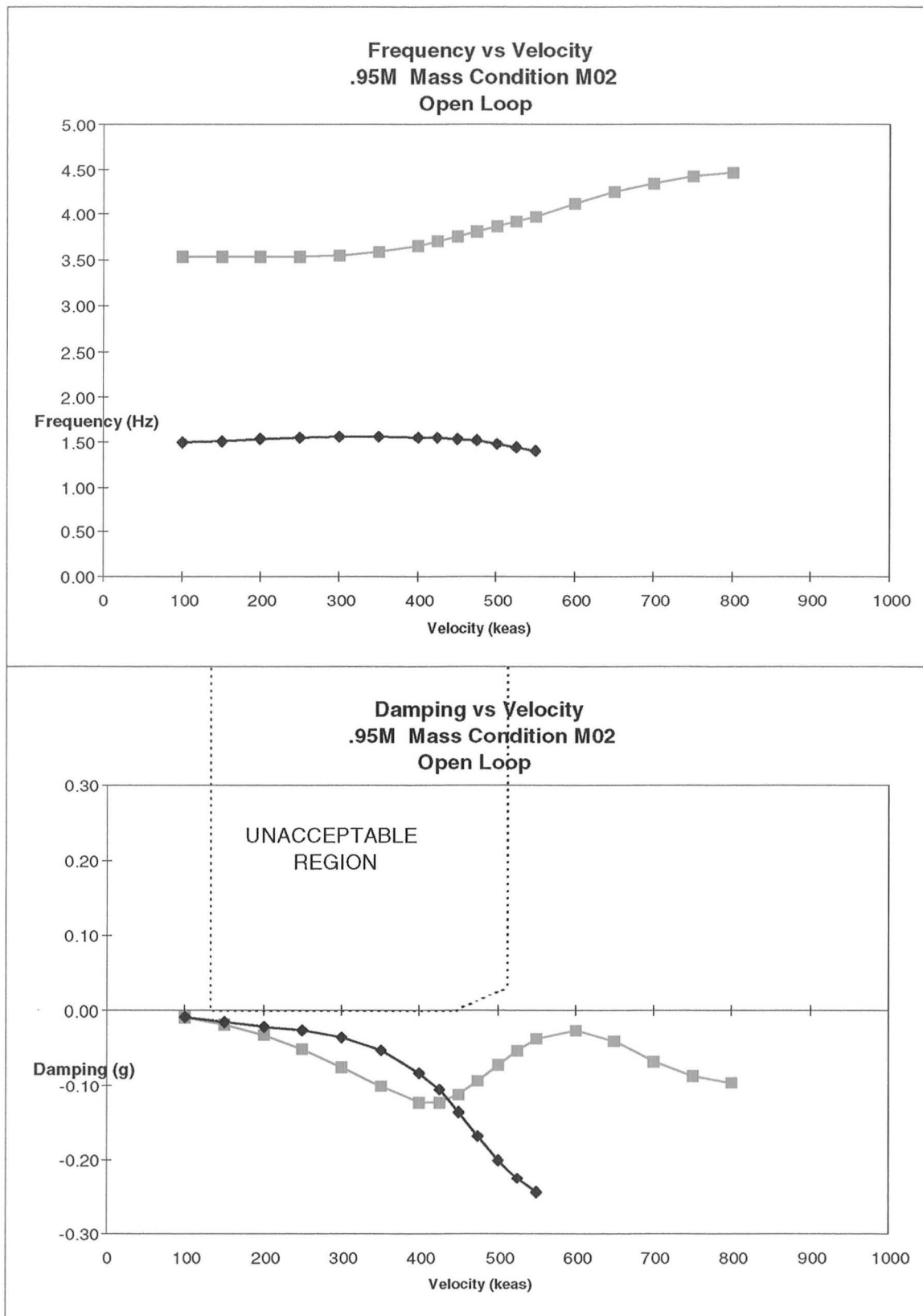


Figure 1: Open Loop Flutter analysis Results, Mass Case MO-2 at Mach 0.95.

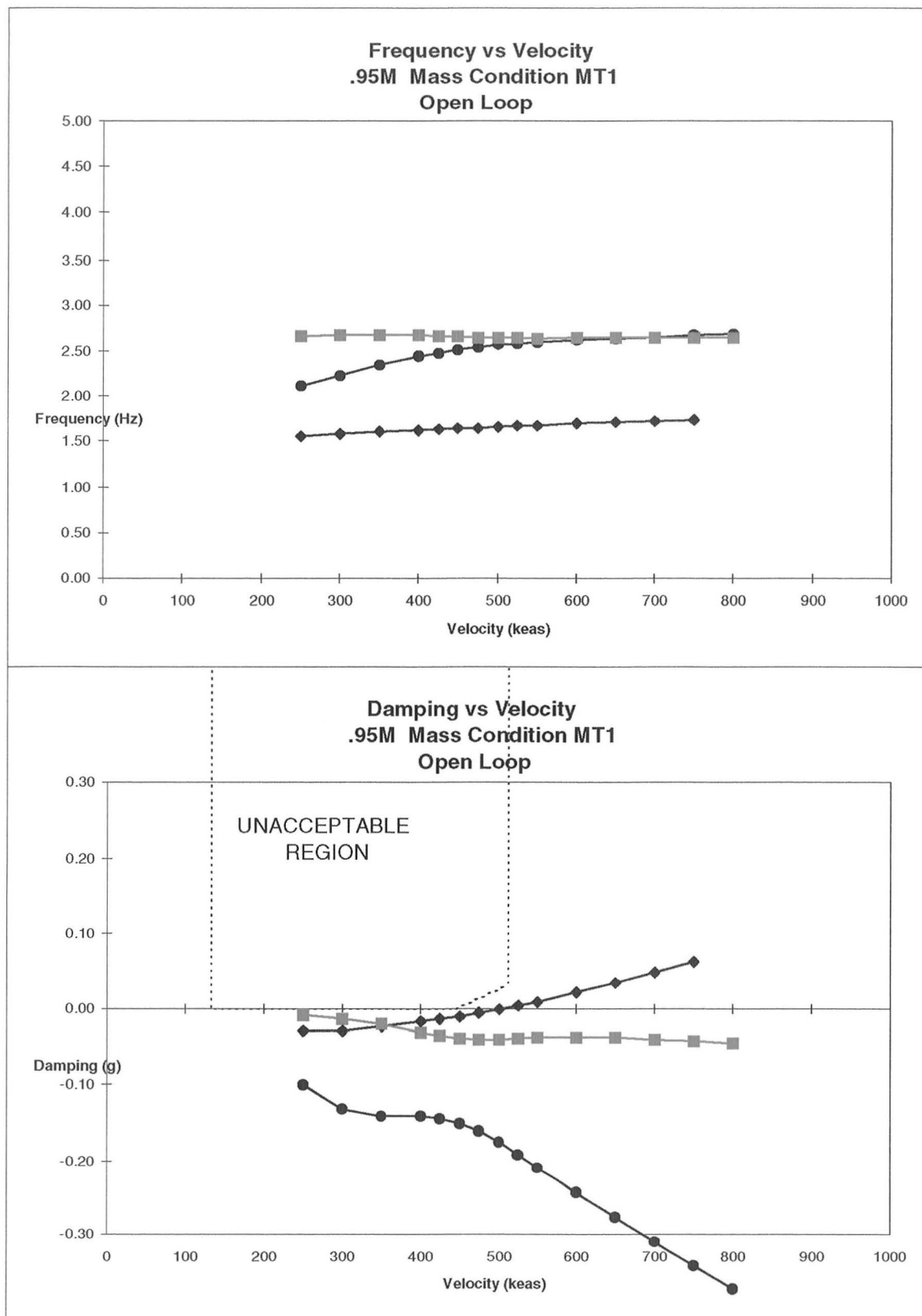


Figure 2: Open Loop Flutter analysis Results, Mass Case MT-1 at Mach 0.95.

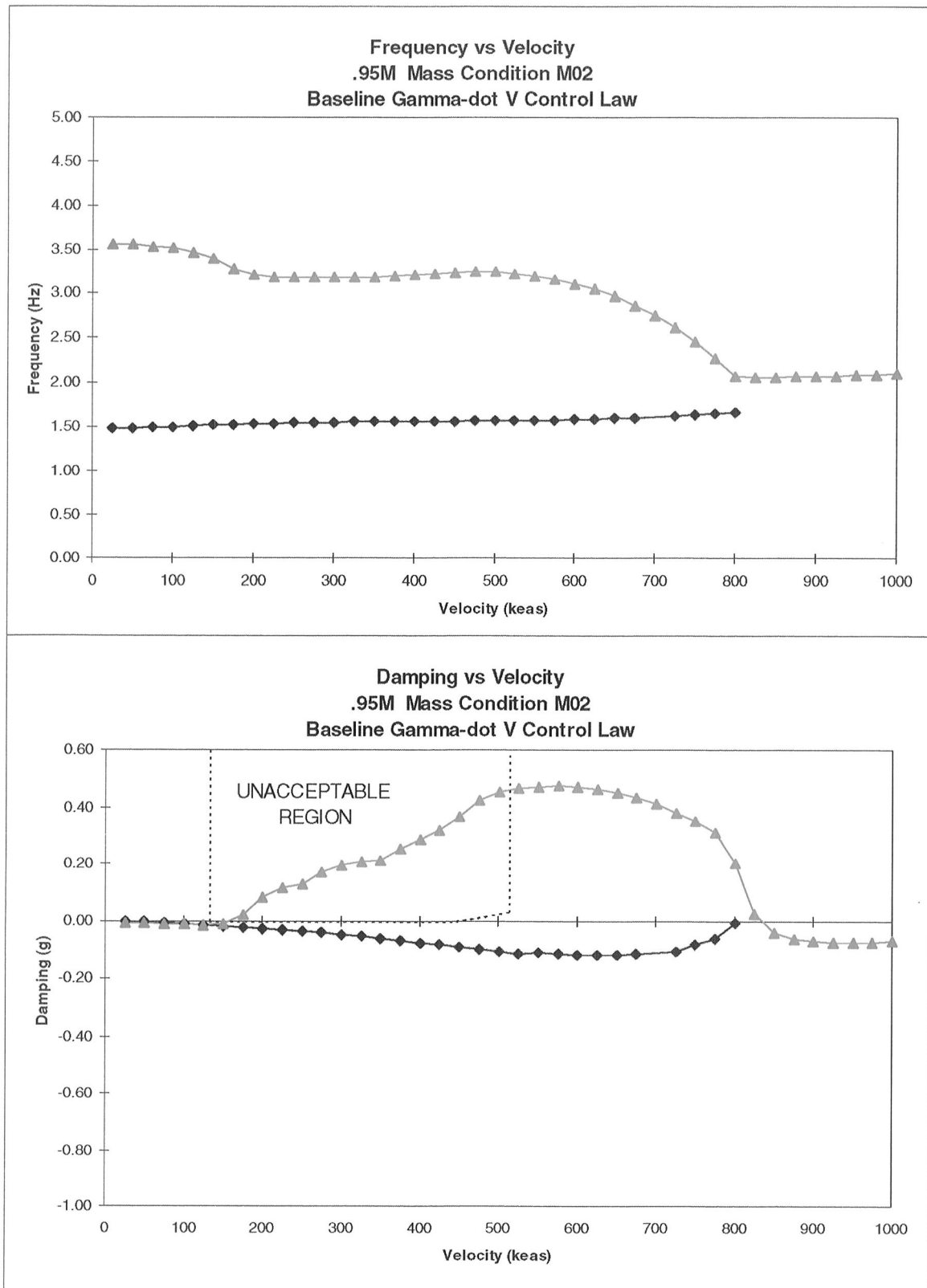


Figure 3: Closed Loop Flutter (Baseline Gamma-dot-V) Analysis Results, Mass Case MO-2 at Mach 0.95.

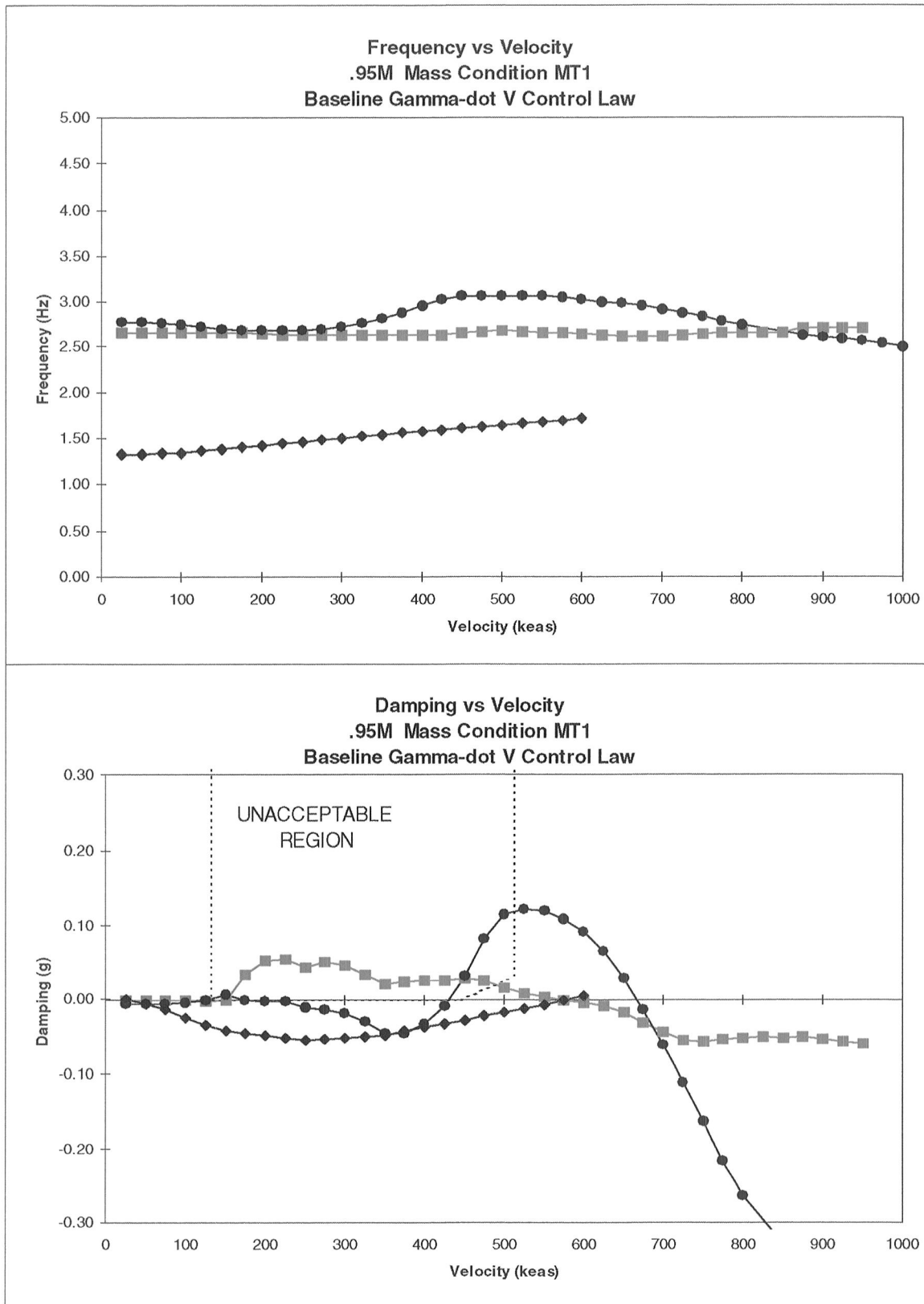


Figure 4: Closed Loop Flutter (Baseline Gamma-dot-V) Analysis Results, Mass Case MT-1 at Mach 0.95.

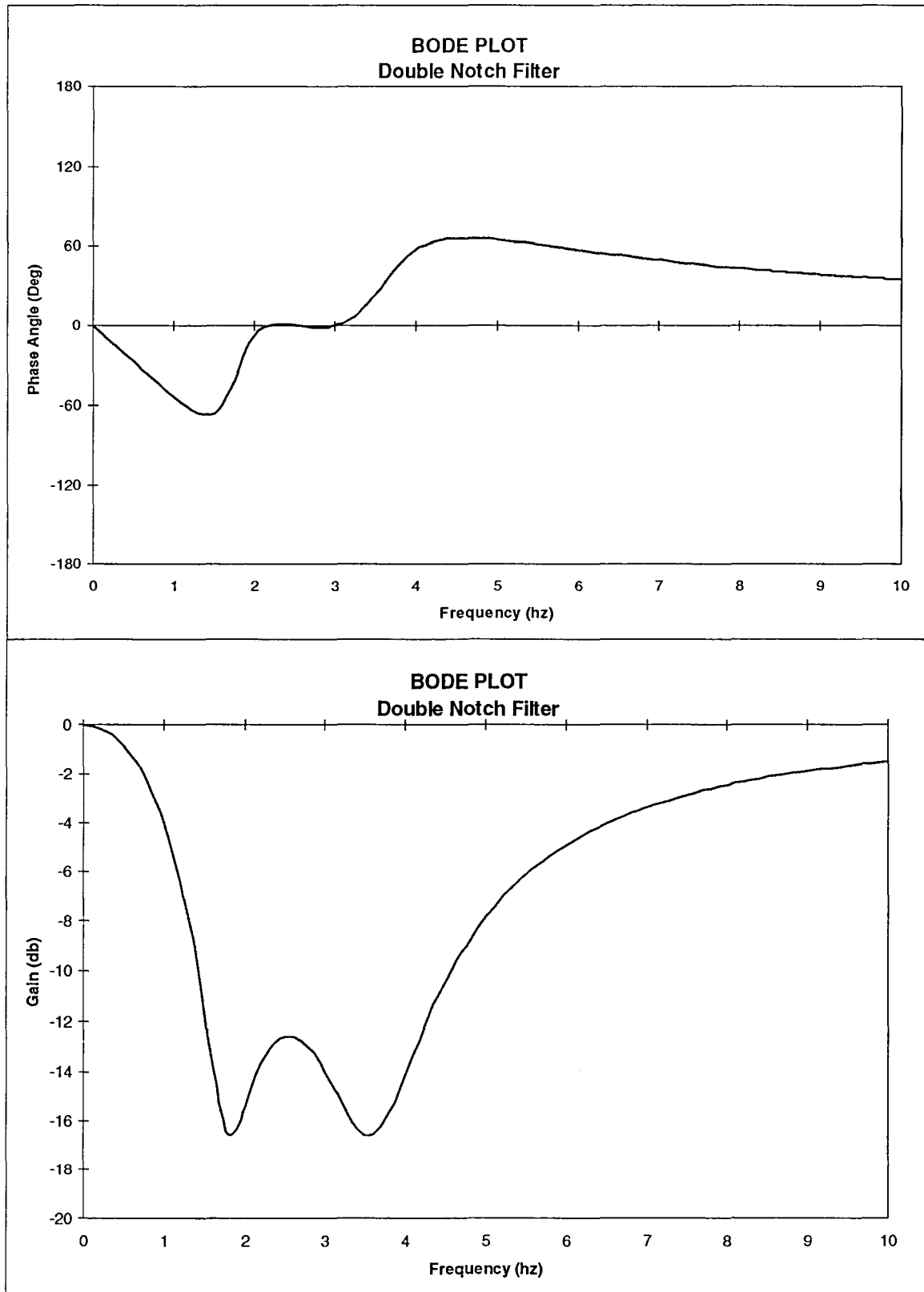


Figure 5: Bode Plot of Double-Notch Filter Used to Eliminate Aeroservoelastic Instabilities.

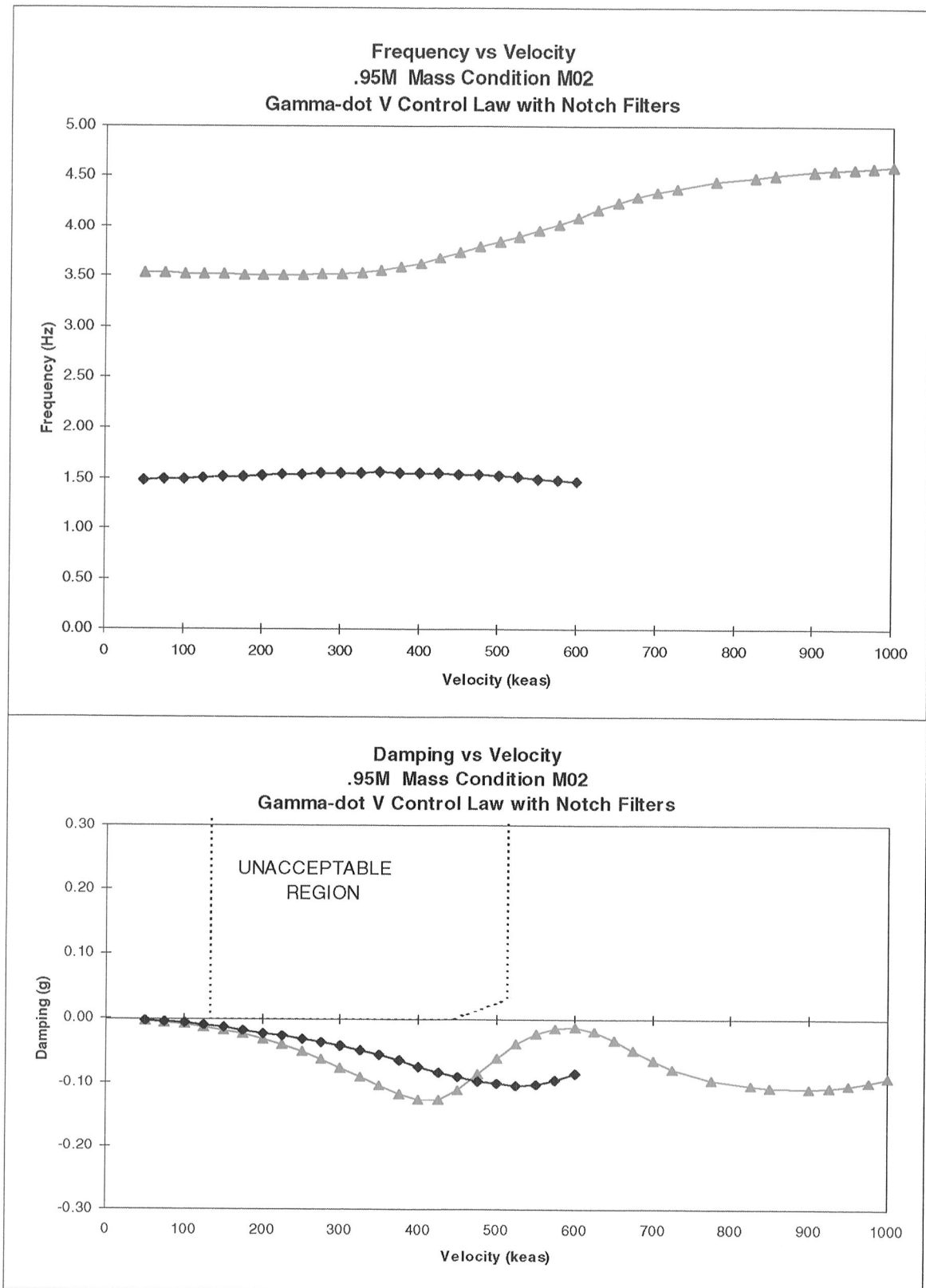


Figure 6: Closed Loop Flutter (Gamma-dot-V with Notch Filter) Analysis Results, Mass Case MO-2 at Mach 0.95.

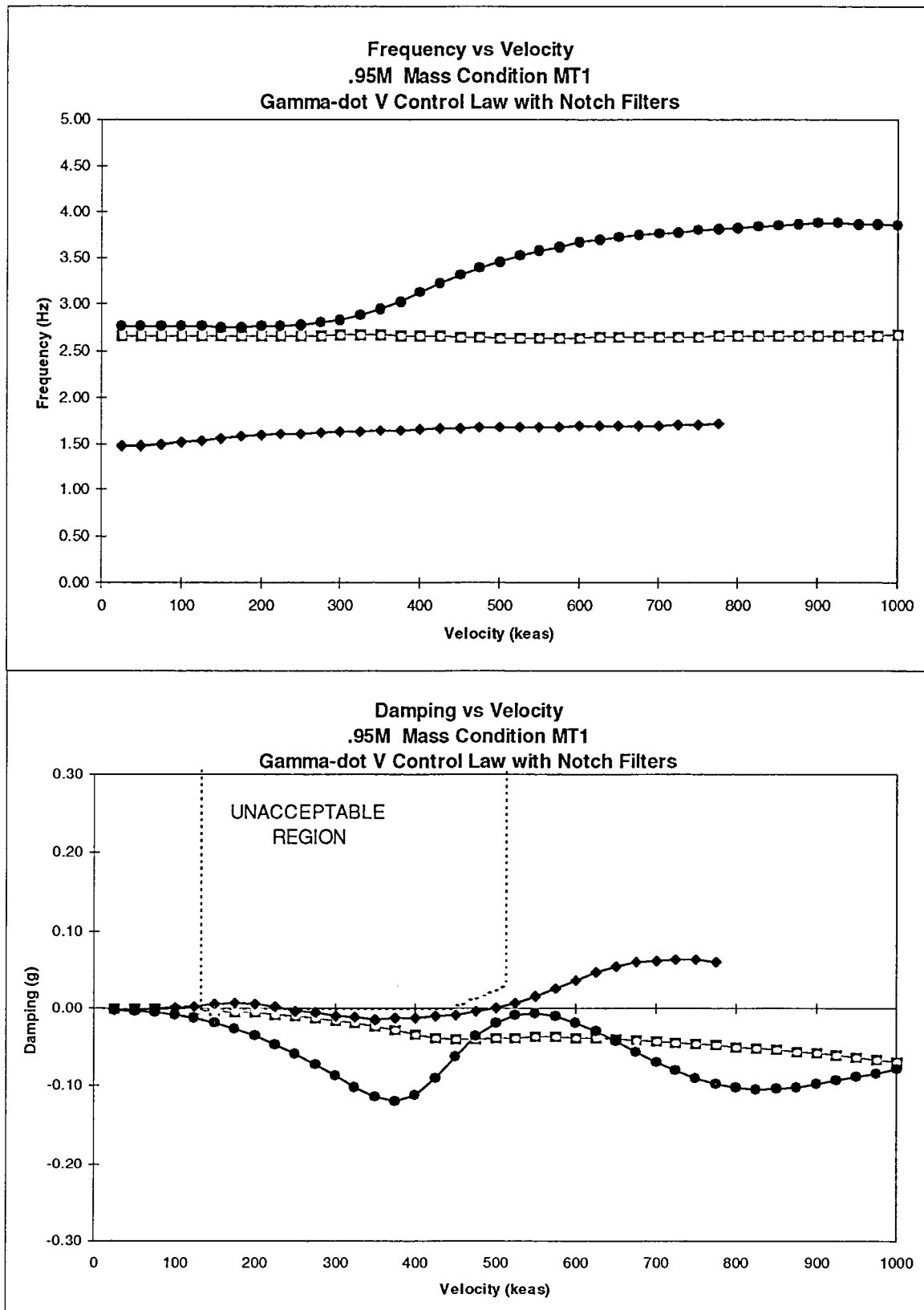


Figure 7: Closed Loop Flutter (Gamma-dot-V with Notch Filter) Analysis Results, Mass Case MT-1 at Mach 0.95.



DELIVERY TRANSMITTAL FORM (DTF)

1. CONTRACT NO: NAS1-20220		TASK ASSIGNMENT NO: Task 20, Subtask 7		2. REFERENCE (DTF) NO: 20-7-02	
3. TITLE OF DELIVERABLE: Evaluation of Aeroservoelastic Effects on Symmetric Flutter				4. DUE DATE March 31, 1998	
				5. DELIVERY DATE: March 31, 1998	
6. NO.	7. ADDRESSEES/ADDRESSES: NAME, OFFICE/CODE/BASE AND CITY/STATE/ZIP			8. QUANTITY: See Distrib.	
	<p>National Aeronautics and Space Administration Langley Research Center Attn: <u>Bill Gilbert</u>, Mail Stop <u>119</u> Contract NAS1-20220 Hampton, VA 23681-0001</p> <p>Attn: Billy Gilbert, Technical Contact, M/S 119, 757-864-6392 (5)</p> <p>R.B Ricketts Carey Butrill ✓ Rob Scott Walt Silva</p> <p>Note: Covers the completion requirement for a milestone under subtask 7.</p> <p>Attn: Cheryl Harrell Attn: R.B. Gardner</p>				
9. REPORTING PERIOD OF PERFORMANCE: N/A					
10. DTF PREPARED/APPROVED BY (SIGN, PRINT NAME, ORGANIZATION, PHONE, MAIL STOP): Kerry Johnsen, Boeing Business Management, (425)965-0238 MS 6H-FP <i>Kerry Johnsen</i> 3/31/98 BOEING COMMERCIAL AIRPLANE GROUP P.O. BOX 3707, Mail Stop 6H-FP SEATTLE, WA 98124-2207					
THE FOLLOWING IS FOR REFERENCE ONLY					
ITEM	ITEM TITLE				DISTRIBUTION REQMTS FOR BLK 6 ABOVE